The Journal of Antibiotics (2009) 62, 539–544

www.nature.com/ja

ORIGINAL ARTICLE

# Synthesis and combinational antibacterial study of 5″-modified neomycin

Jianjun Zhang[1], Katherine Keller[1], Jon Y Takemoto[2], Mekki Bensaci[2], Anthony Litke[1], Przemyslaw Greg Czyryca[3] and Cheng-Wei Tom Chang[1]

**A library of 5″-modified neomycin derivatives were synthesized for an antibacterial structure–activity optimization strategy. Two leads exhibited prominent activity against both methicillin-resistant *Staphylococcus aureus* (MRSA) and vancomycin-resistant enterococci (VRE). Antibacterial activities were measured when combined with other clinically used antibiotics. Significant synergistic activities were observed, which may lead to the development of novel therapeutic practices in the battle against infectious bacteria.**
*The Journal of Antibiotics* (2009) **62,** 539–544; doi:10.1038/ja.2009.66; published online 24 July 2009

**Keywords:** aminoglycoside; antibiotic; MRSA; synergism; VRE

## INTRODUCTION

Aminoglycosides are an important class of antibiotics used against infectious diseases. Their usefulness, however, has been significantly compromised by the emergence of resistant bacteria, especially those equipped with aminoglycoside-modifying enzymes (AMEs).[1–3] Structural modification of aminoglycosides remains an effective approach for reviving their antibacterial activities against resistant bacteria. The typical goal is to provide novel aminoglycosides with structural motifs that cannot be accommodated by AMEs but can still bind to the targeted site on rRNA.[4,5] Most aminoglycosides exert their antibacterial activity by binding selectively to the A-site decoding region of the 16S rRNA and disrupting the functions that are vital to bacteria. Although such modification strategies may lead to the development of novel broad-spectrum antibiotics, X-ray structural and enzymatic studies suggest that higher concentrations of AMEs as compared with that of rRNA, and the substrate promiscuity of AMEs, could limit the success of this approach.[6]

Recently, we discovered that structural modifications of aminoglycosides may alter the traditional mode of action of aminoglycosides and may lead to revived activities against resistant bacteria.[7] Encouraged by these findings and prompted by an article that reported a similar discovery,[8] we conducted further syntheses of derivatives on the basis of the leads to reveal structure–activity relationships (SAR). In an effort to gain more insight into possible modes of action, we also investigated the use of these new aminoglycosides in combination with other clinically used antibiotics with known modes of action.

## RESULTS

### Chemistry

We have demonstrated that neomycin derivatives bearing linear acyl groups at the 5″ position display unusual antibacterial activities. Three additional derivatives with acyl groups of various chain lengths (C7, C16 and C18) were synthesized (Scheme 1). Although the derivative with a heptanoyl group (**4a**)[7] maintains its traditional antibacterial profile, derivatives with a hexadecanoyl group from palmitic acid (C16, **4e**)[7] and an octadecanoyl group from stearic acid (C18, **4f**)[7] manifest unexpected activity against methicillin-resistant *Staphylococcus aureus* (MRSA) and vancomycin-resistant enterococci (VRE). MRSA strains harbor genes that encode APH(3′), ANT(4′) and AAC(6′)/APH(2″), which render the bacteria resistant to various aminoglycosides, such as gentamicin and tobramycin.[9] VRE contains *vanB*-, *ant(6)-I*- and *aac(6′)-aph(2″)*-resistance genes with high levels of resistance to aminoglycosides and vancomycin.[10,11] The *vanB* gene and other genes encode for proteins that produce abnormal D-Ala-D-Lac terminal ends of peptidoglycan precursors.[12] Vancomycin binds to D-Ala-D-Lac with a much lower affinity than does the normal D-Ala-D-Ala, allowing the bacteria to become resistant to vancomycin. As both MRSA and VRE are known to possess high levels of resistance against traditional aminoglycosides,[10,9,13] we decided to further explore SAR with regard to the linear acyl groups by synthesizing **4b**, **4c** and **4d** with a C10 (decanoyl), C12 (dodecanoyl) and C14 (tetradecanoyl) chain length, respectively. The synthesis of these 5″-acylated neomycin derivatives proceeded through the reported method using neomycin B as the starting material (Scheme 1).[7]

[1]Department of Chemistry and Biochemistry, Utah State University, Logan, UT, USA and [2]Department of Biology, Utah State University, Logan, UT, USA and [3]Allosterix Pharmaceuticals, LLC, Providence, UT, USA
Correspondence: Professor C-WT Chang, Department of Chemistry and Biochemistry, Utah State University, 0300 Old Main, Logan, UT 84322-0300, USA.
E-mail: tom.chang@usu.edu
Received 11 April 2009; revised 29 June 2009; accepted 30 June 2009; published online 24 July 2009

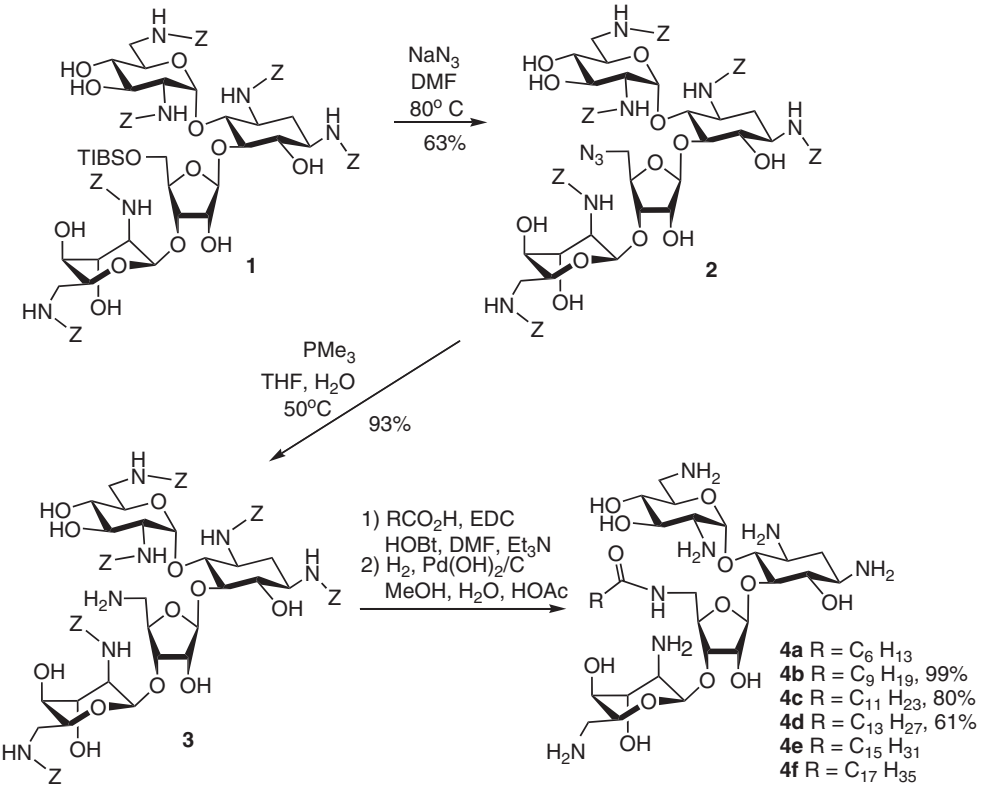


**Scheme 1** Synthesis of neomycin derivatives.

**Table 1 MIC of the 5″-modified neomycin derivatives[a]**

| | *Antibiotic-susceptible strains* | | | | *Antibiotic-resistant strains* | | | |
|---|---|---|---|---|---|---|---|---|
| *Compounds* | *E. coli ATCC 25922* | *S. aureus ATCC 25923* | *K. pneumoniae ATCC13883* | *S. aureus ATCC 33591 (MRSA)* | *K. pneumoniae ATCC 700603* | *P. aeruginosa ATCC 27853* | *E. faecalis ATCC 29212* | *E. faecalis ATCC51299 (VRE)* |
| Neomycin B | 4 | 1 | 4 | 125 | 16–32 | 64 | 64–125 | ⩾250 |
| Amikacin | 1 | 1 | 1 | 8–16 | 0.5 | 0.5–1 | 32–64 | ⩾250 |
| Vancomycin | 125–250 | 0.5–1 | ⩾250 | 1 | ND | ⩾250 | 1–2 | 125 |
| **4a** | 16 | 2–4 | 16–32 | 125 | 32–64 | ⩾250 | 32–64 | ⩾250 |
| **4b** | 32 | 16 | 64–125 | 125–250 | 125 | 16–32 | 32–64 | 64–125 |
| **4c** | 16–32 | 8–16 | 64–125 | 16–32 | 64–125 | 16 | 8–16 | 64–125 |
| **4d** | 8–16 | 2–4 | 64 | 4–8 | 32–64 | 8 | 2–4 | 8–16 |
| **4e** | 4–8 | 1–2 | 8–16 | 2–4 | 16–32 | 4 | 2–4 | 4 |
| **4f** | 4–8 | 2–4 | 8–16 | 2–4 | 32 | 8–16 | 4–8 | 8–16 |

[a]Unit: μg ml$^{-1}$, ND, not determined.

After the protection of amino groups of neomycin B with a carbobenzyloxy (Cbz or Z) group, 5″-OH was selectively substituted by compound **1**[14] with azide, forming compound **2**. After the Staudinger reduction of azide, compound **3**[7] with 5″-$NH_2$ was used and coupled with desired carboxylic acids, leading to the preparation of desired neomycin derivatives.

## Biological testing

The synthesized aminoglycosides were assayed against both Gram-positive (G+) and Gram-negative (G−) susceptible and resistant bacterial strains using neomycin B, amikacin and vancomycin as controls. Aminoglycoside-susceptible *Escherichia coli* (G−, ATCC 25922) and *S. aureus* (G+, ATCC 25923) were used as standard reference strains. Also used were *Klebsiella. pneumoniae* (G−, ATCC 13883) resistant to ampicillin but susceptible to aminoglycosides, *Pseudomonas. aeruginosa* (G−, ATCC 27853), which expresses APH(3′)-IIb and manifests a modest resistance toward aminoglycosides,[15] MRSA (ATCC 33591), *Enterococcus faecalis* (G+, ATCC51299, VRE) and an *E. faecalis* strain (ATCC 29212), which is susceptible to vancomycin but moderately resistant to aminoglycosides. The minimum inhibitory concentrations (MICs) are summarized in Table 1.

From the MIC values, the 5″-acylated neomycin derivatives are found to be generally more active against G+ bacteria than against G− bacteria. When comparing the antibacterial activity of each compound, compound **4a** showed a similar MIC profile as neomycin, although it was four- to eightfold less active than neomycin against aminoglycoside-susceptible strains, although inactive against aminoglycoside-resistant strains. Increasing the acyl chain length from heptanoyl (**4a**) to decanoyl (**4b**) led to a decrease in antibacterial activity: 8- to16-fold less active than neomycin against aminoglycoside-susceptible strains and inactive against aminoglycoside-resistant strains. However, the MIC profile of **4b** remained similar to that of **4a** and neomycin. As the acyl chain length was extended to C14, C16 and C18 (designated **4d**, **4e** and **4f**, respectively), the activities against aminoglycoside-resistant strains increased, which implicates different modes of antibacterial action.

### Quantitative structure–activity relationship analysis

To provide support for our hypothesis of different modes of antibacterial action, we conducted a simple, one-descriptor (logP) quantitative structure–activity relationship (QSAR) analysis. The data set was divided into two groups: results from aminoglycoside-susceptible and results from aminoglycoside-resistant strains (Figures 1 and 2). From the results against susceptible strains, a 'V-shape' relation was obtained instead of a linear, or at least a monotonous relationship. The latter was found in the cases of resistant strains.

### Hemolysis studies

Gram-positive bacteria differ from G− bacteria by the absence of an outer membrane found in the latter with abundant and structurally diverse lipopolysaccharides. Judging from the length of acyl groups and the activity profile of compounds **4d**, **4e** and **4f** with lower MICs against G+ bacteria, we postulate new modes of antibacterial action involving an interaction with bacterial inner membranes. Therefore, one of the concerns of using these newly synthesized compounds as an antibacterial is their potential toxicity to mammalian cells. Thus, we decided to conduct the hemolysis study by using compounds **4e** and **4f** with longer linear acyl chains. From the hemolysis data, it was found that compounds **4e** and **4f** cause an estimated 50% hemolysis at 0.2 and 0.3 mg ml$^{-1}$, respectively (Figure 3).

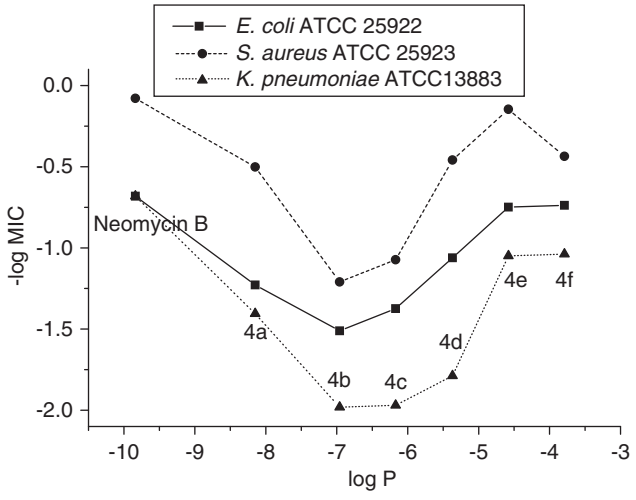


**Figure 1** Quantitative structure–activity relationship (QSAR) analysis of minimum inhibitory concentrations (MICs) from aminoglycoside-susceptible strains.

### Combinational studies

Using a combination of antibiotics is a common practice in the treatment of bacterial infection.[16] Such a practice has the advantages of potentially enhancing the efficacy of treatment, as in the case of synergism, lowering the possibility of inducing drug resistance from microbes and reducing the dose of antibiotics. An example of such synergism is the use of vancomycin (bacterial cell membrane action) in combination with gentamicin, an aminoglycoside.[17] Therefore, we explored the possible use of the new neomycin derivatives in combination with clinically used antibiotics. As **4e** is the most active neomycin derivative, we selected **4e** along with amikacin, neomycin B and vancomycin for combinational antibacterial studies.

We used a checkerboard assay for the antibiotic combinational study.[18] The selected antibiotics were used in combination with the lead, **4e**. The results are summarized in Table 2. The combinational effect can be evaluated on the basis of the fractional inhibitory concentration (FIC) index, which can be calculated on the basis of the following equation:

$$\mathrm{FIC} = [\mathrm{A}]/\mathrm{MICA} + [\mathrm{B}]/\mathrm{MICB}, \text{ synergism} : \mathrm{FIC} = 0.5;$$
$$\text{addition} : \mathrm{FIC} = 0.5 - 1.0; \text{ indifference} :$$
$$\mathrm{FIC} = 1 - 4; \text{ antagonism} : \mathrm{FIC} \geqslant \| 4$$

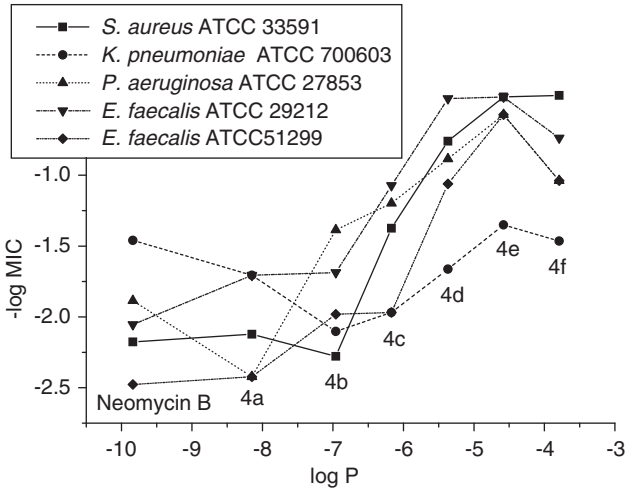


**Figure 2** Quantitative structure–activity relationship (QSAR) analysis of minimum inhibitory concentrations (MICs) from aminoglycoside-resistant strains.

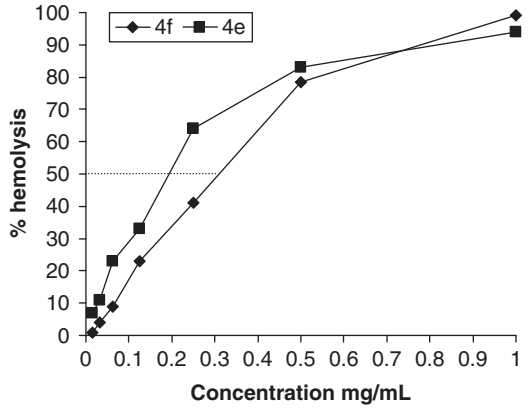


**Figure 3** Hemolysis of **4e** and **4f**.

**Table 2 FIC from combinational studies of 4e**

| *Strains of bacteria* | *Neomycin* | *Amikacin* | *Vancomycin* |
|---|---|---|---|
| *E. coli* ATCC 25922 | 0.27–0.56 (synergism)[a] | 0.38–0.53 (synergism) | ND |
| *S. aureus* ATCC 25923 | ND | 1.0 (addition or indifference) | 0.53–1.5 (addition or indifference) |
| *K. pneumoniae* ATCC 13883 | ND | 0.08–0.16 (synergism) | ND |
| *K. pneumoniae* ATCC 700603 | ND | 0.38–0.53 (synergism) | ND |
| *S. aureus* ATCC 33591 (MRSA) | ND | 0.28–0.53 (synergism) | 0.53–0.56 (addition) |
| *P. aeruginosa* ATCC 27853 | ND | 0.38–0.50 (synergism) | ND |
| *E. faecalis* ATCC 29212 | ND | 0.53–0.56 (addition) | 0.28–0.53 (synergism) |

[a]FIC=[A]/$MIC_A$+[B]/$MIC_B$, synergism: FIC$\leqslant$0.5; addition: FIC=0.5–1.0; indifference: FIC=1–4; antagonism: FIC $\geqslant$4, ND, not determined.

## DISCUSSION

From the relationship between acyl chain length and MIC profile, it seems that when a shorter chain length was incorporated, the derivatives maintain the original mode of antibacterial action as does the parent neomycin (that is, binding to the A-site decoding region of 16S rRNA). The added acyl chain, however, reduces the activity of **4a**, likely because of the steric interference of the acyl group on the binding of the neomycin derivative to rRNA. As the chain length increases, steric hindrance increases, resulting in a further decrease in antibacterial activity. Nevertheless, when even longer acyl chains were incorporated, the derivatives showed significant antibacterial activity with SAR in the order of C16$\approx$C18$>$C14 against both susceptible and resistant strains. As an elevated steric hindrance from these long acyl groups is expected, it is unlikely that compounds **4d**, **4e** and **4f** will regain their antibacterial activity by exerting the same mode of action. Our previous enzymatic and molecular modeling studies also revealed that AMEs can inactivate aminoglycosides with diverse structural motifs.[7] Thus, it is probable that these three neomycin derivatives have different modes of antibacterial action. The activity of **4d**, **4e** and **4f** against enterococci, which are known to be intrinsically resistant against traditional aminoglycosides, also supports this hypothesis.

The results from the QSAR analysis also support our hypothesis that different modes of actions are likely for compounds **4d**, **4e** and **4f** because of the increase in lipophilicity. The compounds presented in the plot of Figure 1 can be roughly divided into two groups: neomycin **4a** (C8) and **4b** (C10) as the first group and compounds **4c** (C12), **4d** (C14), **4e** (C16) and **4f** (C18) as the second group. The linear relationship of the first group suggests that when the sizes of acyl groups are relatively small, compounds **4a** and **4b** still exert the same antibacterial mode of action as that of neomycin. As the sizes of acyl groups increase, the second group shows a different linear relationship with a reverse dependence of the activity on lipophilicity unlike the first group. These two different linear relationships are consistent with our speculation that compounds **4d**, **4e** and **4f** regain their antibacterial activity by exerting different modes of action. The results from Figure 2 also manifest two roughly linear relationships from two groups of compounds as described above. As traditional aminoglycosides are inactive against these resistant bacteria, it is expected to obtain a rather leveling line for the first group. Once again, for the second group, the linear relationship implies a strong connection between the increased lipophilicity and the antibacterial activity.

On the basis of the results of hemolysis studies, the concentrations for 90% hemolysis for both compounds are expected to be higher than 1 mg ml$^{-1}$. Compared with the MIC values of these two compounds (ranging from 2 to 16 $\mu$g ml$^{-1}$), the concentrations that give significant hemolysis are 50- to 500-fold higher. Thus, these neomycin derivatives are not hemolytic at their effective antibacterial concentrations.

According to the FIC index, compound **4e** shows a strong synergistic effect with amikacin and/or neomycin against G− bacteria, including *E. coli*, *K. pneumoniae* and *P. aeruginosa*. As compound **4e** alone is less active against G− bacteria, one possible reason could be that **4e** causes damage to the bacterial membrane and facilitates the entrance of amikacin into bacteria. The synergistic effect with **4e** and amikacin was consistently observed with all G− bacterial strains tested. With G+ bacteria, the synergistic effects with **4e** were inconsistent with the outcomes ranging from synergism to indifference with amikacin and vancomycin. The synergism of amikacin and **4e** against MRSA is of interest. As MRSA is equipped with various AMEs that should drastically reduce the activity of aminoglycosides, including amikacin, the observed synergism is unexpected. The synergism of vancomycin and **4e** against *E. faecali* is difficult to explain. It is possible that the action of **4e** may not interfere with the action of vancomycin, and unlike the combinational effect against G− bacteria, it may depend on individual bacterial strain. The difference in the combinational effect of compound **4e** against G+ and G− could possibly reflect the action of compound **4e** toward inner and outer membranes, respectively.

In conclusion, we have completed the structural optimization of 5″-acylated neomycin derivatives. Interesting antibiotic combinational effects have been revealed. The lead, **4e**, alone has a prominent antibacterial activity against G+ bacteria such as MRSA and VRE. Facing the emergence of vancomycin-resistant *S. aureus*,[19,20] we believe that compound **4e** represents a possible countermeasure against this formidable pathogen. Judging from the data of the QSAR analysis, it is evident that lipophilicity is responsible for the observed antibacterial activity of the lead.

On the basis of the combinational study, compound **4e** will be more effective when used alone against G+ bacteria. Nevertheless, we have shown that it is possible to use **4e** in combination with aminoglycosides against G− bacteria. This finding is consistent with a novel mode of antibacterial action of **4e**. The synergism between **4e** and amikacin against *E. coli* and other G− bacteria may provide a potential application in counteracting food-borne bacterial outbreaks such as those caused by *E. coli* O157 : H7, *Salmonella* spp. and other G− pathogens.

## METHODS

### General experimental procedures

**General procedure for coupling of compound 3 with carboxylic acids.** To a solution of compound **3** (0.20 g, 0.14 mmol) and carboxylic acids (0.28 mmol) in dimethyl formamide (10 ml) and $Et_3N$ (0.04 ml, 0.28 mmol), HOBt (0.030 g, 0.21 mmol) and EDC (0.040 g, 0.21 mmol) were added.[1] The reaction was

stirred at room temperature overnight. After completion of the reaction, the reaction was concentrated and diluted with EtOAc. The organic solution was washed with water, saturated $NaHCO_{3(aq)}$, brine and dried over anhydrous $Na_2SO_4$. After removal of the solvent, followed by a fast gradient column chromatography (eluted from hexane/EtOAc=1/1 to EtOAc/MeOH=9 : 1), the product was usually obtained as a solid, which was subjected to hydrogenation without further purification.

**General procedure for hydrogenation and purification.** The solids from acid/amine coupling reaction (0.1–0.2 mmol) were dissolved in degassed MeOH (9 ml), followed by the addition of 1 ml HOAc : $H_2O$ (1 : 4 ratio) degassed solution. A catalytic amount of $Pd(OH)_2$/C powder was added and the system was well sealed and further degassed. The system was stirred under atmospheric $H_2$ at room temperature for 10 h. The reaction was then quenched by filtering through Celite and the residue was washed with $H_2O$ and the combined solutions were concentrated. The crude product was purified with Amberlite CG50 ($NH_4^+$) eluted with a gradient of $NH_4OH$ solution (0–20%). After collecting the desired fractions and removing the solvent, the product was re-dissolved in water and loaded onto an ion-exchange column packed with Dowex 1X8-200 (Sigma-Aldrich, St Louis, MO, USA) ($Cl^-$ form) and eluted with water. After removal of the solvent, the product was obtained as a white solid.

**5″-Deoxy-5″-decanamidoneomycin B (4b).** $^1$H NMR ($D_2O$, 300 MHz) $\delta$ 5.87. (d, $J$=5.0 Hz, 1H), 5.32 (d, $J$=4.1 Hz, 1H), 5.18 (d, $J$=1.7 Hz, 1H), 4.35 (t, $J$=5.2 Hz, 1H), 4.1–4.2 (m, 4H), 3.9–4.0 (m, 3H), 3.6–3.7 (m, 2H), 3.2–3.6 (m, 12H), 2.40 (dt, $J$=12.4 Hz, $J$=4.1 Hz, 1H), 2.18 (t, $J$=7.2 Hz, 2H), 1.8 (m, 1H), 1.5 (m, 2H), 1.1 (m, 12H), 0.72 (t, $J$=6.5 Hz, 3H); $^{13}$C NMR ($D_2O$, 75 MHz) $\delta$ 178.0, 109.1, 95.7, 94.9, 84.8, 80.7, 77.3, 75.0, 73.5, 72.3, 70.5, 70.2, 69.8, 68.1, 67.6, 67.4, 53.3, 50.9, 49.6, 48.6, 41.1, 40.6, 40.1, 36.0, 31.2, 28.7, 28.5 (2 carbons), 28.4, 28.0, 25.5, 22.1, 13.5; ESI/APCI Calcd for $C_{33}H_{66}N_7O_{13}^+$ ([M+H]$^+$) *m/e* 768.4713; measure *m/e* 768.4698.

**5″-Deoxy-5″-dodecanamidoneomycin B (4c).** $^1$H NMR ($D_2O$, 300 MHz) $\delta$ 5.86. (d, $J$=4.1 Hz, 1H), 5.31 (d, $J$=4.1 Hz, 1H), 5.18 (d, $J$=1.4 Hz, 1H), 4.34 (t, $J$=4.8 Hz, 1H), 4.1–4.2 (m, 4H), 3.9–4.0 (m, 3H), 3.6–3.7 (m, 2H), 3.2–3.6 (m, 12H), 2.40 (dt, $J$=8.2 Hz, $J$=4.1 Hz, 1H), 2.16 (t, $J$=7.2 Hz, 2H), 1.9 (m, 1H), 1.5 (m, 2H), 1.1 (m, 16H), 0.72 (t, $J$=6.5 Hz, 3H); $^{13}$C NMR ($D_2O$, 75 MHz) $\delta$ 177.9, 109.2, 95.7, 94.9, 84.8, 80.7, 77.3, 75.0, 73.5, 72.3, 70.5, 70.2, 69.8, 68.1, 67.6, 67.4, 53.3, 50.8, 49.6, 48.6, 41.1, 40.5, 40.1, 36.0, 31.2, 28.8 (2 carbons), 28.7, 28.6, 28.5, 28.4, 28.0, 25.5, 22.1, 13.5; ESI/APCI Calcd for $C_{35}H_{70}N_7O_{13}^+$ ([M+H]$^+$) *m/e* 796.5026; measure *m/e* 796.5016.

**5″-Deoxy-5″-tetradecanamidoneomycin B (4d).** $^1$H NMR ($D_2O$, 300 MHz) $\delta$ 5.86. (d, $J$=3.8 Hz, 1H), 5.31 (d, $J$=4.1 Hz, 1H), 5.18 (d, $J$=1.7 Hz, 1H), 4.34 (t, $J$=5.2 Hz, 1H), 4.1–4.2 (m, 4H), 3.9–4.0 (m, 3H), 3.6–3.7 (m, 2H), 3.2–3.6 (m, 12H), 2.40 (dt, $J$=12.4 Hz, $J$=4.1 Hz, 1H), 2.17 (t, $J$=7.2 Hz, 2H), 1.8 (m, 1H), 1.5 (m, 2H), 1.1 (m, 20H), 0.72 (t, $J$=6.5 Hz, 3H); $^{13}$C NMR ($D_2O$, 75 MHz) $\delta$ 178.0, 109.1, 95.7, 94.9, 84.8, 80.7, 77.3, 75.0, 73.5, 72.3, 70.5, 70.2, 69.8, 68.1, 67.6, 67.4, 53.3, 50.8, 49.6, 48.6, 41.1, 40.6, 40.1, 36.0, 31.2, 28.9 (2 carbons), 28.8 (2 carbons), 28.7, 28.6, 28.5, 28.4, 28.0, 25.5, 22.1, 13.5; ESI/APCI Calcd for $C_{37}H_{74}N_7O_{13}^+$ ([M+H]$^+$) *m/e* 824.5339; measure *m/e* 824.5333.

### Minimum inhibitory concentration determinations

A solution of selected bacteria was inoculated into trypticase soy broth at 35 °C for 1–2 h.[21] The absorbance at 625 nm was measured and diluted with broth, if necessary, to an absorbance of 0.08–0.1. The adjusted inoculated medium (100 µl) was diluted with 10 ml broth and then applied to a 96-well microtiter plate(50 µl). A series of solutions (50 µl each in twofold dilution) of the tested compounds were added to the testing wells. The 96-well plate was incubated at 35 °C for 12–18 h. MIC is defined as the lowest concentration of compound needed to inhibit the growth of bacteria. Determinations were repeated at least three times.

### Quantitative structure–activity relationship analysis

Minimum inhibitory concentrations presented in Table 1 have been recalculated to molar concentrations (µM). MICs represented as ranges in Table 1 (for example, '16–32') were calculated as arithmetic means of these values. Log P (logarithm of the partition coefficient octanol/water) values for neomycin B and for each of the new compounds were calculated using the HyperChem 7.0 package (HyperCube, Inc., Gainesville, FL, USA), with atomic charges being calculated using the AM1 semi-empirical method.

### Combinational study

A block of 6×6 wells on a 96-well microtiter plate was created with a twofold serial dilution of **4e** and the selected antibiotic to locate the optimal range of inhibitory concentrations. Thereafter, a block of 8×8 wells on a 96-well microtiter plate with a twofold serial dilution of **4e** and the selected antibiotic was created to study the combinational studies. For each compound, there was a row or column with only one compound so that MIC could be determined. FIC index was calculated using the following equation: $FIC=[A]/MIC_A+[B]/MIC_B$. The combinational effect was defined as synergism: $FIC \leqslant 0.5$; addition: FIC=0.5–1.0; indifference: FIC=1–4; antagonism: $FIC \geqslant 4$. The procedure for every combination of compound **4e** and selected antibiotic was repeated two to four times.

### Hemolytic activity

Hemolytic activity was determined using methods described by Dartois *et al.*[22] and Sorensen *et al.*[23] with modification. Sheep erythrocytes were used to test hemolytic activities of **4e** and **5f**. Sheep red blood cells (RBCs) were obtained by centrifuging whole blood at 1000×*g*, washed four times with phosphate-buffered saline (PBS) and resuspended in PBS to a final concentration of $10^8$ erythrocytes per ml. The RBC suspension (80 µl) was added to each well containing different concentrations of **4e** and **5f** (20 µl). The plate was incubated at 37°C for 60 min. Wells with added deionized water and Triton X-100 (1%, w/v) served as negative (blank) and positive controls, respectively. The percentage of hemolysis was calculated using the following equation:

$$\%\,\text{hemolysis} = [(\text{absorbance of sample}) - (\text{absorbance of blank})] \times 100/(\text{absorbance of positive control}).$$

### Supplementary data

Spectroscopic information for the synthesized compounds can be found in the supplementary information in the online version.

## ACKNOWLEDGEMENTS

We acknowledge the National Institutes of Health (AI053138) for financial support.

1 Umezawa, S & Tsuchiya, T. in *Aminoglycoside Antibiotics* (eds Umezawa, H. & Hooper, I. R.) 37–110 (Springer-Verlag, New York, 1982).
2 Haddad, J., Kotra, L. P. & Mobashery, S. in *Glycochemistry Principles, Synthesis, and Applications* (eds Wang, P. G. & Bertozzi, C. R.) 353–424 (Marcel Dekker Inc., New York/Basel, 2001).
3 Wang, J. & Chang, C.-W. T. in *Aminoglycoside Antibiotics* (ed. Arya, D. P.) 141–180 (John Wiley & Sons, Inc., 2007).
4 Wang, J. *et al.* Glycodiversification for optimization of the kanamycin class aminoglycosides. *J. Med. Chem.* **48,** 6271–6285 (2005).
5 Li, J., Chiang, F.-I., Chen, H.-N. & Chang, C.-W. T. Investigation of the regioselectivity for Staudinger reaction and its application for the synthesis of aminoglycosides with N-1 modification. *J. Org. Chem.* **72,** 4055–4066 (2007).
6 Fong, D. H. & Berghuis, A. M. Substrate promiscuity of an aminoglycoside antibiotic resistance enzyme via target mimicry. *EMBO J.* **21,** 2323–2331 (2002).
7 Zhang, J. *et al.* Surprising alteration of antibacterial activity of 5″-modified neomycin against resistant bacteria. *J. Med. Chem.* **51,** 7563–7573 (2008).
8 Bera, S., Zhanel, G. G. & Schweizer, F. Design, synthesis, and antibacterial activities of neomycin-lipid conjugates: polycationic lipids with potent Gram-positive activity. *J. Med. Chem.* **51,** 6160–6164 (2008).
9 Ida, T. *et al.* Identification of aminoglycoside-modifying enzymes by susceptibility testing: epidemiology of methicillin-resistant *Staphylococcus aureus* in Japan. *J. Clin. Microbiol.* **39,** 3115–3121 (2001).
10 Swenson, J. M. *et al.* Molecular characterization and multilaboratory evaluation of *Enterococcus faecalis ATCC 51299* for quality control of screening tests for vancomycin and high-level aminoglycoside resistance in Enterococci. *J. Clin. Microbiol.* **33,** 3019–3021 (1995).

11 Cetinkaya, Y., Falk, P. & Mayhall, C. G. Vancomycin-resistant enterococci. *Clin. Microbiol. Rev.* **13,** 686–707 (2000).
12 Barna, J. C. J. & Williams, D. H. The structure and mode of action of glycopeptide antibiotics of the vancomycin group. *Ann. Rev. Microbiol.* **38,** 339–357 (1984).
13 Fridkin, S. K. *et al.* Monitoring antimicrobial use and resistance: comparison with a national benchmark on reducing vancomycin use and vancomycin-resistant enterococci. *Emerg. Infect. Dis.* **8,** 702–707 (2002).
14 Kling, D., Hesek, D., Shi, Q. & Mobashery, S. Design and synthesis of a structurally constrained aminoglycoside. *J. Org. Chem.* **72,** 5450–5453 (2007).
15 Hachiler, H., Santanam, P. & Kayser, F. H. Sequence and characterization of a novel chromosomal aminoglycoside phosphotransferase gene, aph (3′)-IIb, in *Pseudomonas aeruginosa. Antimicrob. Agents Chemother.* **40,** 1254–1256 (1996).
16 Neu, H. C. & Gootz, T. D. in *Medical Microbiology* (ed. Baron, S.) 4th edn. 183–185 (The University of Texas Medical Branch at Galvaston, 1996).
17 Cottagnoud, P., Cottagnoud, M. & Täuber, M. G. Vancomycin acts synergistically with gentamicin against penicillin-resistant pneumococci by increasing the intracellular penetration of gentamicin. *Antimicrob. Agents Chemother.* **40,** 144–147 (2003).
18 Eliopoulos, G. M. & Moellering, R. C. Jr. in *Antibiotics in Laboratory Medicine* (ed. Lorian, V.) 330–396 (Williams & Wikins, New York, 1996).
19 Zhu, W. *et al.* Vancomycin-resistant *Staphylococcus aureus* isolates associated with Inc18-Like *vanA* plasmids in Michigan. *Antimicrob. Agents Chemother.* **52,** 452–457 (2008).
20 Tenover, F. C. *et al.* Vancomycin-resistant *Staphylococcus aureus* isolate from a patient in pennsylvania. *Antimicrob. Agents Chemother.* **48,** 275–280 (2004).
21 The procedure was modified from *Methods for Dilution Antimicrobial Susceptibility Testing for Bacteria that Grow Aerobically* Approved standard M7-A5, and Performance Standards for Antimicrobial Disk Susceptibility Tests. Approved standard M2-A7, National Committee for Clinical Laboratory Standards, Wayne, PA.
22 Dartois, V. *et al.* Systemic antibacterial activity of novel synthetic cyclic peptides. *Antimicrob. Agents Chemother.* **49,** 3302–3310 (2005).
23 Sorensen, K. N., Kim, K. H. & Takemoto, J. Y. *In vitro* antifungal and fungicidal activities and erythrocyte toxicities of cyclic lipodepsinonapeptides produced by Pseudomonas syringae pv. Syringae. *Antimicrob. Agents Chemother.* **40,** 2710–2713 (1996).

Supplementary Information accompanies the paper on The Journal of Antibiotics website (http://www.nature.com/ja)

The Journal of Antibiotics (2009) 62, 545–549

www.nature.com/ja

ORIGINAL ARTICLE

# Haplofungins, novel inositol phosphorylceramide synthase inhibitors, from *Lauriomyces bellulus* SANK 26899 I. Taxonomy, fermentation, isolation and biological activities

Takashi Ohnuki[1], Tatsuya Yano[2], Yasunori Ono[1], Shiho Kozuma[3], Toshihiro Suzuki[4], Yasumasa Ogawa[4] and Toshio Takatsu[1]

**In the course of screening for antifungal agents, we have discovered eight novel compounds, haplofungin A, B, C, D, E, F, G and H, from a culture broth of the fungus strain *Lauriomyces bellulus* SANK 26899. Haplofungins are composed of an arabinonic acid moiety linked through an ester to a modified long alkyl chain and show potent inhibitory activities against fungal inositol phosphorylceramide (IPC) synthase. Haplofungin A inhibited the activity of IPC synthase from *Saccharomyces cerevisiae* with an $IC_{50}$ value of 0.0015 μg ml$^{-1}$. This inhibitor also suppressed the growth of *Candida glabrata* at the MIC value of 0.5 μg ml$^{-1}$.**
*The Journal of Antibiotics* (2009) **62,** 545–549; doi:10.1038/ja.2009.72; published online 31 July 2009

**Keywords:** antifungal; haplofungin; inhibitor; inositol phosphorylceramide synthase; sphingolipid

## INTRODUCTION

Opportunistic invasive fungal infections are a major cause of morbidity and mortality in cancer and immunocompromised patients. The frequency of such fungal infections is on the rise year after year.[1] Moreover, the increase in aspergillosis and azole -resistant candidiasis makes chemotherapy difficult.[2] Therefore, the discovery of antifungal agents having new mechanisms of action is anticipated.

Glycosphingolipid (GSL) is composed of a hydrophilic sugar chain and a ceramide that consists of hydrophobic sphingosine and fatty acid. In the animal kingdom, GSL is known to take part in a variety of life phenomena, such as cell differentiation and proliferation, organ formation, programmed cell death, etc.[3] Similar to plants, the core structure of GSL in yeast and filamentous fungi consists of inositol-phosphoceramide (IPC) in which phosphatidylinositol is linked to phytoceramide, and is quite different from that of mammalian GSL.[4] It is therefore suggested that IPC synthase, an enzyme that synthesizes fungal-specific IPC from phytoceramide and phosphatidylinositol, is a novel target for antifungal drugs.[5] Aureobasidin A,[6] rustmicin[7,8] and khafrefungin[9] have been reported to inhibit IPC synthase, and also to suppress the growth of clinically important fungi such as *Saccharomyces cerevisiae*, *Candida albicans* and *Cryptococcus neoformans*. Recently, pleofungins were also reported by our group to be IPC synthase inhibitors. It is noteworthy that they suppressed the growth of *Aspergillus fumigatus* at the MIC value of 0.5 μg ml$^{-1}$, in addition to the pathogenic fungi described above.[10] From these results, the screening of IPC synthase inhibitors was suggested to be one of the most efficient ways to discover a novel broad-spectrum fungicide that has potent antifungal activities.

During the course of our continuous screening, novel fungicides named haplofungin A, B, C, D, E, F, G and H (Figure 1) were discovered from a culture broth of the fungus *Lauriomyces bellulus* SANK 26899. (These compounds showed potent inhibitory activities against the IPC synthase from *S. cerevisiae*.) In this paper, we report the taxonomy and fermentation of the producing fungus, as well as the isolation and biological properties of haplofungins. The structure determination and stereochemistry of haplofungins will be reported in succeeding papers.

## RESULTS

### Taxonomy of the producing organism

The producing microorganism, *Lauriomyces bellulus* Crous & MJ Wingf.[11] SANK 26899, was isolated from a soil sample collected in Ohota-shi, Shimane Prefecture, Japan.

Colonies on modified Weitzman and Silva-Hutner[11] agar attained 21–22 mm in diameter in 7 days at 23 °C, plane (Figure 2). They were composed of a thin mycelia layer, white, sparse with sporulation toward the center and entire margins. Exudates and sclerotia were not observed. The mycelia were immersed and superficial, septate,

[1]Exploratory Research Laboratories I, Daiichi Sankyo Co. Ltd., 1-2-58 Hiromachi, Shinagawa-ku, Tokyo, Japan; [2]Biological Research Laboratories II, Daiichi Sankyo Co. Ltd., 1-2-58 Hiromachi, Shinagawa-ku, Tokyo, Japan; [3]Exploratory Research Laboratories II, Daiichi Sankyo Co. Ltd., 1-16-13, Kitakasai, Edogawa-ku, Tokyo, Japan and [4]Process Development Laboratories, Daiichi Sankyo Co. Ltd., 389-4 Shimokawa Otsurugi, Izumimachi, Iwaki-shi, Fukushima, Japan
Correspondence: T Ohnuki, Exploratory Research Laboratories I, Daiichi Sankyo Co. Ltd., 1-2-58 Hiromachi, Shinagawa-ku, Tokyo 140-8710, Japan.
E-mail: ohnuki.takashi.eh@daiichisankyo.co.jp
Received 25 April 2009; revised 8 June 2009; accepted 18 June 2009; published online 31 July 2009

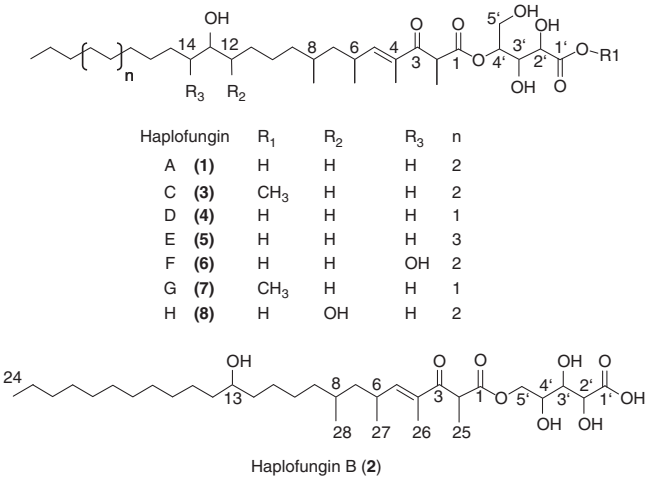


**Figure 1** Structures of haplofungins.

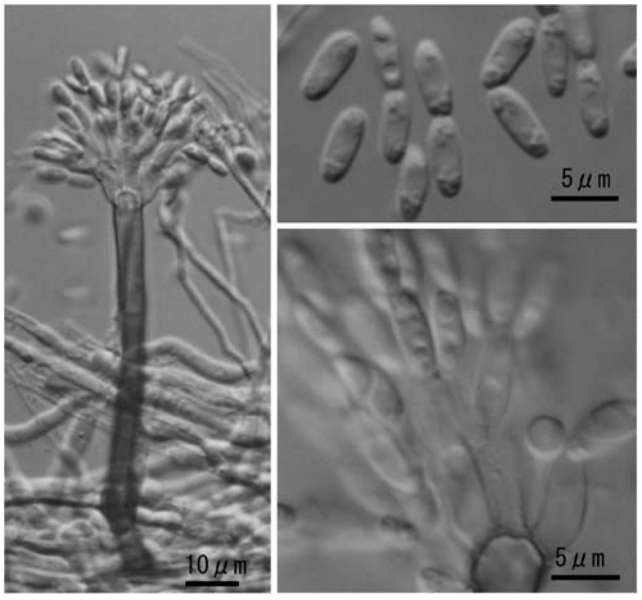


**Figure 2** Microscopic characterisitics of *Lauriomyces bellulus* SANK 26899.

branched, smooth and hyaline, becoming brown near the conidiophores or setae. Setae were 440–650 μm long, 4–6 μm wide at the base, simple, solitary, erect, straight or curved, smooth, septate, dark brown and thick-walled, becoming tapered and light brown toward the apex. The conidiophores were 45–105 μm long, 4–6 μm wide, macronematous, mononematous, simple, solitary, erect, straight or curved, smooth, septate, dark brown and thick-walled at the base, becoming thin-walled and light brown toward the apex. The sporogenous apparatus was complex, consisting of a series of branches or conidiogenous cells arising from the stipe apex. The primary branches were 5–9 μm long, 3.5–5 μm wide, thin-walled, smooth and hyaline. The subsequent branches were hyaline and produced branches or conidia. The ramoconidia were 6–9×2–3 μm, holoblastic, catenate, in acropetal branches or unbranched chains, aseptate, smooth, thin-walled, cylindrical to ellipsoidal, rarely curved, with flattened budding scars at both ends and hyaline.

In our previous patent application document,[12] we reported that the producing strain had been identified as the fungus *Haplographium*

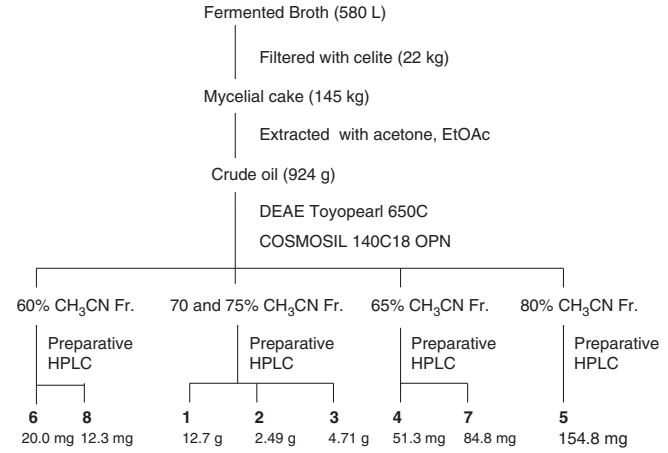


**Figure 3** Isolation procedure for haplofungins.

*heliocephalum* V Rao and de Hoog SANK 26899, according to the description by Zucconi and Pagano[13] and Rao and de Hoog,[14] but *H. heliocephalum* was treated as a synonym of *L. heliocephalus* (Rao and de Hoog) Castañeda and Kendrick.[11] In the course of establishing the genus *Lauriomyces* RF Castañeda, Castañeda and Kendrick[11] recognized four species of *Lauriomyces*, with one of them being reported as *L. heliocephalus*. Subsequently, Crous and Wingfield added *L. bellulus* to the genus *Lauriomyces*, which resembles *L. heliocephalus*.[15] These two species have similar-sized conidia, but can easily be distinguished from each other by the presence or absence of setae. This producing strain does not have setae and therefore SANK 26899 was identified as *Lauriomyces bellulus* Crous and MJ Wingf.[15] It has been deposited with the International Patent Organism Depositary, National Institute of Advanced Industrial Science and Technology, Japan, under accession No. FERM BP-08506.

**Fermentation**

A seed medium (500 ml) consisting of 3% glycerin, 3% glucose, 2% soluble starch, 1% soybean meal, 0.25% gelatin, 0.25% yeast extract, 0.25% $NH_4NO_3$ and 0.01% CB-442 (pH 7.0) was poured into each of two 2-l Erlenmeyer flasks and sterilized at 121 °C for 30 min. A loopful of the slant culture of the strain, SANK 26899, was inoculated to each medium and cultured on a rotary shaker (210 r.p.m.) at 23 °C for 6 days. A second seed medium (30 l) with the same contents was poured into each of two 60-l jar fermentors and sterilized at 121 °C for 30 min. Then, the first seed culture (5%) was transferred to the fermentors and cultivation was carried out at 23 °C for 2 days. A production medium (300 l), consisting of 8% glycerin, 0.25% gelatin, 1% soybean meal, 0.25% yeast extract, 0.25% $NH_2PO_4$, 0.1% $(NH_4)_2SO_4$ and 0.01% CB-442 (pH 7.0) in each of two 600-l tank fermentors, was sterilized at 121 °C for 30 min. The second seed culture (5%) was transferred to the production medium and fermentation was carried out at 23 °C for 7 days.

**Isolation and purification of haplofungins**

The isolation and purification procedures for haplofungins are shown in Figure 3. The culture broth (580 l) was filtered with Celite 545 (22 kg) as a coadjuvant to separate the supernatant and mycelial cake. The mycelial cake (145 kg) was soaked in acetone (240 l) and filtered. Ethyl acetate (240 l) was added to the extract and subsequently partitioned by the addition of 0.1% phosphoric acid (120 l). The organic layer was washed with a saturated NaCl solution, dried over

anhydrous $Na_2SO_4$ and concentrated *in vacuo* to give brown oil (924 g). The oily substance was dissolved in 100 ml of hexane-ethyl acetate-methanol (1:1:1) and applied to a DEAE Toyopearl 650C column ($AcO^-$ type, 6 l, Tosoh, Tokyo, Japan) equilibrated with ethyl acetate. Further, the column was washed with hexane-ethyl acetate (1:1, 12 l), ethyl acetate (12 l) and methanol (12 l) and the active substance was eluted with methanol—acetic acid (9:1, 12 l). Then, the eluate was concentrated *in vacuo* to dryness and the residue (338 g) was dissolved in 50% aqueous acetonitrile containing 0.1% phosphoric acid. This solution was applied to a COSMOSIL 140C18 OPN column (8 l, Nacalai Tesque, Kyoto, Japan). The chromatography was performed stepwise with 60, 65, 70, 75 and 80% aqueous acetonitrile containing 0.1% phosphoric acid. The eluted fractions were further purified as follows.

*Isolation of haplofungin A (**1**), B (**2**) and C (**3**).* Seventy and seventy-five percent acetonitrile fractions were combined and evaporated *in vacuo* to remove the acetonitrile and extracted with ethyl acetate (500 ml). The organic layer was dried over anhydrous $Na_2SO_4$ and concentrated *in vacuo* to dryness to give a residue. The residue was dissolved in 77% aqueous acetonitrile containing 0.1% phosphoric acid, applied to an ODS HPLC column (YMC-pack ODS-AM, 100×500 mm, YMC, Kyoto, Japan) and chromatographed with 80% aqueous acetonitrile containing 0.1% phosphoric acid to obtain three active fractions. Each of the active fractions was evaporated *in vacuo* to dryness to remove the acetonitrile and was extracted with ethyl acetate. The ethyl acetate layer was dried over anhydrous $Na_2SO_4$ and concentrated *in vacuo* to give haplofungin A (**1**, 12.7 g), B (**2**, 2.49 g) and C (**3**, 4.71 g).

*Isolation of haplofungin D (**4**) and G (**7**).* A 65% acetonitrile fraction was extracted with ethyl acetate. The organic layer was dried over anhydrous $Na_2SO_4$ and concentrated *in vacuo* to dryness. The residue was applied to an ODS HPLC column (Develosil ODS HG-5, 20×150 mm, Nomura Chemical, Aichi, Japan) and chromatographed with 77% aqueous acetonitrile containing 0.1% formic acid. The active fractions were concentrated *in vacuo* and lyophilized to give haplofungin D (**4**, 51.3 mg) and G (**7**, 84.8 mg).

*Isolation of haplofungin E (**5**).* An 80% acetonitrile fraction was extracted with ethyl acetate. The organic layer was dried over anhydrous $Na_2SO_4$ and concentrated to dryness. The residue was applied to an ODS HPLC column (Develosil ODS HG-5, 20×150 mm) and chromatographed with 85% aqueous acetonitrile containing 0.1% phosphoric acid. The active fractions were concentrated *in vacuo* to remove the acetonitrile and extracted with ethyl acetate. The ethyl acetate layer was concentrated *in vacuo* to dryness to give haplofungin E (**5**, 154.8 mg).

*Isolation of haplofungin F (**6**) and H (**8**).* A 60% acetonitrile fraction was evaporated *in vacuo* to remove the acetonitrile and extracted with ethyl acetate. The organic layer was concentrated *in vacuo* and the residue was applied to an ODS HPLC column (YMC-pack ODS-AM, 100×500 mm) and chromatographed with 65% aqueous acetonitrile containing 0.1% phosphoric acid. The active fraction was evaporated *in vacuo* to remove the acetonitrile and extracted with ethyl acetate. The active fraction was re-chromatographed with an ODS HPLC column (μBONDASPHERE, 50×100 mm, Waters, Milford, MA, USA) and eluted with 60% aqueous acetonitrile containing 0.1% phosphoric acid. The active fraction was evaporated *in vacuo* to remove the acetonitrile and extracted with ethyl acetate. The organic layer was dried over anhydrous $Na_2SO_4$ and concentrated to dryness.

**Table 1 Inhibitory activity of haplofungins against IPC synthase prepared from *S. cerevisiae* and *A. fumigatus***

| | $IC_{50}$ (μg/ml) | |
|---|---|---|
| *Compounds* | *S. cerevisiae* | *A. fumigatus* |
| **1** | 0.0015 | 0.25 |
| **2** | 0.025 | 0.8 |
| **3** | 0.010 | 0.5 |
| **4** | 0.054 | 0.6 |
| **5** | 0.0015 | 0.24 |
| **6** | 0.053 | 1.3 |
| **7** | 0.059 | 2 |
| **8** | 0.035 | 0.8 |
| Pleofungin A | 0.04 | 0.0095 |
| Khafrefungin | 0.065 | 0.5 |

The active substances were finally separated by ODS HPLC (Develosil ODS HG-5, 20×150 mm) with 65% aqueous acetonitrile containing 0.1% formic acid. Each of the active fractions was concentrated *in vacuo* and lyophilized to give haplofungin F (**6**, 20.0 mg) and H (**8**, 12.3 mg).

### Biological properties of haplofungins

The inhibitory activities of haplofungins and other inhibitors against IPC synthase prepared from *S. cerevisiae* and *A. fumigatus* are summarized in Table 1. All of the haplofungins inhibited IPC synthases from these fungi. Although **1** and **5** were the most potent compounds with an approximate $IC_{50}$ value of 1.5 ng $ml^{-1}$ against the IPC synthase from *S. cerevisiae*, the other related compounds had less activity. Compound **3**, the methyl ester of **1**, was 6-fold less potent than **1** and the results indicated that $IC_{50}$ was affected by the presence of methyl ester in the aldonate moiety. A similar pattern was observed between **5** and **7**. Compound **7**, the methyl ester derivative of **5**, showed 40-fold less potent inhibitory activity against the enzyme from *S. cerevisiae*. The dihydroxyl analogs, **6** and **8**, had less enzyme inhibitory activity than **1** and the others. Thus, the existence of a hydroxyl group, except at C-13 in the alkyl chain, also reduced the $IC_{50}$ value. The alkyl chain length of haplofungins is a very important factor for inhibitory activity. The $IC_{50}$ values of **1**, **4** and **5** indicate that the IPC synthase inhibitory activity of haplofungins depends on the alkyl chain length. Compound **2**, which has an aldonate moiety attached to the C-1 ester carbonyl groups at C-5′, had less inhibitory activity than **1**. Therefore, the results indicate that an aldonate moiety attached to C-1 at C-4′ is essential for eliciting IPC synthase inhibitory activity.

The *in vitro* antifungal activities of haplofungins and the other compounds are summarized in Table 2. In spite of their potent IPC synthase activities, haplofungins did not display any antifungal activity, except for *C. glabrata*. It is suggested that poor membrane permeability or accessibility to the target enzyme of the compounds may affect antifungal activity.

## DISCUSSION

We isolated novel compounds, haplofungins, and found that these compounds are potent IPC synthase inhibitors. Haplofungins were produced by the fungal strain, SANK 26899, which was identified as *Lauriomyces bellulus*.

As shown in Tables 1 and 2, **1** inhibited IPC synthase activity from *S. cerevisiae* with an $IC_{50}$ value of 1.5 ng $ml^{-1}$ and also suppressed the growth of *C. glabrata* at the MIC value of 0.5 μg $ml^{-1}$.

**Table 2** ***In vitro*** **antifungal activities of haplofungins and other IPC synthase inhibitors**

| | *MIC/MIC$_{80}$ (μg ml$^{-1}$)* | | | | | |
|---|---|---|---|---|---|---|
| *Compounds* | *C. albicans ATCC64550* | *C. parapsilosis ATCC22019* | *C. glabrata ATCC90030* | *C. tropicalis SANK59263* | *Cr. neoformans SANK59863* | *A. fumigatus SANK10662* |
| **1** | >64/>64 | >64/>64 | 0.5/0.25 | >64/>64 | 64/4 | >64/>64 |
| **2** | >64/>64 | >64/>64 | >64/32 | >64/>64 | >64/16 | >64/>64 |
| **3** | >64/>64 | >64/>64 | 64/8 | >64/>64 | 64/8 | >64/>64 |
| **4** | >64/>64 | >64/>64 | 8/4 | >64/>64 | >64/>64 | >64/>64 |
| **5** | >64/>64 | >64/>64 | 0.5/0.25 | >64/>64 | >64/>64 | >64/>64 |
| **6** | >64/>64 | >64/>64 | >64/>64 | >64/>64 | >64/>64 | >64/>64 |
| **7** | >64/>64 | >64/>64 | 4/2 | >64/>64 | >64/>64 | >64/>64 |
| **8** | >64/>64 | >64/>64 | >64/>64 | >64/>64 | >64/>64 | >64/>64 |
| Pleofungin A | 2/1 | 1/0.5 | 0.13–0.25/–[a] | 4/2 | 0.06–0.13/–[a] | 0.5/0.13–0.25 |
| Khafrefungin | >64/>64 | >64/>64 | 2/0.5 | >64/>64 | >64/4 | >64/>64 |
| Aureobasidin A | 0.13/0.06 | 1/0.5 | 1/0.5 | 1 | 1/0.5 | 32/4 |

[a]Not tested.

When the inhibitory activities of these compounds were tested against an enzyme from *A. fumigatus*, they showed 10- to 100-fold less potent activities than in the case of *S. cerevisiae*. In particular, the IPC synthase from *A. fumigatus* was significantly less sensitive to **1** and **5**, with an approximate $IC_{50}$ of 0.25 μg ml$^{-1}$, which is 170-fold less potency.

Khafrefungin was reported as an IPC synthase inhibitor isolated from the culture broth of the strain MF6020 by the Merck Group (Whitehouse Station, NJ, USA).[9] The structure is very similar to haplofungins in terms of the structural components of aldonic acid and a modified alkyl chain. The absolute configuration was determined by total synthesis[16] and the aldonic acid moiety was determined to be an arabinonic acid, the same as haplofungins. As shown in Table 1, Khafrefungin also inhibited IPC synthases from *C. albicans* and *A. fumigatus;* however, the activities were 40-fold less active than **1**. Therefore, it is supposed that the structure of a modified C24 alkyl chain moiety in **1** is essential for potent inhibitory activity against the IPC synthase of *S. cerevisiae*. Pleofungin A[10,17] is a cyclic depsipeptide isolated as an IPC synthase inhibitor. Although this compound showed 26-fold more potent inhibitory activity than **1** against the IPC synthase of *A. fumigatus*, it had lower inhibitory activity than **1** against the IPC synthase of *S. cerevisiae*.[10] It is interesting to note that the inhibitory activities of the two distinct types of inhibitors were greatly different. It has been reported that the homology of IPC synthase genes between filamentous fungi and yeast is low.[18,19] These results indicated that the difference in the affinity to the enzyme of these two types of inhibitors may be affected by the antifungal spectrum.

From the viewpoint of the structure–activity relationship, the inhibitory activities of these compounds against IPC synthase indicated that the free arabinonic acid moiety and modified long alkyl chain with one hydroxyl group at C-13 were suggested to be essential for eliciting IPC synthase inhibitory activity. It might be possible that the core structure of haplofungins mimics the structure of phytoceramide, which is the substrate of IPC synthase. If the antifungal activity is improved by structure modification, there is a possibility that haplofungin-derived compounds may be candidates for more safe and effective antifungal agents.

## MATERIALS AND METHODS

### General experimental procedures

The strain, SANK 26899, was isolated from a soil sample collected in Ohota-Shi, Shimane Prefecture. This strain was used for the production of haplofungins. For determination of the amounts of haplofungins in the culture broth, the samples were analyzed on an 1100 HPLC system (Agilent Technologies, Santa Clara, CA, USA) using a reverse phase column (Cadenza CD-C18, 4.6×75 mm, Imtakt, Kyoto, Japan); flow rate, 0.6 ml min$^{-1}$; mobile phase, a 15-min linear gradient from 65% acetonitrile containing 0.1% phosphoric acid to 95% acetonitrile containing 0.1% phosphoric acid; detection, UV at 230 nm.

### Compounds

Pleofungin A, aureobasidin A and khafrefungin were purified from the original strains of Daiichi-Sankyo (Toyko, Japan). Phosphatidyl inositol was purchased from Sigma-Aldrich (St Louis, MO, USA) and BODIPY-FL-C5-ceramide was purchased from Molecular Probes (Carlsbad, CA, USA).

### IPC synthase assay

The method for measuring the inhibitory activity against IPC synthases was previously described.[10] We used *Saccharomyces cerevisiae* and *Aspergillus fumigatus* as the sources of IPC synthase. Crude IPC synthase of *A. fumigatus* and *S. cerevisiae* was prepared from stationary growing fungal cells cultured in yeast extract–peptone–dextrose medium. To measure the IPC synthase activities *in vitro*, crude enzyme was mixed with BODIPY-FL-C5-ceramide and phosphatidyl inositol. After incubation of the reaction mixtures, BODIPY-labeled IPC was extracted by the addition of solvent mixture (MeOH:diethylether, 41:91) and their fluorescent values were measured (Ex/Em, 505/513).

### Antifungal activities

The minimum inhibitory concentrations were evaluated by the microtiter broth dilution method in RPMI-1640 medium.[20] For the determination of the minimum inhibitory concentrations against *Candida* species and *Cryptococcus neoformans*, cells were diluted into 5.0×10$^3$ CFU/ml in RPMI medium. The cell suspensions (100 μl) were transferred into 96-well microtiter plates. Then, 100 μl of diluted samples with RPMI medium was added to the cell suspensions. After mixing the samples and cell suspensions of *Candida* and *Cryptococcus*, the plates were incubated at 37 °C for 24 and 48 h, respectively. For the minimum inhibitory concentrations against the *Aspergillus* species, cell suspensions (90 μl) were distributed into 96-well microtiter plates and 100 μl of diluted samples and 10 μl of Alamar Blue were further added. Then, the plates were incubated at 26 °C for 72 h and the growth conditions were determined by measuring $OD_{595}$.

1 Müller, J. Epidemiology of deep-seated, domestic mycoses. *Mycoses* **37,** 1–7 (1994).
2 Rex, J. H. & Pfaller, M. A. Resistance of *Candida* species to fluconazole. *Antimicrob. Agents Chemother.* **39,** 1–8 (1995).

3 Dickson, R. C. & Lester, R. L. Sphingolipid functions in *Saccharomyces cerevisiae. Biochim. Biophys. Acta.* **1583,** 13–25 (2002).
4 Dickson, R. C. Sphingolipid functions in *Saccharomyces cerevisiae*: comparison to mammals. *Ann. Rev. Biochem.* **67,** 27–48 (1998).
5 Sugimoto, Y. & Yamada, K. IPC synthase as a useful target for antifungal drugs. *Curr. Drug. Targets. Infect. Disord.* **4,** 311–322 (2004).
6 Takesako, K. *et al.* Biological properties of aureobasidin A, a cyclic depsipeptide antifungal antibiotic. *J. Antibiot.* **46,** 1414–1420 (1993).
7 Takatsu, T. *et al.* Rustmicin, a new macrolide antibiotic active against wheat stem rust fungus. *J. Antibiot.* **38,** 1806–1809 (1985).
8 Mandala, S. M. *et al.* Rustmicin, a potent antifungal agent, inhibits sphingolipid synthesis at inositol phosphoceramide synthase. *J. Biol. Chem.* **273,** 14942–14949 (1998).
9 Mandala, S. M. *et al.* Khafrefungin, a novel inhibitor of sphingolipid synthesis. *J. Biol. Chem.* **272,** 32709–32714 (1997).
10 Yano, T. *et al.* Pleofungins, novel inositol phosphorylceramide synthase inhibitors, from *Phoma sp.* SANK 13899. I. Taxonomy, fermentation, isolation, and biological activities. *J. Antibiot.* **60,** 136–142 (2007).
11 Castañeda, R. F. & Kendrick, B. Conidial fungi from Cuba: 1. *Univ Waterloo Biol Ser* **32,** 21 (1990).
12 Ohnuki, T., Takatsu, T., Yano, T. & Ono, Y. (Sankyo, Co. LTD.), Novel anti fungal compound of F-15949. JP252834, September 10 (2003).
13 Zucconi, L. & Pagano, S. Concerning the generic limits in *Haplographium. Mycotaxon* **66,** 11–18 (1993).
14 Rao, V. & de Hoog, G. S. New or critical Hyphomycetes from India. *Stud. Mycol.* **28,** 1–84 (1986).
15 Crous, P. W. & Wingfield, M. J. *Sporendocladia fumosa* and *Lauriomyces bellulus* sp. nov. from *Castanea* cupules in Switzerland. *Sydowia* **46,** 193–203 (1994).
16 Wakabayashi, T., Mori, K. & Kobayashi, S. Total synthesis and structure elucidation of khafrefungin. *J. Am. Chem. Soc.* **123,** 1372 (2001).
17 Aoyagi, A., Yano, T., Kozuma, S. & Takatsu, T. Pleofungins, novel inositol phosphorylceramide synthase inhibitors, from *Phoma sp.* SANK 13899. II. Structural elucidation. *J. Antibiot.* **60,** 143–152 (2007).
18 Heidler, S. A. & Radding, J. A. Inositol phosphoryl transferase from pathogenic fungi. *Biochem. Biophys. Acta* **1500,** 147–152 (2000).
19 Zhong, W., Jeffries, M. W. & Georgopapadakou, N. H. Inhibition of inositol phosphorylceramide synthase by aureobasidin A in *Candida* and *Aspergillus* Species. *Antimicrob. Agents and Chemother.* **44,** 651–653 (2000).
20 Barchiesi, F., Colombo, A. L., McGough, D. A. & Rinaldi, M. G. Comparative study of broth macrodilution and microdilution techniques for *in vitro* antifungal susceptibility testing of yeasts by using the National Committee for Clinical Laboratory Standards' proposed standard. *J. Clin. Microbiol.* **32,** 2494–2500 (1994).

The Journal of Antibiotics (2009) 62, 551–557

www.nature.com/ja

ORIGINAL ARTICLE

# Haplofungins, new inositol phosphorylceramide synthase inhibitors, from *Lauriomyces bellulus* SANK 26899 II. Structure elucidation

Takashi Ohnuki[1], Tatsuya Yano[2] and Toshio Takatsu[1]

**Eight new inositol phosphorylceramide synthase inhibitors: haplofungin A, B, C, D, E, F, G and H, were discovered in a culture broth of the fungus *Lauriomyces bellulus* SANK 26899. The planar structures for these haplofungins were elucidated by various spectroscopic analyses and a GC/MS analysis of their degradation products. All eight compounds were found to comprise an arabinonic acid moiety linked through an ester bond to a modified long alkyl chain.**
*The Journal of Antibiotics* (2009) **62,** 551–557; doi:10.1038/ja.2009.73; published online 31 July 2009

**Keywords:** antifungal; haplofungin; inhibitor; inositol phosphorylceramide synthase; physicochemical properties; sphingolipid; structure

## INTRODUCTION

In our screening program for new inositol phosphorylceramide (IPC) synthase inhibitors, we discovered eight new compounds named haplofungin A (**1**), B (**2**), C (**3**), D (**4**), E (**5**), F (**6**), G (**7**) and H (**8**) from a culture broth of *Lauriomyces bellulus* SANK 26899 (Figure 1). In the preceding paper,[1] we described the taxonomy of the producing strain and the production, isolation and biological activities of these haplofungins. Here, we report the physicochemical properties and structure elucidation of these haplofungins.

## RESULTS

### Physicochemical properties

The physicochemical properties of **1–8** are summarized in Table 1. These compounds were soluble in methanol, ethyl acetate and dimethylsulfoxide, but were insoluble in water and *n*-hexane. The IR spectra of these compounds showed characteristic absorption bands for hydroxyl (3400 $cm^{-1}$), carbonyl and carboxyl groups (1740–1661 $cm^{-1}$). The similarity of the UV spectra ($\lambda_{max}$ 236–238 nm) of these compounds indicated that they have the same α,β-unsaturated carbonyl system. $^{1}H$ and $^{13}C$ NMR data of haplofungins are summarized in Tables 2 and 3, respectively.

### Structure elucidation of haplofungins

*Structure of 1.* The structure of **1** was established on the basis of the NMR and MS data. The molecular formula of **1** was determined to be $C_{33}H_{60}O_9$ based on high-resolution time-of-flight mass spectrometry (HRTOF-MS), which gave an $(M+Na)^+$ ion at *m/z* 623.4122 (calculated for $C_{33}H_{60}O_9Na$, 623.4135). The $^{13}C$ NMR spectra indicated that **1** contains five methyls, 15 methylenes, one oxygenated methylene, three methines, four oxygenated methines, one $sp^2$ methine, one $sp^2$ quaternary carbon, one carbonyl carbon, one ester carbonyl carbon and one carboxyl carbon. To fulfill the molecular formula of **1**, the presence of four hydroxyl groups was suggested. The presence of a long alkyl chain was readily inferred from a broad equivalent signal resonating from δ 1.26 to δ 1.32, which was observed in the $^{1}H$ NMR spectrum. The connectivity of protons and carbons was established by the heteronuclear single quantum coherence (HSQC) spectrum. Double quantum filtered correlation spectroscopy (DQF COSY) and heteronuclear single quantum coherence homonuclear Hartmann–Hahn spectroscopy (HSQC-HOHAHA) experiments showed the three proton spin systems drawn in bold lines (Figure 2). The first proton spin system was found to be a long alkyl chain moiety from the H-5 olefinic methine through the H-13-oxygenated methine to the terminal methyl at H-24. Two blanched methyl groups (C-27, C-28) connected to the C-6 and C-8 methine carbons at δ 33.0 and δ 32.1 were also included in this system. The second proton spin system consisted of an H-2 methine adjacent to an H-25 methyl. The connectivities of three oxygenated methines (H-2′, H-3′ and H-4′) and one oxygenated methylene (C-5′) were established as the third spin system.

A heteronuclear multiple bond correlation (HMBC) experiment was used to confirm the assignments of above proton spin systems and establish the connectivity between the partial structures constructed above (Figure 2). The H-5 allylic methine proton at δ 6.64, in the first spin system, was assigned at the β-position of α,β-unsaturated carbonyl system by the observation of $^{1}H$–$^{13}C$ long-range correlations

[1]Exploratory Research Laboratories I, Daiichi Sankyo Co. Ltd, Hiromachi, Shinagawa-ku, Tokyo, Japan and [2]Biological Research Laboratories II, Daiichi Sankyo Co. Ltd, Hiromachi, Shinagawa-ku, Tokyo, Japan
Correspondence: T Ohnuki, Exploratory Research Laboratories I, Daiichi Sankyo Co. Ltd, 1-2-58 Hiromachi, Shinagawa-ku, Tokyo 140-8710, Japan.
E-mail: ohnuki.takashi.eh@daiichisankyo.co.jp
Received 25 April 2009; revised 1 July 2009; accepted 7 July 2009; published online 31 July 2009

from the H-5 olefinic proton to C-3 keto carbonyl and C-4 quaternary $sp^2$ carbon. The correlations with the H-26 methyl group at δ 1.80 to C-3, C-4 and C-5 confirmed the assignment of the methyl to be directly attached at C-4. The correlations with the H-25 methyl group to C-2, C-1 ester carbonyl carbon and C-3 keto carbonyl carbon and from the H-2 methine proton at δ 4.47 to C-1, C-3 and C-4 confirmed a 1,3-dicarbonyl-2-methyl system. The configuration of the $\Delta^4$ double bond was determined to be *E* by NOEs observed between the H-26 methyl protons and the other two methyl protons at H-25 and H-27. The presence of an aldonate moiety in **1** was shown by the observation of the $^1H$–$^{13}C$ long-range coupling from oxygenated H-2′ methine proton at δ 4.05 to C-1′ carboxyl carbon in the third spin system. As the long-range correlation with the H-4′-oxygenated methine proton at δ 4.97 to C-1 ester carbonyl carbon was observed in the HMBC experiment, it was shown that the aldonate moiety was connected to the 1,3-dicarbonyl system through an ester bond between C-1 and C-4′.

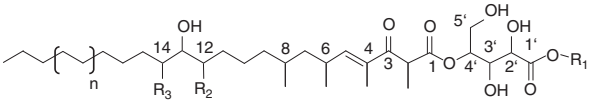

| Haplofungin | $R_1$ | $R_2$ | $R_3$ | n | M.W. |
|---|---|---|---|---|---|
| A (**1**) | H | H | H | 2 | 600 |
| C (**3**) | $CH_3$ | H | H | 2 | 614 |
| D (**4**) | H | H | H | 1 | 572 |
| E (**5**) | H | H | H | 3 | 628 |
| F (**6**) | H | H | OH | 2 | 616 |
| G (**7**) | $CH_3$ | H | H | 1 | 586 |
| H (**8**) | H | OH | H | 2 | 616 |

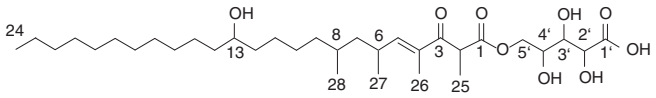

Haplofungin B (**2, M**.W. 600)

**Figure 1** Structures of haplofungins.

To identify the aldonate, **1** was treated with 5% HCl/MeOH and then with *N,O*-bis-(trimethylsilyl)trifluoroacetamide (BSTFA). The reaction mixture was applied to GC/MS directly. The TMS derivative of the aldonate moiety was detected as a peak with a retention time of 12.56 min, which was identical to that of the authentic arabinono-1,4-lactone derivative.

It was thought that it would be possible to determine the length of the alkyl chain and the substituted position of the hydroxyl group by analyzing the EI-MS fragmentation of the keto analog obtained through the decarboxylation at C-1 of the fatty-acid chain because the β-keto acid was unstable under acidic or alkaline conditions when

**Table 1 Physicochemical properties of haplofungins**

| | *1* | *2* | *3* | *4* |
|---|---|---|---|---|
| *Appearance* | *White powder* | *White powder* | *White powder* | *White powder* |
| Molecular weight | 600 | 600 | 614 | 572 |
| Molecular formula | $C_{33}H_{60}O_9$ | $C_{33}H_{60}O_9$ | $C_{34}H_{62}O_9$ | $C_{31}H_{56}O_9$ |
| HR-MS (*m/z*) | | | | |
| Calculated: | 623.4135 | 623.4135 | 637.4291 | 595.3822 |
| Found: | 623.4122 $(M+Na)^+$ [a] | 623.4134 $(M+Na)^+$ [a] | 637.4292 (M+Na)+ [a] | 595.3830 $(M+Na)^+$ [b] |
| UV $\lambda_{max}$ (methanol) nm (ε) | 238 (5,970) | 236 (8,588) | 236 (7,970) | 236 (10,800) |
| IR $\nu_{max}$ (KBr) $cm^{-1}$ | 3407, 3137, 2928, 2856, 1737, 1679, 1449, 1381, 1316, 1213, 1146, 1037, 845, 803, 726 | 3353, 2955, 2919, 2850, 1785, 1737, 1666, 1465, 1456, 1377, 1317, 1283, 1251, 1201, 1131, 1093, 1052 | 428, 2953, 2925, 2854, 2729, 1744, 1663, 1456, 1376, 1251, 1216, 1130, 1073, 1036, 951 | 3408, 2926, 2855, 1740, 1663, 1457, 1377, 1312, 1249, 1201, 1129, 1073, 1040, 968 |
| $[\alpha]_{24}^D$ (methanol) | −20.0° (*c* 2.0) | −33.0° (*c* 1.0) | −58.0° (*c* 1.1) | −38.0° (*c* 1.0) |
| HPLC retention time (min)[c] | 15.2 | 15.6 | 17.4 | 13.5 |
| | *5* | *6* | *7* | *8* |
| *Appearance* | *White powder* | *White powder* | *White powder* | *White powder* |
| Molecular weight | 628 | 616 | 586 | 616 |
| Molecular formula | $C_{35}H_{64}O_9$ | $C_{33}H_{60}O_{10}$ | $C_{32}H_{58}O_9$ | $C_{33}H_{60}O_{10}$ |
| HR-MS (*m/z*) | | | | |
| Calculated: | 651.4448 | 639.4084 | 609.3978 | 661.3903 |
| Found: | 651.4479 $(M+Na)^+$ [a] | 639.4105 $(M+Na)^+$ [b] | 609.4000 $(M+Na)^+$ [b] | 661.3920 $(M+2Na-H)^+$ [b] |
| UV $\lambda_{max}$ (methanol) nm (ε) | 237 (20,000) | 237 (12,000) | 236 (12,500) | 236 (16,300) |
| IR $\nu_{max}$ (KBr) $cm^{-1}$ | 3378, 2956, 2920, 2851, 1739, 1665, 1466, 1457, 1377, 1249, 1215, 1131, 1074, 1040, 967 | 3372, 2924, 2854, 1738, 1661, 1457, 1377, 1314, 1245, 1215, 1127, 1073, 1038, 967 | 3394, 2955, 2928, 2855, 1743, 1161, 1456, 1377, 1216, 1130, 1074, 1037, 952 | 3336, 2954, 2922, 2872, 2853, 1737, 1664, 1458, 1377, 1247, 1213, 1127, 1069, 1042, 947 |
| $[\alpha]_{24}^D$ (methanol) | −28.0° (*c* 0.1) | −50.0° (c 0.1) | −50.0° (*c* 0.1) | −32.0° (*c* 0.1) |
| HPLC retention time (min)[c] | 18.2 | 11.9 | 10.6 | 11.2 |

[a]LC/ESI-TOF MS, liquid chromatography coupled with time of flight mass spectrometry using electrospray ionization.
[b]HRFAB MS, high-resolution fast atom bombardment mass spectrscopy
[c]Condition of HPLC analysis is described in experimental section.

**Table 2 $^{1}$H NMR spectral data of haplofungins**

| | *1* | | *2* | | *3* | | *4* | | *5* | | *6* | | *7* | | *8* | |
|---|---|---|---|---|---|---|---|---|---|---|---|---|---|---|---|---|
| *Carbon no.* | $\delta_H$[a] | *mult., J=Hz* | $\delta_H$[b] | *mult., J=Hz* | $\delta_H$[c] | *mult., J=Hz* | $\delta_H$[a] | *mult., J=Hz* | $\delta_H$[a] | *mult., J=Hz* | $\delta_H$[a] | *mult., J=Hz* | $\delta_H$[a] | *mult., J=Hz* | $\delta_H$[a] | *mult., J=Hz* |
| 2 | 4.47 | 1H, d, 7.1 | 4.56 | 1H, d, 6.9 | 4.42 | 1H, d, 7.0 | 4.47 | 1H, d, 7.1 | 4.47 | 1H, d, 7.1 | 4.47 | 1H, d, 7.1 | 4.47 | 1H, d, 7.1 | 4.47 | 1H, d, 7.1 |
| 5 | 6.64 | 1H, dd, 1.1, 9.3 | 6.77 | 1H, d, 9.4 | 6.61 | 1H, dd, 1.1, 9.3 | 6.64 | 1H, d, 9.3 | 6.64 | 1H, d, 9.6 | 6.64 | 1H, d, 9.5 | 6.64 | 1H, d, 9.6 Hz | 6.64 | 1H, d, 9.3 |
| 6 | 2.77 | 1H, m | 2.70 | 1H, m | 2.64 | 1H, m | 2.75 | 1H, m | 2.76 | 1H, m | 2.76 | 1H, m | 2.78 | 1H, m | 2.77 | 1H, m |
| 7 | 1.32 | 2H, m | 1.22 | 1H, m | 1.17 | 1H, m | 1.33 | 1H, m | 1.34 | 2H, m | 1.25 | 2H, m | 1.25 | 2H, m | 1.32 | 2H, m |
| | | | 1.34 | 1H, m | 1.31 | 1H, m | 1.40 | 1H, m | | | | | | | | |
| 8 | 1.65 | 1H, m | 1.44 | 1H, m | 1.35 | 1H, m | 1.45 | 1H, m | 1.45 | 1H, m | 1.65 | 1H, m | 1.42 | 1H, m | 1.65 | 1H, m |
| 9 | 1.12 | 2H, m | 1.41 | 2H, m | 1.03 | 1H, m | 1.14 | 1H, m | 1.15 | 1H, m | 1.12 | 2H, m | 1.12 | 1H, m | 1.12 | 2H, m |
| | | | | | 1.17 | 1H, m | 1.39 | 1H, m | 1.40 | 1H, m | | | | | | |
| 10 | 1.29 | 2H, m | 1.46 | 2H, m | 1.29 | 2H, m | 1.30 | 2H, m | 1.30 | 2H, m | 1.29 | 2H, m | 1.29 | 2H, m | 1.29 | 2H, m |
| 11 | 1.29 | 2H, m | 1.14 | 1H, m | 1.29 | 2H, m | 1.30 | 2H, m | 1.30 | 2H, m | 1.29 | 2H, m | 1.29 | 2H, m | 1.58 | 2H, m |
| | | | 1.62 | 1H, m | | | | | | | | | | | | |
| 12 | 1.42 | 2H, m | 1.69 | 2H, m | 1.23 | 2H, m | 1.42 | 2H, m | 1.42 | 2H, m | 1.54 | 2H, m | 1.37 | 2H, m | 3.29 | 1H, m |
| 13 | 3.49 | 1H, m | 3.90 | 1H, m | 3.40 | 1H, m | 3.45 | 1H, m | 3.48 | 1H, m | 3.33 | 1H, m | 3.49 | 1H, m | 3.29 | 1H, m |
| 14 | 1.44 | 2H, m | 1.68 | 2H, m | 1.29 | 2H, m | 1.42 | 2H, m | 1.42 | 2H, m | 3.33 | 1H, m | 1.37 | 2H, m | 1.58 | 2H, m |
| 15 | 1.29 | 2H, m | 1.74 | 2H, m | 1.29 | 2H, m | 1.30 | 2H, m | 1.29 | 2H, m | 1.54 | 2H, m | 1.29 | 2H, m | 1.30 | 2H, m |
| 16 | 1.29 | 2H, m | 1.29 | 2H, m | 1.29 | 2H, m | 1.30 | 2H, m | 1.29 | 2H, m | 1.30 | 2H, m | 1.29 | 2H, m | 1.30 | 2H, m |
| 17 | 1.29 | 2H, m | 1.29 | 2H, m | 1.29 | 2H, m | 1.30 | 2H, m | 1.29 | 2H, m | 1.30 | 2H, m | 1.29 | 2H, m | 1.30 | 2H, m |
| 18 | 1.29 | 2H, m | 1.29 | 2H, m | 1.29 | 2H, m | 1.30 | 2H, m | 1.29 | 2H, m | 1.30 | 2H, m | 1.29 | 2H, m | 1.30 | 2H, m |
| 19 | 1.29 | 2H, m | 1.29 | 2H, m | 1.29 | 2H, m | 1.30 | 2H, m | 1.29 | 2H, m | 1.30 | 2H, m | 1.29 | 2H, m | 1.30 | 2H, m |
| 20 | 1.29 | 2H, m | 1.29 | 2H, m | 1.29 | 2H, m | 1.30 | 2H, m | 1.29 | 2H, m | 1.30 | 2H, m | 1.29 | 2H, m | 1.30 | 2H, m |
| 21 | 1.29 | 2H, m | 1.29 | 2H, m | 1.29 | 2H, m | 1.33 | 2H, m | 1.29 | 2H, m | 1.30 | 2H, m | 1.33 | 2H, m | 1.30 | 2H, m |
| 22 | 1.29 | 2H, m | 1.25 | 2H, m | 1.29 | 2H, m | 0.90 | 3H, m | 1.29 | 2H, m | 1.30 | 2H, m | 0.89 | 3H, m | 1.30 | 2H, m |
| 23 | 1.33 | 2H, m | 1.27 | 2H, m | 1.33 | 2H, m | 1.30 | 3H, d, 4.5 | 1.29 | 2H, m | 1.41 | 2H, m | 1.31 | 3H, d, 7.1 | 1.41 | 2H, m |
| 24 | 0.89 | 3H, m | 0.88 | 3H, m | 0.89 | 3H, m | 1.80 | 3H, m | 1.29 | 2H, m | 0.89 | 3H, m | 1.80 | 3H, brs | 0.90 | 3H, m |
| 25 | 1.31 | 3H, m | 1.51 | 3H, d, 6.9 | 1.32 | 3H, m | 1.05 | 3H, d, 6.7 | 1.34 | 2H, m | 1.31 | 3H, d, 7.1 | 1.06 | 3H, d, 6.6 | 1.31 | 3H, d, 7.0 |
| 26 | 1.80 | 3H, d, 1.1 | 1.92 | 3H, brs | 1.80 | 3H, d, 1.1 | 0.91 | 3H, m | 0.89 | 3H, m | 1.80 | 3H, d, 7.2 | 0.91 | 3H, d, 6.3 | 1.81 | 3H, brs |
| 27 | 1.06 | 3H, d, 6.6 | 1.03 | 3H, d, 6.3 | 1.06 | 3H, d, 6.6 | | | 1.30 | 3H, d, 7.1 | 1.05 | 3H, d, 6.0 | | | 1.04 | 3H, d, 6.6 |
| 28 | 0.92 | 3H, m | 0.90 | 3H, m | 0.92 | 3H, m | | | 1.80 | 3H, brs | 0.91 | 3H, d, 7.0 | | | 0.91 | 3H, d, 6.3 |
| 29 | | | | | | | | | 1.31 | 3H, d, 6.7 | | | | | | |
| 30 | | | | | | | | | 0.90 | 3H, m | | | | | | |
| 2′ | 4.05 | 1H, d, 2.3 | 5.46 | 1H, brs | 4.05 | 1H, d, 2.3 | 4.07 | 1H, d, 2.3 | 4.05 | 1H, d, 2.3 | 4.06 | 1H, d, 2.3 | 4.11 | 1H, d, 1.3 | 4.05 | 1H, d, 2.3 |
| 3′ | 4.09 | 1H, dd, 2.5, 9.3 | 4.82 | 1H, m | 4.09 | 1H, dd, 2.3, 9.3 | 4.11 | 1H, dd, 2.3, 9.3 | 4.09 | 1H, dd, 2.3, 9.3 | 4.08 | 1H, dd, 2.3, 9.5 | 4.06 | 1H, dd, 1.3, 9.3 | 4.09 | 1H, dd, 2.3, 9.5 |
| 4′ | 4.97 | 1H, ddd, 1.5, 4.5, 9.3 | 4.83 | 1H, m | 4.97 | 1H, ddd, 1.9, 9.3, 4.5 | 4.98 | 1H, ddd, 1.9, 4.5, 9.3 | 4.97 | 1H, ddd, 1.9, 4.5, 12.1 | 4.97 | 1H, ddd, 2.5, 4.6, 9.5 | 4.98 | 1H, ddd, 2.6, 4.5, 9.3 | 4.97 | 1H, ddd, 1.9, 4.5, 9.3 |
| 5′ | 3.76 | 1H, dd, 1.9, 12.1 | 4.94 | 1H, dd, 5.1, 10.9 | 3.76 | 1H, dd, 1.9, 12.1 | 3.78 | 1H, dd, 4.5, 12.1 | 3.76 | 1H, dd, 1.9, 12.1 | 3.76 | 1H, dd, 4.6 , 12.3 | 3.77 | 1H, dd, 2.6, 12.3 | 3.76 | 1H, dd, 1.9, 12.1 |
| | 3.88 | 1H, dd, 4.5, 12.1 | 5.12 | 1H, dd, 1.9, 10.9 | 3.88 | 1H, dd, 4.5, 12.1 | 3.89 | 1H, dd, 1.9, 12.1 | 3.88 | 1H, dd, 4.5, 12.1 | 3.88 | 1H, dd, 2.5, 12.3 | 3.87 | 1H, dd, 4.5, 12.3 | 3.88 | 1H, dd, 4.5, 12.1 |
| 5′-$OCH_3$ | | | | | 3.63 | 3H, s | | | | | | | 3.75 | 3H, s | | |

[a]Chemical shifts are shown with reference to methanol-$d_4$ as $\delta_H$ 3.31.
[b]Chemical shifts are shown with reference to pyridine-$d_5$ as $\delta_H$ 8.74.
[c]Chemical shifts are shown with reference to dimethylsulfoxide-$d_6$ as $\delta_H$ 2.50.

**Table 3** $^{13}$C NMR spectral data of haplofungins

| | *1* | | *2* | | *3* | | *4* | | *5* | | *6* | | *7* | | *8* | |
|---|---|---|---|---|---|---|---|---|---|---|---|---|---|---|---|---|
| *Carbon no.* | $\delta_C$[a] | *mult.* | $\delta_C$[b] | *mult.* | $\delta_C$[c] | *mult.* | $\delta_C$[a] | *mult.* | $\delta_C$[a] | *mult.* | $\delta_C$[a] | *mult.* | $\delta_C$[a] | *mult.* | $\delta_C$[a] | *mult.* |
| 1 | 172.1 | s | 172.8 | s | 170.2 | s | 172.7 | s | 172.7 | s | 172.6 | s | 175.7 | s | 172.0 | s |
| 2 | 47.6 | d | 49.9 | d | 45.8 | d | 48.2 | d | 48.4 | d | 47.7 | d | 48.2 | d | 47.6 | d |
| 3 | 200.9 | s | 198.6 | s | 197.8 | s | 201.6 | s | 201.5 | s | 201.0 | s | 201.6 | s | 200.9 | s |
| 4 | 135.5 | s | 135.1 | s | 133.4 | s | 136.2 | s | 136.5 | s | 135.9 | s | 136.1 | s | 135.5 | s |
| 5 | 153.3 | d | 151.5 | d | 150.9 | d | 153.9 | d | 153.9 | d | 153.3 | d | 153.9 | d | 153.3 | d |
| 6 | 33.0 | d | 32.2 | d | 31.0 | d | 33.6 | d | 33.6 | d | 33.1 | d | 33.6 | d | 33.0 | d |
| 7 | 45.6 | t | 44.9 | t | 43.6 | t | 46.2 | t | 46.2 | t | 45.6 | t | 46.2 | t | 45.5 | t |
| 8 | 32.1 | d | 31.4 | d | 30.1 | d | 32.7 | d | 32.7 | d | 32.2 | d | 32.7 | d | 32.1 | d |
| 9 | 38.0 | t | 37.7 | t | 36.2 | t | 38.0 | t | 38.0 | t | 38.1 | t | 38.9 | t | 38.2 | t |
| 10 | 28.3 | t | 28.0 | t | 26.5 | t | 29.0 | t | 28.9 | t | 28.4 | t | 28.9 | t | 23.9 | t |
| 11 | 26.9 | t | 27.0 | t | 25.6 | t | 27.9 | t | 27.9 | t | 27.2 | t | 27.9 | t | 34.1 | t |
| 12 | 38.8 | t | 39.0 | t | 37.2 | t | 39.2 | t | 39.2 | t | 33.8 | t | 39.2 | t | 76.1 | d |
| 13 | 75.6 | d | 71.5 | d | 69.5 | d | 73.2 | d | 73.2 | d | 76.2 | d | 73.2 | d | 76.2 | d |
| 14 | 38.6 | t | 39.1 | t | 37.2 | t | 39.1 | t | 39.2 | t | 76.2 | d | 39.1 | t | 33.8 | t |
| 15 | 27.2 | t | 27.3 | t | 25.2 | t | 27.6 | t | 27.6 | t | 33.7 | t | 27.6 | t | 27.2 | t |
| 16 | 30.6 | t | 30.1 | t | 28.8 | t | 31.3 | t | 31.3 | t | 24.0 | t | 31.3 | t | 30.5 | t |
| 17 | 31.0 | t | 30.4 | t | 29.2 | t | 31.7 | t | 31.5 | t | 30.9 | t | 31.5 | t | 30.9 | t |
| 18 | 30.9 | t | 30.6 | t | 29.1 | t | 31.6 | t | 31.5 | t | 30.9 | t | 31.6 | t | 30.9 | t |
| 19 | 30.9 | t | 30.5 | t | 29.1 | t | 31.5 | t | 31.5 | t | 30.9 | t | 31.7 | t | 30.9 | t |
| 20 | 30.9 | t | 30.5 | t | 29.1 | t | 33.9 | t | 31.5 | t | 30.9 | t | 33.9 | t | 30.9 | t |
| 21 | 30.9 | t | 30.8 | t | 29.1 | t | 24.6 | t | 31.5 | t | 30.9 | t | 24.6 | t | 30.9 | t |
| 22 | 33.2 | t | 32.6 | t | 31.3 | t | 15.3 | q | 31.5 | t | 33.3 | t | 12.6 | q | 33.2 | t |
| 23 | 23.9 | t | 23.4 | t | 22.1 | t | 15.6 | q | 31.5 | t | 26.4 | t | 15.6 | q | 24.5 | t |
| 24 | 14.6 | q | 14.8 | q | 14.1 | q | 15.2 | q | 33.9 | t | 14.7 | q | 15.3 | q | 14.6 | q |
| 25 | 15.0 | q | 15.2 | q | 14.0 | q | 20.8 | q | 24.6 | t | 15.0 | q | 20.9 | q | 15.0 | q |
| 26 | 12.0 | q | 12.5 | q | 11.3 | q | 21.2 | q | 15.3 | q | 12.0 | q | 21.2 | q | 12.0 | q |
| 27 | 20.1 | q | 20.3 | q | 19.3 | q | — | | 15.6 | q | 20.2 | q | — | | 20.1 | q |
| 28 | 20.6 | q | 20.6 | q | 19.9 | q | — | | 12.7 | q | 20.6 | q | — | | 20.6 | q |
| 29 | — | | — | | — | | — | | 20.8 | q | — | | — | | — | |
| 30 | — | | — | | — | | — | | 21.2 | q | — | | — | | — | |
| 1′ | 176.7 | s | 178.0 | s | 173.3 | s | 177.4 | s | 177.1 | s | 176.6 | s | 172.6 | s | 176.5 | s |
| 2′ | 71.6 | d | 72.4 | d | 70.4 | d | 72.1 | d | 72.2 | d | 71.6 | d | 72.5 | d | 71.5 | d |
| 3′ | 71.4 | d | 74.5 | d | 69.4 | d | 72.0 | d | 72.0 | d | 71.1 | d | 72.0 | d | 71.3 | d |
| 4′ | 75.5 | d | 70.3 | d | 73.7 | d | 76.1 | d | 76.1 | d | 75.5 | d | 75.8 | d | 75.4 | d |
| 5′ | 61.7 | t | 69.3 | t | 59.3 | t | 62.3 | t | 62.4 | t | 61.7 | t | 62.3 | t | 61.7 | t |
| 5′-OCH3 | — | | — | | 51.6 | q | — | | — | | — | | 49.3 | q | — | |

[a]Chemical shifts are shown with reference to methanol-$d_4$ as $\delta_C$ 49.0.
[b]Chemical shifts are shown with reference to pyridine-$d_6$ as $\delta_C$ 150.4.
[c]Chemical shifts are shown with reference to dimethylsulfoxide-$d_6$ as $\delta_C$ 39.5.

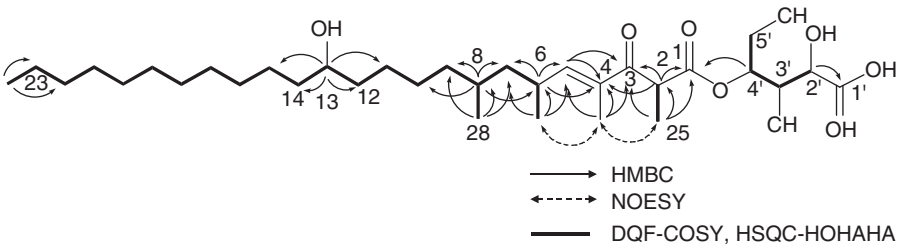


**Figure 2** Selected $^1$H–$^1$H COSY, HMBC and NOE correlations in haplofungin A (**1**).

making hydorolysate of haplofungins. For this purpose, **1** was treated with 5% HCl/MeOH at 105°C for 10 h. The resultant was concentrated *in vacuo* followed by treatment with BSTFA in pyridine for 5 min. Their EI-MS fragment patterns and retention times in the GC/MS analysis are shown in Figure 3 and Table 4. The substituted position of the hydroxyl group was determined by the alkyl chain length from the α-cleavage sites at each side of the hydroxyl group. Fragmentation of the alkyl chain derivative (**1a**) from **1** on EI-MS gave fragments at *m/z* 257 and 325, indicating that the oxidation site is C-13 (Figure 3). From these results, the planar structure of **1** was established as shown in Figure 1.

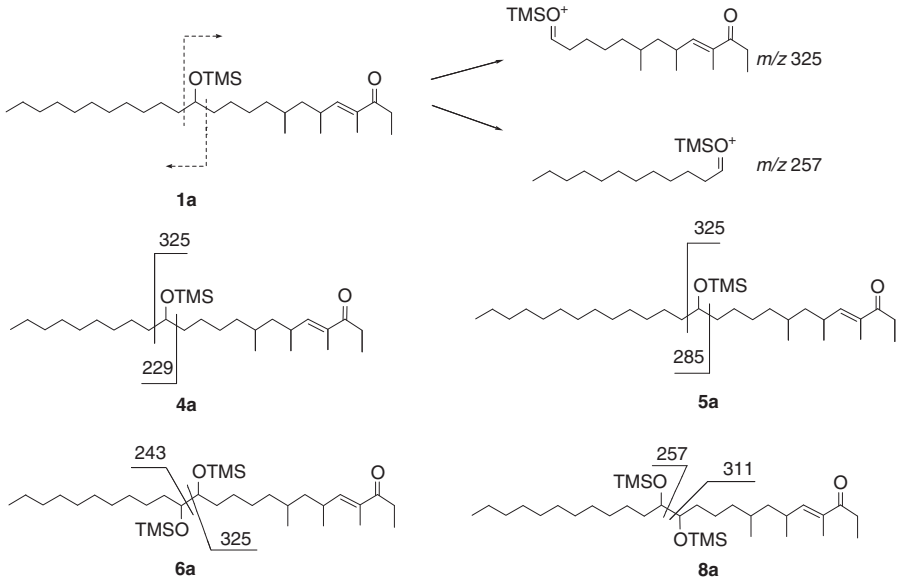


**Figure 3** EI-MS fragmentation patterns of derived alkyl chain moieties. The ketone and long-chain moieties were produced by α-cleavage reactions that occur on either side of the hydroxyl group with loss of enol ether moiety. For example, fragmentation of **1a** on EI-MS gave fragments at *m/z* 357 and 325, indicating that the oxidation site is C-13.

**Table 4 GC-MS retention times and EI-MS fragmentation patterns of TMS derivatives**

| | $t_R$ (min) | | | | |
|---|---|---|---|---|---|
| *Compound* | *Arabinono lactone* | *Alkyl chain* | *Derivative* | *EI-MS fragment ions (m/z)* | |
| **1** | 12.56 | 33.91 | **1a** | 257 | 325 |
| **3** | 12.62 | 33.96 | **1a** | 257 | 325 |
| **4** | 12.58 | 31.23 | **4a** | 229 | 325 |
| **5** | 12.63 | 36.52 | **5a** | 285 | 325 |
| **6** | 12.55 | 35.52 | **6a** | 243 | 325 |
| **7** | 12.62 | 31.26 | **4a** | 229 | 325 |
| **8** | 12.54 | 35.39 | **8a** | 257 | 311 |

**Structure elucidation of the minor components**

As described in the preceding paper,[1] compounds **2–8** were isolated as minor components from a culture broth of SANK 26899. The analysis of each compound by LC/MS afforded molecular weights ranging from 572 Da to 628 Da. Their mass differences were easily explained as the number of $CH_2$ units or hydroxyl substituents from **1**. To determine the location of hydroxyl groups, number of aliphatic carbons, and to identify an aldonic acid moiety, GC/MS analysis of TMS derivatives prepared from the methanolysis products of all minor compounds were used.

In addition to the results shown in Figure 3 and Table 4, the structures of the minor components were finally determined by 1D and 2D NMR spectra, as follows:

*Structure of haplofungin B (**2**).* The molecular formula of **2** was determined as $C_{33}H_{60}O_9$ by HRTOF-MS, which was the same as that of **1**. The $^1H$ and $^{13}C$ NMR spectra of **2** were very similar to those of **1**, except for the signals for the aldonic acid moiety. In the HMBC experiment, $^1H$–$^{13}C$ long-range correlations were observed from H-5′a- and 5′b-oxygenated methylene protons at δ 4.94 and 5.12 to the C-1 ester carbonyl carbon at δ 172.8, which established that the C-5′ in aldonate moiety is attached to the C-1 in the fatty-acid moiety (Figure 1). During purification, it was observed that **1** was easily converted to **2** under alkaline conditions (data not shown). The structure of **2** was thus determined to be an acyl rearrangement product of **1**.

*Structure of haplofungin C (**3**).* The molecular formula of **3**,determined as $C_{34}H_{62}O_9$ by HRTOF-MS, differed from that of **1** by one $CH_2$ unit. The $^1H$ and $^{13}C$ NMR spectra in DMSO-$d_6$ indicated the presence of methyl ester ($\delta_H$ 3.63, $\delta_C$ 51.6). The structures of the aldonate moiety and the fatty-acid moiety were identified by GC/MS analysis (Table 4). The fragment patterns of the hydrolyzed TMS derivatives of the methanolysis products were identical with those of **1**. In the HMBC spectrum, correlation from 1′-$OCH_3$ methoxyl protons at δ 3.63 to C-1′ carbonyl carbon at δ 173.3 in the aldonic acid moiety was observed. A $^1H$–$^{13}C$ long-range correlation was also observed from H-4′-oxygenated methine proton at δ 4.97 to C-1 ester carbonyl carbon at δ 170.2, which established that the C-4′ in aldonate moiety is attached to the C-1 in the fatty acid moiety. From these results, the structure of **3** was elucidated to be the methyl ester of **1** (Figure 1).

*Structure of haplofungin D (**4**).* The molecular formula of **4** was determined as $C_{31}H_{56}O_9$ by high-resolution fast atom bombardment mass spectrscopy (HR-FABMS), which was different from that of **1** by two $CH_2$ units. The structures of the aldonate moiety and the fatty-acid moiety were also determined by GC/MS analysis and the fragment ion (*m/z* 229) originated from the TMS derivative (**4a**) of the fatty acid indicated that the length of the alkyl chain was shorter than **1** by two $CH_2$ units (Figure 3, Table 4). The $^{13}C$ NMR spectrum readily showed the absence of two methylene units in the alkyl chain. In the HMBC spectrum, $^1H$–$^{13}C$ long-range correlation was observed from oxygenated H-4′ methine proton at 4.98 to C-1 ester carbonyl carbon at 172.7, which established that the C-4′ in aldonic acid moiety is attached to the C-1 in the fatty-acid moiety. Combining the results of the NMR and GC/MS experiments, the structure of **4** was determined to be as shown in Figure 1.

*Structure of haplofungin E (**5**).* The molecular formula of **5** was determined as $C_{35}H_{64}O_9$ by HRTOF-MS and it was shown that **5** was two $CH_2$ units larger than **1**. The identification of the aldonate moiety and the structure analysis of the fatty-acid moiety were carried out by GC/MS analysis. The fragment ion (*m/z* 285) from the TMS derivative (**5a**) of the fatty acid indicated that the alkyl chain length was longer than that of **1** by two $CH_2$ units (Figure 3, Table 4). Two newly appeared methylene carbons, in the alkyl chain, were observed in the $^{13}C$ NMR spectrum. In the HMBC spectrum, $^{13}C$–$^{1}H$ long-range correlation from the oxygenated methine proton at δ 4.97 (H-4′) to the ester carbonyl carbon at δ 172.7 (C-1) indicated that the C-4′ in the aldonate moiety is attached to ester carbonyl carbon (C-1) in the fatty-acid moiety. From these results, the structure of **5** was determined to be as shown in Figure 1.

*Structure of haplofungin F (**6**).* The molecular formula of **6** was determined to be $C_{33}H_{60}O_{10}$ by HR-FABMS and shown to have one additional oxygen in the molecule compared to **1**. The $^{13}C$ NMR spectrum readily showed the presence of one newly observed oxygenated methine carbon signal at δ 76.2. These data strongly suggested that one hydroxyl group was introduced into the structure of **1**. To clarify the oxygenated sites, TMS derivatives of the aldonate moiety and fatty-acid moiety were subjected to GC/MS analysis and the appearance of the fragment ions (*m/z* 243 and 325) caused by the oxidative cleavage of 1,2-diol in the TMS derivative of the fatty acid (**6a**) showed the substituted positions of two hydroxyl groups to be at C-13 and C-14 (Figure 3, Table 4). In the HMBC spectrum, $^{1}H$–$^{13}C$ long-range correlation was observed from H-4′-oxygenated methine proton at δ 4.97 to C-1 ester carbonyl carbon at δ 172.6, which established that the C-4′ in aldonic acid moiety is attached to C-1 in the fatty-acid moiety. From these results, the structure of **6** was determined to be as shown in Figure 1.

*Structure of haplofungin G (**7**).* The molecular formula of **7** was determined to be $C_{32}H_{58}O_9$ by HR-FABMS. It differs from that of **4** by one $CH_2$ unit. The $^{1}H$ and $^{13}C$ NMR spectra indicated the presence of a methoxyl group ($\delta_H$ 3.75, $\delta_C$ 49.3). GC/MS analysis of the TMS derivative showed the same fragment pattern as that of **4** (Figure 3, Table 4). In the HMBC spectrum, correlation between 1′-$OCH_3$ protons at δ 3.75 to C-1′ carbonyl carbon at δ 172.6 in the aldonic acid moiety was observed. $^{1}H$–$^{13}C$ long-range correlation was also observed from the H-4′ oxygenated methine proton at δ 4.98 to the C-1 ester carbonyl carbon at δ 175.7, which established that the C-4′ in the aldonic acid moiety is attached to C-1 in the fatty-acid moiety (Figure 1). From these results, the structure of **7** was established to be the methyl ester of **4**.

*Structure of haplofungin H (**8**).* The molecular formula of **8** was determined to be $C_{33}H_{60}O_{10}$ by HR-FABMS, which was the same as **6**. Typical two fragment ions (m/z 311 and 257) derived from the TMS derivative of the fatty acid (**8a**) by the 1,2-diol cleavage between C-12 and C-13 were observed. The $^{13}C$ NMR spectrum readily showed the presence of one newly observed oxygenated methine carbon signal at 76.1 in the alkyl chain. As the same hydroxylation sites as **6** were expected in this case, GC/MS analysis was carried out. Consequently, the substituted positions of the two hydroxyl groups were determined to be at C-12 and 13 (Figure 3, Table 4). $^{1}H$–$^{13}C$ long-range correlation was observed from the oxygenated H-4′ methine proton at δ 4.97 to the C-1 ester carbonyl carbon at δ 172.0, which established that the C-4′ in the aldonic acid moiety is attached to the C-1 in the fatty-acid moiety. Thus, the structure of **8** was determined to be the C-12-hydroxylated homolog of **1** as shown in Figure 1.

## DISCUSSION

Eight new compounds were isolated as fungal IPC synthase inhibitors. Their planer structures have been elucidated by 1D and 2D NMR experiments and GC/MS analysis of the TMS derivatives from degradation products prepared by methanolysis. From these results, it was shown that these homologs were composed of an arabinonic acid moiety and a β-keto acid with a long unsaturated hydroxyalkyl chain as partial structures. Interestingly, these units have a high similarity to the partial structures of two known IPC synthase inhibitors, khafrefungin[3] and rustmicin.[4,5] The arabinonic acid and the hydroxylated long-chain fatty-acid units are common to khafrefungin and the α-methyl-β-keto acid unit is common to rustmicin. These units are reported to be indispensable for the biological activities of these compounds.[6–8] A 14-membered macrolide, the same as rustmicin, has been obtained by macrolactonization between C-1 and C-13 of β-keto acid prepared from **1** by hydrolysis under mild alkaline condition. However, this macrolide showed no biological activity (data not shown). It was evident that haplofungin has a very unique structure which possesses partial structures of these two known compounds. The core structure of haplofungins also seems to mimic the structure of phytoceramide, which is the substrate of IPC synthase. However, their antifungal activities were weak,[1] in contrast to the strong inhibitory activities against IPC synthase. If the structural features and the antifungal activities of haplofungins are improved, these derivatives will be candidates for new chemotherapeutic drugs for fungal diseases. The absolute structure of haplofungin A will be reported in the succeeding paper.[9]

## EXPERIMENTAL SECTION

### General experimental procedures

The 1D and 2D NMR spectra of haplofungins were recorded on a Bruker AVANCE 500 spectrometer (Bruker, Rheinstetten, Germany) equipped with a cryogenic probe. The data set acquired for each sample consisted of 1D $^{1}H$, $^{13}C$ NMR, gs-DQF-COSY, NOESY, gs-HSQC, gs-HMBC and gs-HSQC-HOHAHA experiments which were adopted from Bruker standard pulse microprograms. The HR-FABMS spectra were recorded on a Micromass Autospec mass spectrometer (Micromass, Manchester, UK). The HRTOF-MS spectra were obtained on a Micromass LCT equipped with an electrospray ion (ESI) source. Optical rotations were measured with a JASCO DIP-370 spectropolarimeter (JASCO, Tokyo, Japan). IR spectra were obtained on a JASCO FT/IR-8900 spectrometer. The UV spectra were recorded on a Shimadzu UV-265FW spectrometer (Shimadzu, Kyoto, Japan). GC/MS analyses were carried out using an Agilent GC/MSD spectrometer (Agilent, Santa Clara, CA, USA; EI-MS detector, 5973; GC system, 6890; carrier gas, He). The LC/MS analyses were carried out using an Agilent LC/MSD equipped with an ESI ion source. The analytical HPLC operations were performed on an Agilent HP1100 HPLC system. The HPLC analyses were measured on an Agilent 1100 system (column, Cadenza CD-C18 (4.6×75 mm, Imtakt Co., Japan); mobile phase, A: 0.1% trifluoroacetic acid, B: acetonitrile, 65–95% B (0–15 min), 95% B (15–20 min), linear gradient, flow rate, 0.6 ml $min^{-1}$; detection UV 240 nm).

### GC/MS analysis of components prepared from haplofungins by methanolysis

The compound **1** was treated with methanol containing 5% HCl at 80°C for 4 h in a sealed ampoule, and the reaction mixture was dried over a stream of $N_2$ gas. The residue was then dissolved in pyridine and BSTFA was added. The mixture was allowed to stand at room temperature for 5 min. The product was subsequently subjected to GC/MS analysis under the following conditions: HP-5 MS capillary column (Agilent, 0.25×30 mm). The column temperature was programmed to rise 5°C $min^{-1}$ from 120°C to 240°C. The flow rate of the He carrier gas was 1.5 ml $min^{-1}$. The retention times of the TMS-derivatives are shown in Table 4. Authentic D-arabinono-1,4-lactone was prepared from D-arabinose by oxidation according to the method of Han *et al.*[10]

1 Ohnuki, T. *et al.* Haplofungins, novel inositol phosphorylceramide synthase inhibitors, from Lauriomyces bellulus SANK 26899 I. Taxonomy, fermentation, isolation, and biological activities. *J. Antibiot.* (e-pub ahead of print 31 July 2009; doi:10.1038/ja.2009.72).
2 Vértesy, L. *et al.* Novel hormone-sensitive lipase inhibitors from *Streptomyces sp.* DSM13381. II. Isolation, structure elucidation and biological properties. *J. Antibiot.* **55,** 480–489 (2002).
3 Mandala, S. M. *et al.* Khafrefungin, a novel inhibitor of sphingolipid synthesis. *J. Biol.Chem.* **272,** 32709–327014 (1997).
4 Takatsu, T. *et al.* Rustmicin, a new macrolide antibiotic active against wheat stem rust fungus. *J. Antibiot.* **38,** 1806–1809 (1985).
5 Mandala, S. M. *et al.* A potent antifungal agent, inhibits sphingolipid synthesis at inositol phosphoceramide synthase. *J. Biol. Chem.* **273,** 14942–14949 (1998).
6 Wakabayashi, T., Mori, K. & Kobayashi, S. Total synthesis and structure elucidation of khafrefungin. *J. Am. Chem. Soc.* **123,** 1372–1375 (2001).
7 Kobayashi, S., Mori, K., Wakabayashi, T., Yasuda, S. & Hanada, K. Convergent total synthesis of khafrefungin and its inhibitory activity of fungal sphingolipid syntheses. *J. Org. Chem.* **66,** 5580–5584 (2001).
8 Sakoh, H. *et al.* Novel galbonolide derivatives as IPC synthase inhibitors: design, synthesis and *in vitro* antifungal activities. *Bioorg. Med. Chem. Lett.* **14,** 143–145 (2004).
9 Ohnuki, T., Yano, T., Furukawa, Y. & Takatsu, T. Haplofungins, novel inositol phosphorylceramide synthase inhibitors, from Lauriomyces bellulus SANK 26899 III. Absolute structure of haplofungin A. *J. Antibiot.* (In press).
10 Han, S. Y., Joullié, M. M., Fokin, V. V. & Petasis, N. A. Spectroscopic, crystallographic and computational studies of the formation and isomerization of cyclic acetals and ketals of pentonolactones. *Tetrahedron Asymmetry* **5,** 2535–2562 (1994).

The Journal of Antibiotics (2009) 62, 559–563

www.nature.com/ja

ORIGINAL ARTICLE

# Haplofungins, novel inositol phosphorylceramide synthase inhibitors, from *Lauriomyces bellulus* SANK 26899 III. Absolute structure of haplofungin A

Takashi Ohnuki[1], Tatsuya Yano[2], Youji Furukawa[1] and Toshio Takatsu[1]

**The absolute structure of haplofungin A, a potent fungal inositol phosphoceramide (IPC) synthase inhibitor from *Lauriomyces bellulus* SANK 26899, was determined by chiral GC/MS analysis, NMR and X-ray crystallographic analysis of the derivatives of degradation products.**

*The Journal of Antibiotics* (2009) **62,** 559–563; doi:10.1038/ja.2009.74; published online 7 August 2009

**Keywords:** absolute structure; antifungal; haplofungin; inhibitor; inositol phosphorylceramide synthase; X-ray crystallography

## INTRODUCTION

Haplofungins were isolated from the fungus strain *Lauriomyces bellulus* SANK 26899 and were found to show potent inhibitory activities against fungal inositol phosphoceramide (IPC) synthase. In the preceding papers, we described the taxonomy of the strain SANK 26899 and its production, isolation, biological activities[1] and physicochemical properties as well as the planar structure of haplofungin A.[2] The structures of haplofungins are composed of an arabinonic acid moiety and an unsaturated β-ketoacyl moiety and some of these partial structures are in common with the reported IPC synthase inhibitors, rustmicin[3,4] and khafrefungin.[5,6] Moreover, it is supposed that the structures of haplofungins mimic that of phytoceramide, which is the substrate of IPC synthase. Therefore, information on the absolute structure of haplofungins would be very useful not only for the study of the structure–activity relationship but also for the design of new antifungal drugs based on haplofungins.

In this paper, we report the absolute structure of haplofungin A (**1**), the most potent IPC synthase inhibitor among the reported natural products.

## RESULTS AND DISCUSSION

The strategy for determination of the absolute configuration of **1** is summarized in Figure 1.

As **1** could not be crystallized in all the solvents tested, stereochemical studies were performed on the two composition elements, an arabinonic acid moiety and a long-chain β-keto acid moiety. As the aldonic acid moiety in **1** was identified earlier as arabinonic acid,[2] its absolute configuration in the moeity was assumed as a result of chiral GC/MS analysis. In contrast, that of the long-chain β-keto acid was elucidated by NMR and an X-ray crystallographic analysis.

### Stereochemistry of the arabinonic acid moiety

To determine the absolute configuration of the arabinonic acid moiety, the trifluoroacetyl (TFA) derivative (**1c**) prepared from the hydrolysate (**1a**) was analyzed by gas chromatography using a chiral column (HP-Chiral-20β capillary column, Agilent Technologies, Santa Clara, CA, USA). As shown in Figure 2, the peak with a retention time of 21.55 min was identical to that of authentic trifluoroacetyl-D-arabinono-1,4-lactone prepared from D-arabinonic acid.[7] Thus, the aldonic acid moiety in **1** was determined to be D-arabinonic acid.

### Absolute configuration of the secondary alcohol at C-13

To determine the absolute configuration of position 13 in the alkyl chain of **1**, we chose α-methoxy-2-naphthylacetic acid (2-NMA) as an anisotropic reagent.[8] 2-NMA is known as a very suitable reagent for the configurational analysis of secondary alcohol in a long alkyl chain. The lipid moiety **1b** was prepared from **1** by methanolysis through the decarboxylation at C-1. **1b** was treated with (*R*)- or (*S*)-2-NMA, triethylamine, 2,4,6-trichlorobenzoyl chloride and 4-(dimethylamino) pyridine (DMAP) in THF at room temperature for 1 h to give (*R*)- or (*S*)-2-NMA ester derivatives (**1d**, **1e**). $^1$H NMR signals of **1d** and **1e** were assigned by 1D and 2D NMR experiments. As shown in Figure 3, completely opposite signs of $\Delta\delta$ values ($=\delta R-\delta S$), which were systematically oriented in the right and left sides of C-13, were observed. This anisotropic effect clearly indicated that the configuration of C-13 was *S*.

### Absolute structure of the long alkyl chain moiety of 1

Among the three undetermined chiral centers (C-2, C-6 and C-8), C-2 is an α-carbon of β-keto acid. It can easily be racemized under conventional hydrolysis conditions. Moreover, decarboxylation

[1]Exploratory Research Laboratories I, Daiichi Sankyo Co. Ltd, Hiromachi, Shinagawa-ku, Tokyo, Japan and [2]Biological Research Laboratories II, Daiichi Sankyo Co. Ltd, Hiromachi, Shinagawa-ku, Tokyo, Japan
Correspondence: T Ohnuki, Exploratory Research Laboratories I, Daiichi Sankyo Co. Ltd, 2/1/1958 Hiromachi, Shinagawa-ku, Tokyo 140-8710, Japan.
E-mail: ohnuki.takashi.eh@daiichisankyo.co.jp
Received 25 April 2009; revised 5 July 2009; accepted 7 July 2009; published online 7 August 2009

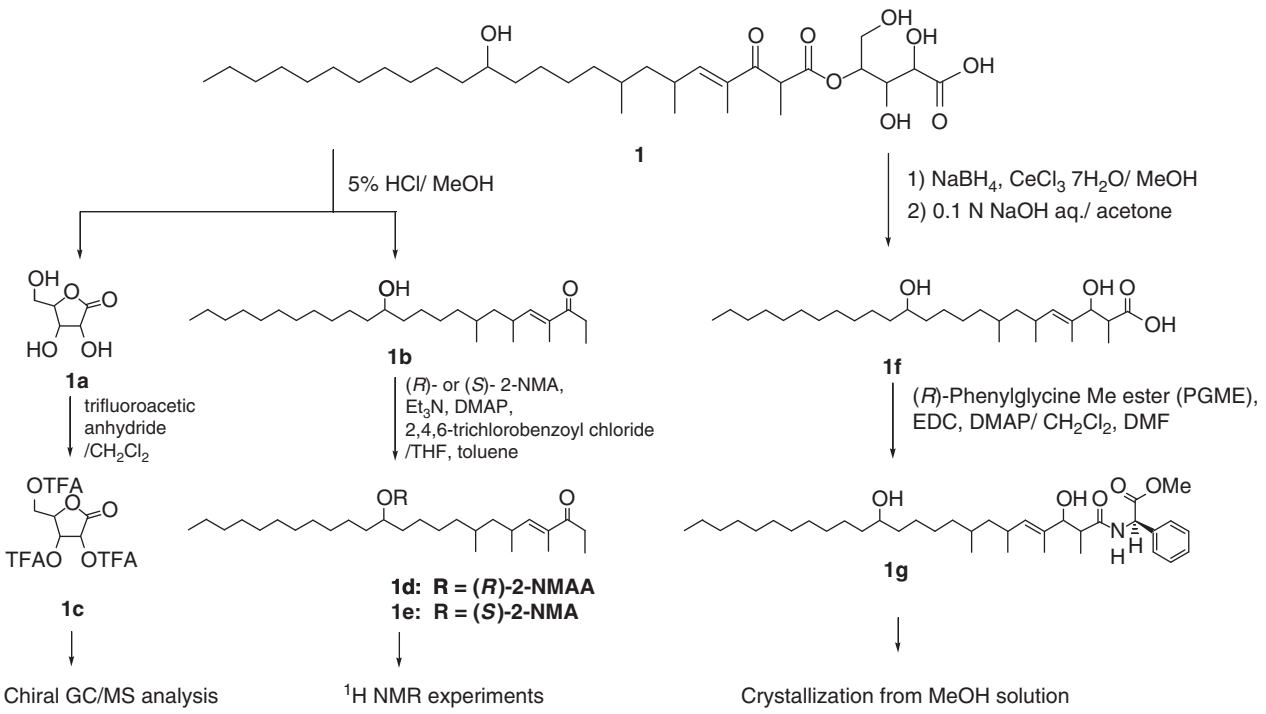


**Figure 1** Planar structure of haplofungin A and the elucidation strategy for the stereochemistry.

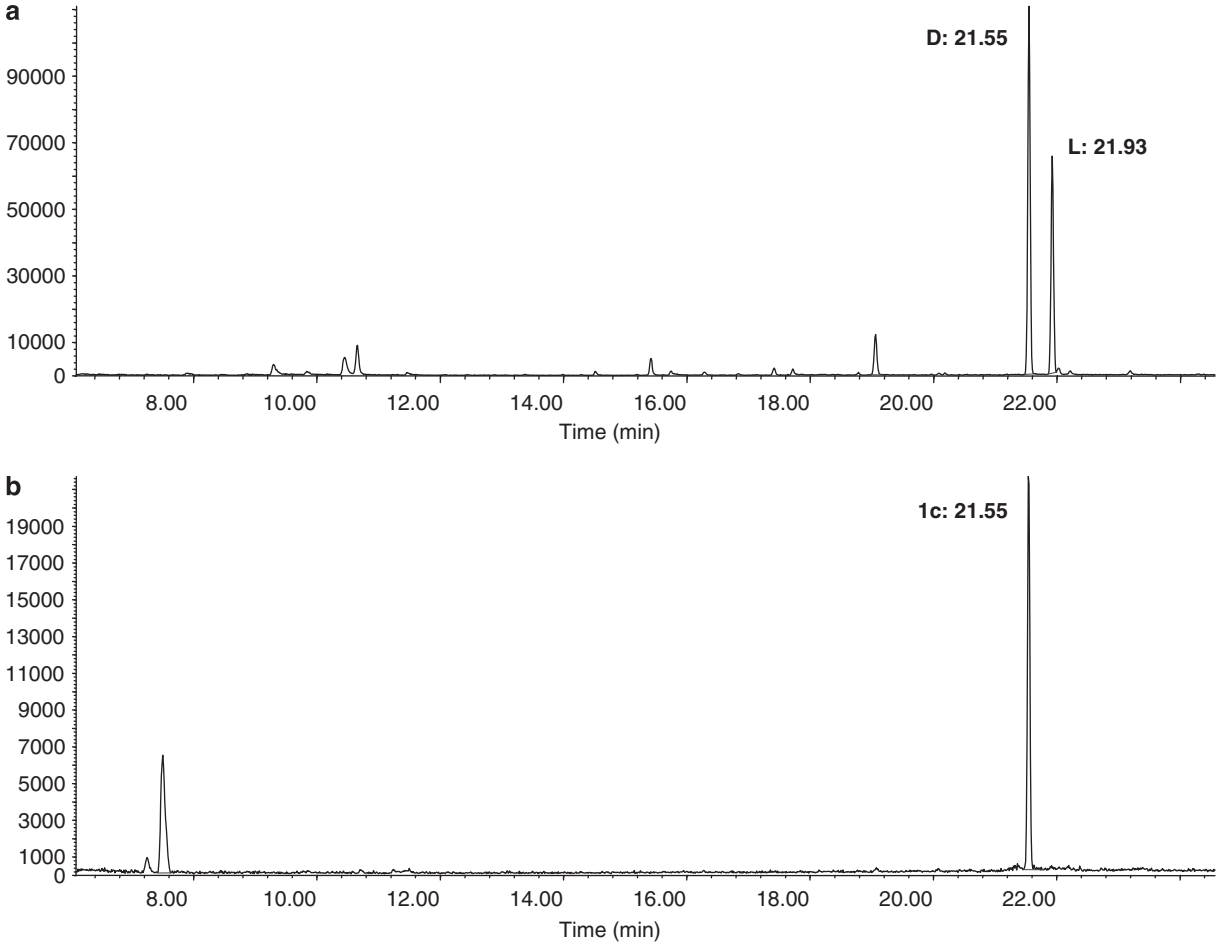


**Figure 2** Chiral GC/MS analysis of trifluoroacetylated hydrolysate. (**a**) Authentic D- and L-arabinono-1,4-lactone. (**b**) Hydrolysate prepared from **1**.

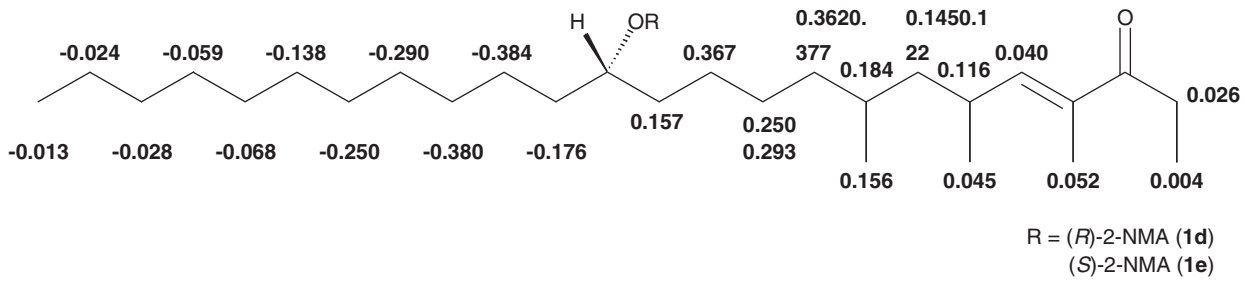


**Figure 3** $\Delta\delta$ values obtained from **1d** and **1e**.

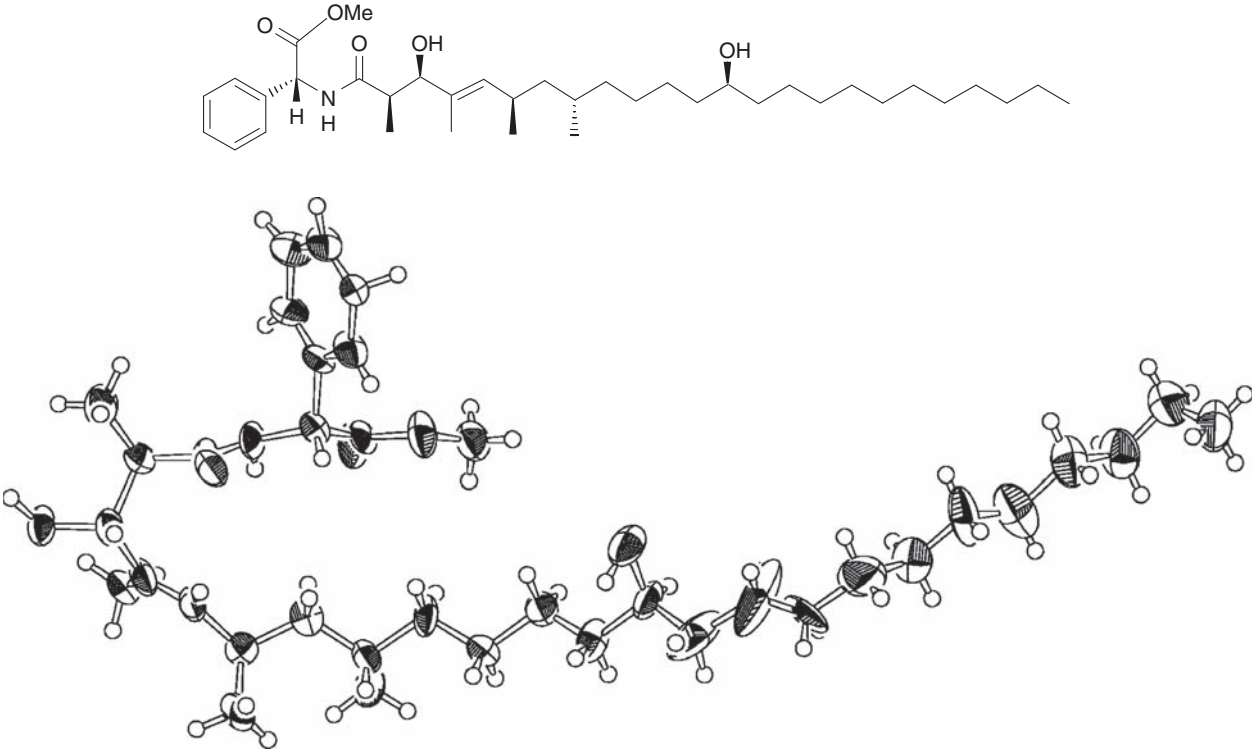


**Figure 4** *ORTEP* diagram and structure of (*R*)-PGME-amide derivative (**1g**).

occurred at C-1 under acidic conditions, with the disappearance of chirality at C-2.

To avoid such decomposition, C-3 carbonyl was converted to a corresponding alcohol before alkaline hydrolysis. For this purpose, **1** was treated with $CeCl_3$ and $NaBH_4$ in methanol[9] to selectively reduce C-3 carbonyl and the reaction was accomplished without the racemization at C-2. Following hydrolysis by 0.1 N NaOH gave **1f** as a single isomer. Subsequently, (*R*)-phenylglycine methylester (PGME) derivative (**1g**) was obtained by the condensation of **1f** and (*R*)-PGME in DMF. **1g** was crystallized by the hanging drop vapor diffusion method from 75% methanol solution and X-ray crystal structure analysis of **1g,** unequivocally confirming the substructure of **1** determined by the NMR experiments.[2] As the absolute configuration of the PGME moiety was *R*, the absolute chemistries of C-2, C-6, C-8 and C-13 of 1 were determined to be 2*R*, 6*R*, 8*S* and 13*S*, respectively (Figure 4), and the absolute chemistry of C-13 was identical with the result determined by NMR experiments with the 2-NMA derivatives mentioned earlier.

Together with the absolute stereochemistry of the arabinonic acid moiety as described above, the absolute structure of **1** was established to be 2*R*, 6*R*, 8*S*, 13*S*, 2′*S*, 3′*S* and 4′*R*, as shown in Figure 5. Haplofungins are related to khafrefungin, which is an IPC synthase inhibitor isolated by the Merck Group in 1997.[5] Khafrefungin is composed of one aldonate moiety and one hydroxylated fatty acid moiety and its absolute chemistry has been determined by total synthesis.[6] Although the absolute configuration of the arabinonic acid in **1** is consistent with that of khafrefungin, the stereochemistry of each corresponding hydroxylated carbon in the fatty acid was different. In an SAR study of khafrefungin,[10] it has been reported that the stereochemistry of the methyl group at C-4 in the alkyl chain and the aldonic acid moiety were indispensable for its biological activities. In haplofungins, the importance of the stereochemistry of the aldonic acid moiety is thought to be the same as that of khafrefungin. This information suggests that the absolute structure of the aldonic acid moiety of these molecules might mimic the hydrophilic terminal of the widely distributed (2*R*, 3*S*, 4*S*)-form phytosphingosine in the plant kingdom. The stereochemistry at C-2 was determined to be *R* by the selective reduction of C-3 keto carbonyl, the PGME derivatization and X-ray structural analysis of the derivative. An α-methyl-β-keto acid

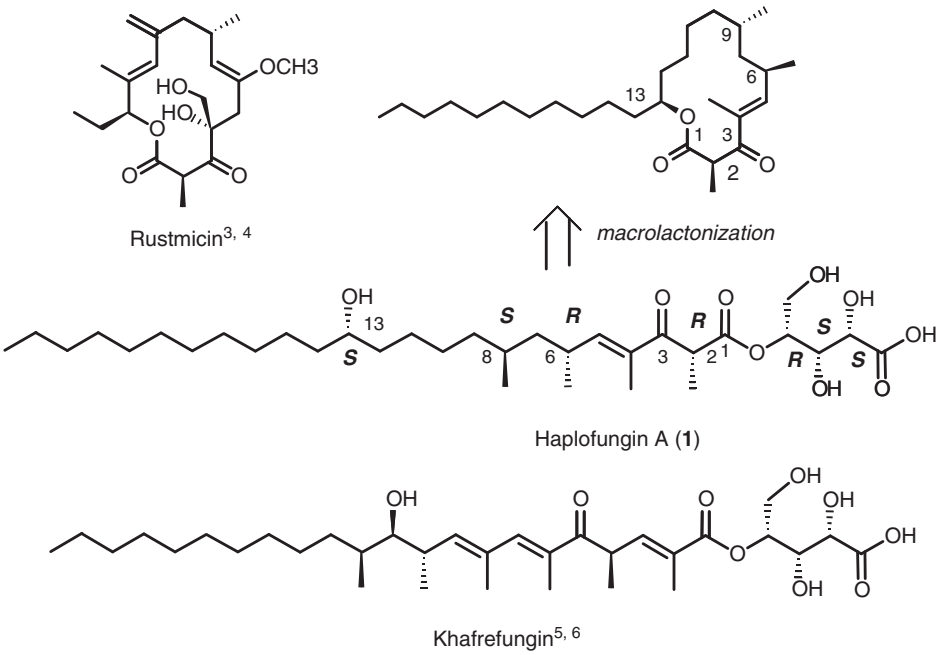


**Figure 5** The absolute configuration of haplofungin A (**1**), khafrefungin and rustmicin.

moiety is a common substructure of haplofungins and rustmicin, isolated from a cultured broth of *Micromonospora chalce*a 980-MC as IPC synthase inhibitor, and the stereochemistry of the unit is also the same[3,4] If the long-chain moiety between C-1 and C-13 of haplofungins were macrolactonized, the carbon skeleton of the product would have the same 14-membered macrolide ring system as that of rustmicin. The configuration of C-2 in rustmicin is essential for its inhibitory activity against IPC synthase.[4] If the substructure of hapolofungin acts on the active site of IPC synthase on which rustmicin acts, the stereochemistry of C-2 in haplofungin would be very important for the binding affinity. Haplofungins are unique hybrid compounds that have the dual structural features of two known IPC synthase inhibitors. It is expected that such stereochemical information will contribute to SAR studies using organic synthesis based on the frame of haplofungins to create effective antifungal agents.

## EXPERIMENTAL SECTION

### Materials

Haplofungin A (**1**) was purified as described in a preceding paper. 2-Naphthaldehyde was purchased from Sigma-Aldrich (St Louis, MO, USA). Trifluoroacetic anhydride was purchased from Kanto Chemical, Tokyo, Japan. (*R*)-Phenylglycine methyl ester was purchased from Tokyo Chemical Industry, Tokyo, Japan.

### General experimental procedures

1D and 2D NMR spectra were recorded on a Bruker AVANCE 500 spectrometer (Bruker, Rheinstetten, Germany) equipped with a Bruker cryoprobe. The data set acquired for each sample consisted of 1D $^{1}H$, $^{13}C$ NMR, gs-DQF-COSY, gs-HSQC, gs-HMBC and gs-HSQC-HOHAHA experiments using Bruker standard microprograms. The GC/MS analysis was performed using an Agilent GC/MSD spectrometer (EI-MS detector, 5973; GC system, 6890; carrier gas, He). The LC/MS analysis was performed using an Agilent LC/MSD equipped with an electrospray ion source. Analytical HPLC was performed on an Agilent HP1100 HPLC system.

### Chiral GC/MS analysis of arabinonic acid moiety in 1

Compound **1** (0.5 mg) was dissolved in 5% methanolic hydrochloride (200 µl), and methanolysis was performed in a sealed ampoule at 105 °C for 8 h. After the reaction mixture was dried under a stream of $N_2$ gas, the residue was dissolved in $CH_2Cl_2$ (100 µl) and trifluoroacetic anhydride (100 µl) was added. The mixture was allowed to stand at room temperature for 5 min. The product was subsequently applied to chiral GC/MS analysis under the following conditions: HP-Chiral-20β capillary column (0.25×30 mm, Agilent Technologies) coated with 0.25 mm film thickness. The column temperature was programed to rise in the ratio of 4 °C/min from 70 to 150 °C and then to rise to 190 °C. The flow rate of the He carrier gas was 1.5 ml min$^{-1}$. When the authentic pertrifluoroacetyl-D,L-arabinono-1,4-lactone showed the retention times of 21.54 and 21.93 min, the product **1c** obtained from **1** was eluted at 21.55 min.

### Preparation of 2-NMA esters from 1

α-Methoxy-2-naphthylacetic acid was obtained as follows: 2-naphthaldehyde was treated with bromoform and KOH in methanol to obtain the racemic 2-NMA, according to the method of Jiang and Compere.[11] After esterification with (−)-menthol, the diastereoisomeric esters were purified by preparative HPLC (column, Develosil C30 UG-5 (20×150 mm, Nomura Chemical, Aichi, Japan); mobile phase, 85% aqueous methanol; flow rate, 11.0 ml min$^{-1}$; detection, UV 310 nm). Each diastereomer was dissolved in 4 N HCl/dioxane and refluxed for 10 h. The mixture was purified by HPLC (column, Pegasil ODS (20×250 mm, Senshu Scientific, Tokyo, Japan); mobile phase, A, 0.1% phosphoric acid, B, 90% acetonitrile containing 0.1% phosphoric acid; linear gradient program from 30 to 100% of B in A in 30 min; flow rate, 10.0 ml min$^{-1}$; detection, UV 310 nm) to give each enantiomer, (*S*)- and (*R*)-2-NMA. Each optical rotation was as follows: (*S*)-2-NMA: $[\alpha]^{D}_{24}$ + 100° (*c* 1.3, methanol). Lit. $[\alpha]^{D}_{25}$ +100.5° (*c* 0.63, methanol)[8] (*R*)-2-NMA: $[\alpha]^{D}_{24}$ -110° (*c* 1.0, methanol). Lit. $[\alpha]^{D}_{25}$ -138.7° (*c* 0.35, methanol).[8] **1** (50 mg, 0.08 mmol) was refluxed with 5% methanolic hydrochloride (10 ml) for 4 h and the mixture was evaporated *in vacuo* to dryness. The residue was extracted with ethyl acetate, and washed with brine. The organic layer was dried over anhydrous $Na_2SO_4$, and concentrated *in vacuo* to give a crude mixture containing **1b** (29 mg, 87.5%). A dry THF solution (2 ml) containing the crude **1b** (25 mg, 0.06 mmol), (*R*)-2-NMA (14.6 mg, 0.07 mmol), triethylamine (17 µl, 0.12 mmol), DMAP (15 mg, 0.123 mmol) and 2,4,6-trichlorobenzoyl chloride

(11 µl, 0.07 mmol) was stirred at room temperature for 1 h. After dilution with toluene (20 ml), the mixture was stirred again at room temperature for 1 h followed by filtration and concentration. The resulting residue was purified by preparative HPLC (column, Develosil C30UG-5, Nomura Chemical (20×150 mm); mobile phase, methanol; flow rate, 10.0 ml $min^{-1}$; detection, UV 254 nm) to afford the (*R*)-2-NMA ester (**1d**, 10.2 mg, 33%). (*S*)-2-NMA ester (**1e**, 8.3 mg, 16.7%) was prepared by the same method.

### Preparation of (*R*)-PGME amide from 1

The carbonyl group at C-3 in **1** was reduced by the method of Larock *et al.*[9] **1** (140 mg, 0.23 mmol) was dissolved in methanol (5 ml) containing $CeCl_3$ (280 mg), and $NaBH_4$ (30 mg) was slowly added by stirring. The mixture was allowed to react at room temperature for 10 min followed by neutralization with 0.1 N HCl. The mixture was evaporated *in vacuo* to remove the methanol and the aqueous suspension was extracted with ethyl acetate (10 ml). The organic layer was dried over anhydrous $Na_2SO_4$ and evaporated *in vacuo*. Then, the crude mixture was dissolved in acetone (5 ml) and treated with 0.1 N NaOH (500 µl) at room temperature for 5 min. The mixture was neutralized with 0.1 N HCl and extracted with ethyl acetate (50 ml). The organic layer was dried over anhydrous $Na_2SO_4$ and concentrated *in vacuo*. The residue was purified by preparative HPLC (column, Capcell Pak C8UG-120, Shiseido Co. Ltd., Tokyo, Japan (20×250 mm); mobile phase, 90% aqueous acetonitrile containing 0.1% phosphoric acid; flow rate, 12.0 ml $min^{-1}$; detection, UV 210 nm). The fraction was concentrated *in vacuo* and extracted with ethyl acetate. The organic layer was dried over anhydrous $Na_2SO_4$ and concentrated *in vacuo* to give a reduced hydrolysate (**1f**, 70.8 mg, 37%). To a stirred dry DMF solution (5 ml) of **1f** (70 mg, 0.15 mmol) and (*R*)-PGME (22.0 mg, 0.13 mmol) were successively added EDC hydrochloride (30 mg, 0.16 mmol) and DMAP (3 mg, 0.025 mmol) followed by standing at room temperature for 8 h. Then, the reaction mixture was extracted with ethyl acetate and the organic layer was successively washed with 5% HCl, saturated $NaHCO_3$ solution and brine. The organic layer was dried over anhydrous $Na_2SO_4$ and concentrated *in vacuo*. The resulting residue was purified by preparative HPLC (column, Develosil C30 UG-5 (20 i.d.×150 mm); mobile phase, methanol—5 mM $HCOONH_4$ (93:7); flow rate, 12.0 ml $min^{-1}$; detection, UV 210 nm) to afford the (*R*)-PGME amide derivative (**1 g**, 59.0 mg, 67%).

### X-ray crystallographic analysis of 1 g

Compound 1**g** was crystallized by the hanging drop vapor diffusion method from 75% methanol solution at room temperature. Crystal with the approximate dimensions of 0.5×0.3×0.04 mm was used for the X-ray analysis. All measurements were made on an AFC-7 diffractometer (Rigaku Corporation, Tokyo, Japan) at −150 °C with graphite monochromated Cu-Kα radiation. The crystal data are as follows: $C_{37}H_{63}NO_5$, MW 601.91, orthorhombic, space group $P2_12_12_1$. $a$=20.565(3) Å, $b$=34.364(8) Å, $c$=5.163(2) Å, $Z$=4, $Dc$=1.096 g $cm^{-3}$. The structure was solved by a direct method with the program SIR88.[12] The non-hydrogen atoms were refined anisotropically. Hydrogen atoms were included as isotropical but not refined. The final cycle of full-matrix least squares refinement was based on 1234 observed reflections ($I > 3.0\sigma(I)$) and converged with $R$=7.0% and Rw=9.6%, where $w=1/\sigma 2(Fo)$.

### Supplementary Information

The Crystal Data Form can be found in the supplementary information in the online version.

## ACKNOWLEDGEMENTS

We thank Dr Shuichiro Ito for the determination of the X-ray crystallographic analyses in this paper.

1 Ohnuki, T. *et al.* Haplofungins, novel inositol phosphorylceramide synthase inhibitors, from *Lauriomyces bellulus* SANK 26988 I. Taxonomy, fermentation, isolation, and biological activities. *J. Antibiot.* (e-pub ahead of print 31 July 2009; doi:10.1038/ja.2009.72).
2 Ohnuki, T., Yano, T. and Takatsu, T. Haplofungins, novel inositol phosphorylceramide synthase inhibitors, from *Lauriomyces bellulus* SANK 26899 II. structure elucidation. *J. Antibiot.* (e-pub ahead of print 31 July 2009; doi:10.1038/ja.2009.73).
3 Takatsu, T. *et al.* Rustmicin, a new macrolide antibiotic active against wheat stem rust fungus. *J. Antibiot.* **38,** 1806–1809 (1985).
4 Mandala, S. M. *et al.* Rustmicin, a potent antifungal agent, inhibits sphingolipid synthesis at inositol phosphoceramide synthase. *J. Biol. Chem.* **273,** 14942–14949 (1998).
5 Mandala, S. M. *et al.* Khafrefungin, a novel inhibitor of sphingolipid synthesis. *J. Biol. Chem.* **272,** 32709–32714 (1997).
6 Wakabayashi, T., Mori, K. & Kobayashi, S. Total synthesis and structural elucidation of khafrefungin. *J. Am. Chem. Soc.* **123,** 1372–1375 (2001).
7 Han, S. Y., Joullié, M. M., Fokin, V. V. & Petasis, N. A. Spectroscopic, crystallographic and computational studies of the formation and isomerization of cyclic acetals and ketals of pentonolactones. *Tetrahedron Asym.* **5,** 2535–2562 (1994).
8 Kusumi, T. *et al.* New chiral anisotropic reagents, NMR tools to elucidate the absolute configuration of long-chain organic compounds. *Tetrahedron Lett.* **35,** 4397–4400 (1994).
9 Larock, R. C., Yum, E. K. & Yang, H. Palladium-catalyzed intermolecular arylation of functionally-substituted cycloalkenes by aryl iodides. *Tetrahedron* **50,** 305–321 (1994).
10 Kobayashi, S., Mori, K., Wakabayashi, T., Yasuda, S. & Hanada, K. Convergent total synthesis of khafrefungin and its inhibitory activity of fungal sphingolipid syntheses. *J. Org. Chem.* **66,** 5580–5584 (2001).
11 Jiang, J. & Compere, E. L. The synthesis of 4,4′-(1,n-dioxaalkane)-bisbenzaldehydes and 4,4′-(1,n-dioxaalkane)-bis(α-methoxy phenylacetic acids. *Synthetic Communications* **28,** 1041–1050 (1998).
12 Burla, M. C. *et al.* SIR88—a direct-method program for the automatic solution of crystal structures. *J. Appl. Cryst.* **22,** 289 (1989).

Supplementary Information accompanies the paper on The Journal of Antibiotics website (http://www.nature.com/ja)

The Journal of Antibiotics (2009) 62, 565–570

www.nature.com/ja

ORIGINAL ARTICLE

# TLN-05220, TLN-05223, new Echinosporamicin-type antibiotics, and proposed revision of the structure of bravomicins*

Arjun H Banskota[1], Mustapha Aouidate[2], Dan Sørensen[3], Ashraf Ibrahim[2], Mahmood Piraee[4], Emmanuel Zazopoulos[2], Anne-Marie Alarco[2], Henriette Gourdeau[2], Christophe Mellon[2], Chris M Farnet[2], Pierre Falardeau[2] and James B McAlpine[2]

**The deposited strain of the hazimicin producer, *Micromonospora echinospora* ssp. *challisensis* NRRL 12255 has considerable biosynthetic capabilities as revealed by genome scanning. Among these is a locus containing both type I and type II PKS genes. The presumed products of this locus, TLN-05220 (1) and TLN-05223 (2), bear a core backbone composed of six fused rings starting with a 2-pyridone moiety. The structures were confirmed by conventional spectral analyses including MS, and 1D and 2D NMR experiments. Comparison of both the $^{1}H$ and $^{13}C$ NMR data of the newly isolated compound with those of echinosporamicin and bravomicin A led us to propose a revision of the structure of the latter to include a 2-pyridone instead of the pyran originally postulated. Both compounds (1 and 2) possessed strong antibacterial activity against a series of gram-positive pathogens including several strains of methicillin-resistant *Staphylococcus aureus* and vancomycin-resistant *Enterococci* (VRE), and cytotoxic activities against several human tumor cell lines. The TLN compounds are the first of this group with reported anticancer activity.**

*The Journal of Antibiotics* (2009) **62,** 565–570; doi:10.1038/ja.2009.77; published online 14 August 2009

**Keywords:** antibacterial; anticancer; bravomicin; *Micromonospora echinospora*; polycyclic aromatic; TLN-05220; TLN-05223

## INTRODUCTION

The genomics of secondary metabolite biosynthesis recently evolved to the point in which analysis of the genome of an organism can define its biosynthetic capabilities for secondary metabolites. A genome scanning technique, requiring minimal amount of sequencing, has been developed in our laboratories, and used with our DECIPHER technology to analyze the genomes of bacteria for their secondary metabolite biosynthetic genes, greatly reducing the amount of sequencing required to define this capability.[1–4] This approach not only ascertains the biosynthetic potential of a producing organism, but it provides the scientist with a handle to detect, isolate and structurally define a specific metabolite. We have shown this approach in the isolation and structural determination of an antifungal agent, ECO-02301 from *Streptomyces aizunensis*[5] and three 5-alkenyl-3,3(*2H*)-furanones from two different *Streptomyces* species.[6] This genome scanning approach, which was applied to define the biosynthetic capabilities of *Micromonospora echinospora* ssp. *challisensis* NRRL 12255 (this strain was deposited (as SCC 1411) to support US Patent 4,440,751),[7] revealed 13 secondary metabolite biosynthetic loci. In our experience, this is an unusually high number to find in a *Micromonospora* species and led to the prioritization of this strain for investigation. A preliminary DECIPHERIT analysis annotated these loci as encoding a terpenoid, five mixed PKS/NRPS, four NRPS and three PKS biosynthetic systems. In this article, we describe the use of the genome scanning technique[8,9] to identify and isolate new polycyclic aromatic antibiotics (TLN-05220, **1** and TLN-05223, **2**) from this strain, the former was previously referred to as ECO-3396.[1,2] Both compounds (**1** and **2**) possessed strong antibacterial activity against broadly resistant, gram-positive pathogens, and cytotoxic activities against several human tumor cell lines.

## RESULTS AND DISCUSSION

*M. echinospora* ssp. *challisensis* NRRL 12255 was obtained from the National Center for Agricultural Utilization Research (NCAUR) in Peoria, IL, USA and was grown in shaken flasks in a dozen different fermentation media designed for the production of secondary metabolites. The whole cultures were then extracted by equal volumes of MeOH and the resultant aqueous/MeOH extracts were subjected to HPLC/MS/UV analyses. A number of these extracts contained a compound with UV absorption $\lambda_{max}$ at 248 and 508 nm, as might

[1]Institute for Marine Biosciences, National Research Council, Halifax, Nova Scotia, Canada; [2]Thallion Pharmaceuticals, Alexander-Fleming, Montréal, Quebec, Canada; [3]Merck-Frosst Canada, Trans Canada Highway, Kirkland, Quebec, Canada and [4]Biotica Technology, Chesterford Research Park, Cambridge, UK
Correspondence: Dr JB McAlpine, 730 Benson Lane, Green Oaks, IL 60048, USA.
E-mail: jmcalpine@thallion.com
*Part IV in a series on Genomic Analysis for the Discovery of Novel Secondary Metabolites. TLN-05220 was previously referred to as ECO-3396.
Received 30 April 2009; revised 9 July 2009; accepted 22 July 2009; published online 14 August 2009

be expected for a type II polyketide. This compound had MS peaks at *m/z* 738.1 (in the positive mode) and 736.1 (in the negative mode). Larger scale (20×500 ml) fermentations of *M. echinospora* ssp. *challisensis* NRRL 12255 were carried out in the two media, which gave the best yields of this metabolite. On harvest, the EtOAc extract gave TLN-05220 (**1**) and TLN-05223 (**2**) (Figure 1) by Sephadex LH-20 (Sigma-Aldrich Canada, Oakville, ON, Canada) column chromatography followed by reversed phase HPLC.

TLN-05220 (**1**) was isolated as a red amorphous solid with molecular formula $C_{30}H_{31}N_3O_{13}$ calculated from the MS data (*m/z* 738.15 $(M+H)^+$ and 736.10 $(M-H)^-$). The $^1H$ NMR spectrum (Table 1) of **1** displayed five aromatic protons including two sets of ortho-coupling protons, one methoxy, two methine, three methylene and three C-methyl groups. The carbon NMR spectrum (Table 2) on the other hand had 38 carbon signals including 23 quaternary carbons in aromatic and carbonyl region ($\delta$ 111.4–187.1), indicating the presence of a complex aromatic system. The UV absorption of TLN-05220 (**1**) at $\lambda_{max}$ 508 nm further suggested that the rest of the molecule should be constructed by an extended conjugated system.

In-depth analyses of the gCOSY together with heteronuclear single quantum coherence (gHSQC) and heteronuclear multiple bond coherence (gHMBC) spectra led to the identification of the piperazinone and 1-methyl propyl groups as two partial structures. Additional sets of proton and carbon signals of the piperazinone moiety were also observed in the NMR spectra and are ascribed to the presence of slowly interchangeable rotamers. The presence of five carbonyl carbons ($\delta$ 187.1 (×2), 183.3, 181.9 and 159.0), two sets of ortho-coupled aromatic protons ($\delta$ 8.63 and 8.39; 7.47 and 7.44) and a singlet aromatic proton signal ($\delta$ 6.73) strongly suggested the presence of a polycyclic aromatic with a core backbone composed of six fused rings, similar to the albofungins,[10] simaomicins[11] and echinosporamicin **3**.[12,13] The presence of a carbonyl carbon at $\delta$ 187.1 (C-5) resembles the situation with echinosporamicin **3**, suggesting the presence of p-benzoquinone ring (ring E) instead of a γ-pyrone, as reported in the albofungin and simaomicin antibiotics, in which it could be derived through the oxidative cleavage of an echinosporamicin-like ring E. Furthermore, the proton and carbon NMR data of TLN-05220 (**1**) were very similar to that of echinosporamicin **3**, isolated from *M. echinospora* ssp. *echinospora* LL-P175. The only difference is the substitution patterns of ring A and ring E. The presence of the second set of the ortho-coupled aromatic protons at $\delta$ 7.47 and 7.44 and two hydroxyl protons at $\delta$ 13.19 strongly suggested that the ring F should be 6,9-dihydroxy substituted. The attachment of the 1-methyl propyl group was placed at C-16 based on the HMBC correlations observed between H-12 and C-16. An additional broad methylene signal at $\delta$ 5.23 having HMBC correlation with carbonyls at $\delta$ 165.9 and 159.0 indicated the connection of the piperazinone to the *N*-alkyl pyridinone of the polycyclic chain through an amide linkage. Finally, the position of the methoxy group was determined to be at C-11 based on the HMBC correlation between the methoxyl protons at $\delta$ 4.04 and C-11 at $\delta$ 153.2. Accordingly, the planar structure of TLN-05220 was determined as **1**. On the basis of the coupling constant of the protons on piperazinone moiety and the presence of similar rotamer signals as described for echinosporamicin, we are led to postulate a similar stereo-structure for these molecules. The stereochemistry of the 1-methyl propyl group remains undetermined.

An examination of related compounds in the literature brought our attention to the bravomicins, exemplified by the parent, bravomicin A, **4**.[14] The spectral data in this patent suggested a strong similarity between the structures of TLN-05220, echinosporamicin and bravomicin A, although these spectral data require some reinterpretation as the data given in the table do not mess with the spectra presented in the figures. Unfortunately, a sample of bravomicin A was not available to us to allow a thorough 2D NMR analysis and direct comparison of spectra measured under identical conditions. In the proton spectra (Table 1), the US patent lists the protons on C-17 at $\delta$ 1.31 as a doublet and those on C-29 at $\delta$ 0.95 as a triplet, whereas the Figure 3 in the patent indicates that the coupling patterns are reversed. Moreover, the triplet should clearly be assigned to the C-19 protons. (Note that the numbering system used in this article is that in Figure 1 and not the one given in the US patent.) The CMR table in the US patent does not include a carbon at ~$\delta$ 45; however, such a carbon is

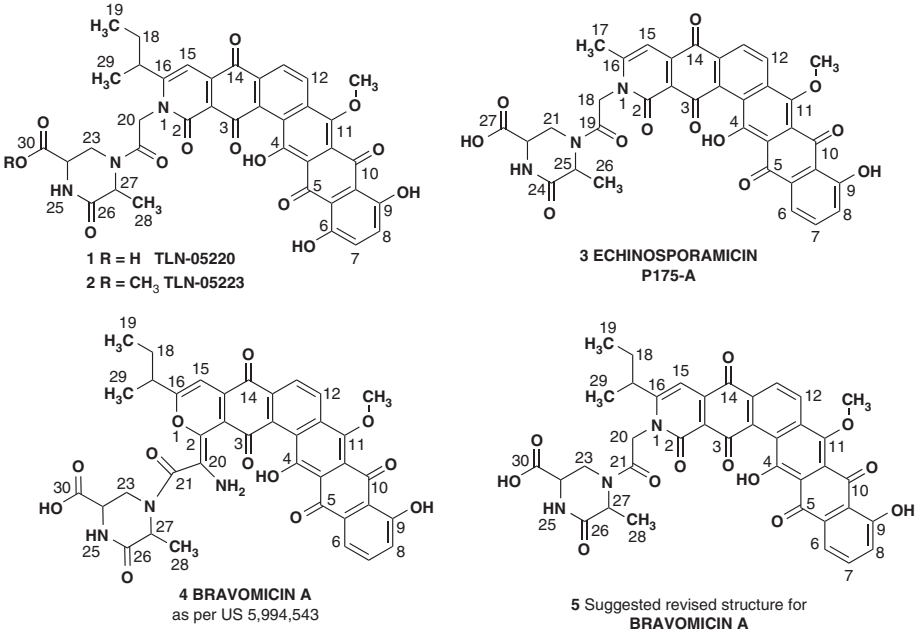


**Figure 1** Structures.

**Table 1 The $^1$H NMR data of TLN-05220 (1), TLN-05223 (2), Echinosporamicin (3) and Bravomicin (4)**

| | *Echinosporamicin (3)*[a] | *TLN-05220 (1)*[a] | *TLN-05223 (2)*[a] | *Bravomicin (4)*[a] | *Revised bravomicin (4)*[a] |
|---|---|---|---|---|---|
| 4-OH | 15.37 | 14.64 | 14.64 | 15.38 | 15.38 |
| 6 | 7.77 | — | — | 7.64 | 7.64 |
| 6-OH | — | 13.19 | 13.28 | — | — |
| 7 | 7.75 | 7.47 | 7.19 | 7.69 | 7.69 |
| 8 | 7.35 | 7.44 | 7.12 | 7.29 | 7.29 |
| 9-OH | 12.90 | 13.19 | 13.28 | 12.83 | 12.83 |
| 12 | 8.52 | 8.63 | 8.23 | 8.48 | 8.48 |
| 13 | 8.27 | 8.39 | 8.11 | 8.22 | 8.22 |
| 15 | 6.75 | 6.73 | 6.69 | 6.72 | 6.72 |
| 17 | 2.42, (2.39) | 2.67 | 2.62 | 2.68 | 2.68 |
| 18[b] | | 1.74, 1.64 | 1.74, 1.62 | 1.70, 1.80 | 1.70, 1.80 |
| 19[b] | | 0.91 | 0.90 | 0.95 | 0.95 |
| 18, 20[b] | 5.10 (5.20) | 5.12 (5.23) | 5.09 (br) | — | 5.10 (br) |
| 21, 23[b] | $H_{ax}$: 3.39 (4.69) | $H_{ax}$: 3.38 (3.81) | $H_{ax}$: 3.42 (3.84) | $H_{ax}$: 3.42 (3.84) | $H_{ax}$: 3.42 (3.84) |
| | $H_{eq}$: 4.69 (4.34) | $H_{eq}$: 4.65 (4.40) | $H_{eq}$: 4.57 (4.40) | $H_{eq}$: 4.68 (4.41) | $H_{eq}$: 4.68 (4.41) |
| 22, 24[b] | 4.02 (4.18) | 4.01 (4.17) | 4.34 (4.17) | 4.02 (4.18) | 4.02 (4.18) |
| 23-NH, 25-NH[b] | 8.20 (8.26) | 8.20 (8.30) | 8.37 (8.51) | | |
| 25, 27[b] | 4.60 (4.55) | 4.67 (4.54) | 4.75 (4.53) | 4.60 (4.55) | 4.60 (4.55) |
| 26, 28[b] | 1.57 (1.31) | 1.60 (1.32) | 1.60 (1.32) | 1.57 (1.31) | 1.57 (1.31) |
| 29[b] | — | 1.27 | 1.24 | 1.31 | 1.31 |
| 30-$OCH_3$[b] | — | — | 3.61 | — | — |
| 11-$OCH_3$ | 4.00(s) | 4.04 | 3.86 | 3.97 (s) | 3.97 |

[a]Chemical shifts on the parentheses belong to the minor rotamer.
[b]Carbon numbers for TLN-05220 (**1**), TLN-05223 (**2**) and Bravomicin (**4**) 17-$NH_2$ in the patent structure of Bravomicin is assigned as $\delta$ 5.10.

clearly evident in Figure 4 of the patent. The corresponding carbon, the attached protons at $\sim\delta$ 5.1 and their HMBC correlations have a critical role in the attachment of the piperazinone moiety in the structural determinations of both TLN-05220 and echinosporamicin. Clearly the data for the revised structure of bravomicin A (6-deoxy TLN-05220) cannot be regarded as rigorous; however, it is highly suggestive.

TLN-05223 (**2**) was also isolated as a red amorphous solid with molecular formula $C_{39}H_{33}N_3O_{13}$ calculated from the MS data (*m/z* 752.6 $(M+H)^+$ and 750.4 $(M-H)^-$). The $^1$H and $^{13}$C NMR signals of **2** were identical to that of **1** except the presence of an additional *O*-methyl group ($\delta$ 3.61). The identical mass fragment of both **1** and **2** at *m/z* 580, that is, $(M+H-$piperazinone moiety$)^+$ suggested that **2** is the methyl ester of **1**, and may possibly be an artifact of the isolation procedure.

One of the 13 biosynthetic loci determined using the DECIPHER genomic analysis platform was ascribed to the biosynthesis of TLN-05220 and TLN-05223. This locus (the DNA and protein sequences that comprise the TLN-05220 gene cluster are deposited in GenBank under accession number FJ915123) spanned approximately 65 Kb and contained a small PKS type I gene in which the adenylation (AT) domains each contained the YASH motif specifying the incorporation of methylmalonate. This PKS type I gene is assumed to result in carbons 16 through 19 and 29, and was slightly upstream of the PKS type II genes that would give rise to the hexacyclic system. Moreover, in the vicinity were a number of genes responsible for oxidative and cyclization functions, and an *O*-methyl transferase. Surprisingly, there were no genes in this locus as sequenced, nor in any of the other 12 loci detected, which would be annotated as NRPS genes encoding a glycine, an alanine and one other (possibly serine) amino acid residue that would be expected to give rise to the glycyl piperazinone moiety, as defined by carbons 20 through 28 and 30. As extensive sequencing analysis was performed on both extremities of this locus, it is possible that the NRPS genes presumed to be involved in the biosynthesis of glycyl piperazinone moiety of compounds **1** and **2** are provided *in trans* by a yet undefined region of the genome.

The compounds were tested for their antibacterial activity against seven pathogenic strains. The MICs are summarized in Table 3. Both compounds (**1** and **2**) possessed significant antibacterial activity against all strains tested. The MIC values were comparable to those of vancomycin, which was used as a control. The potency of the polycyclic aromatics was stronger than that of vancomycin against all tested pathogens except *Streptococcus pneumoniae* PenR (LSPQ 3349). Although the specific strains were different, the activity of TLN-05220 seems to be similar to that reported for echinosporamicin[12,13] and bravomicin A.[14]

Compound **1** was also evaluated for antitumor activity. Bravomicin and echinosporamicin were reported as gram-positive antibacterial agents, the latter specifically described as having no significant anti-cancer activity against HCT-116[13]. As summarized in Table 4, TLN-05220 had potent growth inhibitory activity (sub-micromolar range) on the four human solid tumor cell lines examined. The compound was less active on K-562, an erythroleukemia cell line derived from a chronic myeloid leukemia patient in blast crisis.

As the prostate cell line was the most sensitive, the *in vivo* antitumor activity of TLN-05220 was evaluated in nude mice bearing human prostate (PC3) tumors (Figure 2). Animals from the vehicle control group were killed when the tumor volume reached $\sim$1000 mm$^3$. Out of 10 mice used in the control group, 1 mouse reached the end point by day 26, 7 mice reached the end point by day 40 and the remaining 3 animals on day 43. At 25 mg kg$^{-1}$ on alternate days, i.p. administration of TLN-05220 caused severe abdominal trauma by day 7 and a death on day 13. In total, seven more deaths occurred between days 27 and 50. On day 36, the median tumor volume for this group (six mice) was 467 mm$^3$. The median tumor volume for the vehicle-treated group (nine mice) was 615 mm$^3$. This reflects a tumor reduction of 24% and is not statistically significant. An i.v. administration of TLN-05220 at

**Table 2 CMR assignments**

| *Carbon*[a] | *Echinosporamicin* | *TLN-05220* | *Bravomicin* | *Revised bravomicin* |
|---|---|---|---|---|
| 2 | 157.7, 157.7 | 159.0, 159.1 | 164.3, 164.3 | 157.7, 157.7 |
| 2a | 119.8, 119.9 | 121.4, 121.4 | 120.0, 120.0 | 120.0, 120.0 |
| 3 | 181.9, 181.9 | 181.9, 181.9 | 180.7. 180.7 | 180.7. 180.7 |
| 3a | 137.4, 137.4 | 138.6, 138.6 | 141.6, 141.6 | 141.6, 141.6 |
| 3b | 124.6, 124.6 | 127.9, 127.9 | 124.3, 124.3 | 124.3, 124.3 |
| 4 | 161.0, 161.0 | 165.2, 165.2 | 161.0, 161.0 | 161.0, 161.0 |
| 4a | 110.1 110.1 | 111.4, 111.4 | 109.9, 109.9 | 109.9, 109.9 |
| 5 | 187.2, 187.2 | 187.1, 187.1 | 187.0, 187.0 | 187.0, 187.0 |
| 5a | 132.7, 132.7 | 114.6, 114,6 | 132.6, 132.6 | 132.6, 132.6 |
| 6 | 118.5, 118.5 | 157.1, 157.1 | 118.4, 118.4 | 118.4, 118.4 |
| 7 | 136.9, 136.9 | 130.2, 130.2 | 136.9, 136.9 | 136.9, 136.9 |
| 8 | 124.4, 124.4 | 130.2, 130.2 | 124.7, 124.7 | 124.7, 124.7 |
| 9 | 161.8, 161.8 | 157.9, 157.9 | 161.8, 161.8 | 161.8, 161.8 |
| 9a | 117.3, 117.3 | 116.1, 116.1 | 117.2, 117.2 | 117.2, 117.2 |
| 10 | 186.5, 186.5 | 187.1, 187.1, | 186.3, 186.3 | 186.3, 186.3 |
| 10a | 120.1, 120.1 | 122.0, 122.0 | 119.9, 119.9 | 119.9, 119.9 |
| 11 | 151.8, 151.8 | 153.2, 153.2 | 151.9, 151.9 | 151.9, 151.9 |
| 11a | 138.5, 138.5 | 140.2, 140.2 | 137.5, 137.5 | 137.5, 137.5 |
| 12 | 128.4, 128.4 | 129.8, 129.8 | 128.5, 128.5 | 128.5, 128.5 |
| 13 | 126.8, 126.8 | 128,3, 128.3 | 126.8, 126.8 | 126/8, 126.8 |
| 13a | 133.8, 133.8 | 134.9, 134.9 | 133.8, 133.8 | 133.8, 133.8 |
| 14 | 180.8, 180.8 | 183.3, 183.3 | 182.0, 182.0 | 182.0, 182.0 |
| 14a | 141.6, 141.5 | 143.0, 143.0 | 138.5, 138.5 | 138.5, 138.5 |
| 15 | 100.5, 100.5 | 98.4, 98.4 | 97.0, 97.0 | 97.0, 97.0 |
| 16 | 155.4, 155.6 | 165.3, 165.3 | 163.9, 163.9 | 163.9, 163.9 |
| 17 | 21.0, 21.2 | 39.6, 39.6 | 20.0, 20.0 | 38.1, 38.1 |
| 18[b] | | 30.1, 30.1 | 38.1, 38.1 | 28.3, 28.3 |
| 19[b] | | 13.1, 13.1 | 28.3, 28.3 | 11.8, 11.8 |
| 18, 20[b] | 45.7, 45.6 | 45.9, 45.9 | 157.7, 157.7 | ~45[a] |
| 19, 21[b] | 164.4, 163.9 | 165.9, 165.5 | 164.7,164.7 | 164.7,164.3 |
| 21, 23[b] | 37.3, 40.4 | 38.6, 42.1 | 37.1, 40.3 | 37.1, 40.3 |
| 22, 24[b] | 52.5, 53.1 | 54.1, 54.6 | 52.6, 53.2 | 52.6, 53.2 |
| 24, 26[b] | 168.5, 168.8 | 169.9, 170.1 | 168.8, 168.8 | 168.8, 168.8 |
| 25, 27[b] | 52.7, 51.0 | 54.1, 52.5 | 52.7, 51.1 | 52.7, 51.1 |
| 26, 28[b] | 17.5, 16.0 | 19.0, 17.5 | 17.5, 16.0 | 17.5, 16.0 |
| 29[b] | | 21.6, 21.6 | 11.8, 11.8 | 20.0, 20.0 |
| 27, 30[b] | 172.3, 172.3 | 173.5, 173.3 | 172.4, 172.2 | 172.4, 172.2 |
| $OCH_3$ | 62.7, 62.7 | 64.4, 64.4 | 62.7, 62.7 | 62.7, 62.7 |

[a]In the patent, this peak does not appear in the assigned peaks in Table 2; however, it is clearly evident in Figure 4, the CMR spectrum of bravomicin A.
[b]The difference in structures requires different numbering for structurally comparable carbons.

**Table 3 Antibacterial activity of compound 1 and 2; MICs are expressed in $\mu g\,ml^{-1}$**

| *Strain* | *TLN-05220 (1)* | *TLN-05223 (2)* | *Vancomycin* |
|---|---|---|---|
| *S. aureus ATCC 6538P* | 0.016 | 0.0625 | 1 |
| *S. aureus* MRS3 ATCC 700699 | 0.016 | 0.125 | 4 |
| *S. pneumoniae* LSPQ13412 | 0.5–1 | 1 | 0.5 |
| *S. pneumoniae* PenR LSPQ 3349 | 4–16 | 1 | 0.5 |
| *E. faecalis* VRE-1 ATCC 29212 | 0.063 | 1 | 4-8 |
| *E. faecalis* VRE-2 ATCC 51299 | 0.125 | 1 | 32 |
| *Clostridium difficile* ATCC 9689 | 0.06 | 2 | 0.5 |

$10\,mg\,kg^{-1}$ caused severe toxicity to the tail vein, necessitating the i.p. route for subsequent dosing. The median tumor volume for this group on day 36 (eight mice—two animals had to be killed due to their tumors reaching $1000\,mm^3$) was $634\,mm^3$, and thus not significantly different from the vehicle control group. In summary, although TLN-05220 was potent in inhibiting the growth of PC3 cells, it failed to produce *in vivo* antitumor efficacy. It was felt that the compound had a narrow therapeutic index and also that the pharmacokinetics of the drug were not suitable for i.v. or i.p. dosing.

## EXPERIMENTAL SECTION

### General

Optical rotations were measured at 589 nm in a 1-dm cell on a Perkin Elmer polarimeter Model 241 (Perkin Elmer, Waltham, MA, USA). The NMR spectra were measured on a Varian Unity Inova 500 MHz spectrophotometer (Varian, Palo Alto, CA, USA) with dimethylsulfoxide-$d_6$ solution and are referenced to TMS. The analytical HPLC was carried out with a Waters Alliance 2690 instrument (Waters, Milford, MA, USA) equipped with Micromass ZQ electrospray (Waters) source and Waters 996 diode array UV detectors (Waters). Semi-preparative HPLCs were performed on Waters 600 Controller instrument (Waters) with Waters 996 diode array UV detector (Waters). All the chemicals and solvents used for the purifications were HPLC grade.

### Genome scanning

The genome of *M. echinospora* ssp. *challisensis NRRL 12255* was analyzed by the genome scanning technique as described previously by Zazopoulos *et al.*[3,4] and the nucleotide and protein sequenced were deposited in GenBank (accession number FJ915123).

### Fermentation

*M. echinospora* ssp. *challisensis NRRL 12255*, which was obtained from the NCAUR in Peoria, IL, USA, was maintained and sporulated on agar plates of ATCC culture medium 172 (glucose $10\,g\,l^{-1}$, soluble starch $20\,g\,l^{-1}$, yeast extract $5\,g\,l^{-1}$, N-Z-amine A $5\,g\,l^{-1}$, $CaCO_3$ $19\,g\,l^{-1}$ and agar $15\,g\,l^{-1}$ in distilled water). The surface growth from the agar plate was homogenized and transferred to a 125 ml flask containing three glass beads (5 mm diameter), and 25 ml of sterile FBB medium (potato dextrin $24\,g\,l^{-1}$, beef extract $3\,g\,l^{-1}$, Bacto Casitone $5\,g\,l^{-1}$, glucose $5\,g\,l^{-1}$, yeast extract $5\,g\,l^{-1}$ and $CaCO_3$ $4\,g\,l^{-1}$ in distilled water). The pH of the medium was adjusted at 7.0 before adding $CaCO_3$ and then autoclaved. This vegetative culture was incubated at 28 °C for about 70–72 h on a shaker with a 2.5 cm throw and set at 250 r.p.m.

The vegetative culture (10 ml aliquots) was used to inoculate 2-l baffled flasks each containing 500 ml of sterile media; medium A (glucose $10\,g\,l^{-1}$, sucrose $20\,g\,l^{-1}$, cane molasses $20\,g\,l^{-1}$, Soytone-peptone $5\,g\,l^{-1}$ and $CaCO_3$ $2.5\,g\,l^{-1}$ in distilled water) and medium B (maltose $4\,g\,l^{-1}$, yeast extract $4\,g\,l^{-1}$ and malt extract $10\,g\,l^{-1}$ in distilled water). Both media were adjusted at pH 7.0 before sterilization. The fermentation batches were incubated aerobically on a shaker (200 r.p.m.) with a 2.5 cm throw at 28°C for a period of 4 days.

### Extraction and isolation

*Method A.* The whole fermentation broth of the culture medium A (20×500 ml) was adjusted to pH 3.5 adding sulfuric acid and extracted with ethyl acetate (2×5 l). The organic phase was dried over anhydrous $MgSO_4$ and concentrated under reduced pressure. The residue was then dissolved in methanol (12 ml) and the MeOH soluble part was subjected to a Sephadex LH-20 column (3.5×100 cm) eluted with MeOH under gravity. The fractions (10 min per fraction) were collected after 2 h of sample injection. Fractions 17–21 were pooled and concentrated under reduced pressure, which gave a red precipitate. The red precipitate was collected by filtration to give pure TLN-05220 (**1**, 7.93 mg).

*Method B.* The fermentation broth of the culture medium B (20×500 ml) was adjusted to pH 3.5 adding sulfuric acid and extracted with ethyl acetate (2×5 l). The organic phase was dried over anhydrous $MgSO_4$ and evaporated under reduced pressure. The residue was dissolved in methanol/dimethyl sulfoxide (DMSO) (9:1, 20 ml) and subjected to a Sephadex LH-20 column (3.5×100 cm) eluted with MeOH under gravity. The fractions (10 min per fraction) were collected after 2 h of sample injection. Fractions 2–10 were pooled and concentrated under reduced pressure. The residue was then dissolved in DMSO/MeOH mixture (3:1, 5 ml) and subjected to HPLC purification after filtering through a 0.45 μm 13-mm Acrodisc GHP syringe

filter (Waters). The HPLC was performed on a Waters 600 Controller instrument (Waters) using a Waters NovaPak C18 column (Waters) (5 μm, 25×550 mm), and a gradient of 0.01% aqueous acetic acid/acetonitrile (20 ml min$^{-1}$, 80:20 to 20:80 (0–15 min); 20:80 to 0:100 (15–20 min)). TLN-05220 (**1**, 8.63) and TLN-05223 (**2**, 0.5 mg) were obtained from multiple injections, eluting at 14.5 and 17.1 min, respectively.

**1**: $[\alpha]^{20}_{D}$ −60° (~0.001 MeOH) UV ($\lambda_{max}$) 249, 280 (sh), 335 (sh) and 508 nm; MS (ESI in positive mode) *m/z* 760.0 $(M+Na)^+$, 738.1 $(M+H)^+$, 579.8 $(M+)^+$; MS (ESI in negative mode) *m/z* 736.1 $(M-H)^-$; HRMS 738.1939 calcd for $C_{38}H_{31}N_3O_{13}$ $(M+H)^+$ 738.1935 Δ=0.57 p.p.m. The $^1$H and $^{13}$C NMR data are in Table 1 and 2, respectively.

**2**: UV ($\lambda_{max}$) 249, 280 (sh), 335 (sh) and 508 nm; MS (ESI in positive mode) *m/z* 774.6 (M+Na)+, 752.6 $(M+H)^+$, 580.4 $(M+)^+$; MS (ESI in negative mode) *m/z* 750.4 $(M-H)^-$; HRMS 752.2083 calcd for $C_{39}H_{33}N_3O_{13}$ $(M+H)^+$ 752.2086 Δ=0.40 p.p.m. The $^1$H and $^{13}$C NMR data are in Table 1 and 2, respectively.

## Antibacterial activity

Antibacterial activity of the isolated compounds was measured by determining the MIC against seven pathogenic strains, namely *Staphylococcus aureus* (ATCC 6538P), *S. aureus* MRS3 (ATCC 700699), *S. pneumoniae* (LSPQ 13412), *S. pneumoniae* PenR (LSPQ 3349), *Enterococcus faecalis* VRE-1 (ATCC 29212), *E. faecalis* VRE-2 (ATCC 51299) and *Clostridium difficile* (ATCC 9689). The antibacterial experiments were performed according to the National Committee for Clinical Laboratory Standards (NCCLS) guideline M7-A5.[15]

Stock solutions of the tested compounds were prepared in DMSO (100×) and diluted with Mueller-Hinton test medium as twofold series over 11 points from 64 to 0.06 μg ml$^{-1}$. An aliquot of each stock solution was diluted 50-fold in test medium described below to give a set of eleven 2× solutions. In total, 50 μl of each of the eleven 2× solutions were aliquoted into the corresponding wells of a 12-well row microtiter plate, with the final well reserved for a medium-alone control. Vancomycin (Sigma-Aldrich Canada), used as positive control, was prepared as 2× stock solutions in Mueller-Hinton test medium ranging from 64 to 0.06 μg ml$^{-1}$ (a twofold dilution series over 11 points). An aliquot of 50 μl of each concentration (at 2×) was then transferred to 96-well microtiter plate to obtain a series of eleven twofold dilutions.

An isolated colony of each of the seven indicator strains was used to inoculate tubes containing 2 ml of test medium. Mueller-Hinton test medium was used for *S. aureus* (ATCC 6538P), *S. aureus MRS3* (ATCC 700699), *S. pneumoniae* (LSPQ 13412), *S. pneumoniae* PenR (LSPQ 3349), *C. difficile* (ATCC 9689) and Brain Heart Infusion test medium was used for *E. faecalis* VRE-1 (ATCC 29212) and *E. faecalis* VRE-2 (ATCC 51299) indicator strains. Cells were grown overnight at 35 °C with shaking. Inoculum density for each indicator strain was adjusted to $OD_{600}$=0.1 in 5 ml 0.85% saline, then further diluted 1/100 in appropriate medium. In total, 50 μl of the final dilution (in test medium) of each indicator strain was added to each well of a 12-well row. This brings the final dilution of the test compound or control compound in solution to 1×. The final inoculum has approximately 5×10$^5$ CFU ml$^{-1}$.

The indicator strains were incubated with 11 concentrations of each of test compounds, vancomycin (Sigma) control and one medium-alone control. For MIC determination, assay plates were incubated at 35 °C for 16–20 h. The MIC for each indicator was assessed as the lowest concentration of the test compound resulting in total absence of growth and is shown in Table 3.

**Table 4 Effect of TLN-05220 on cell growth**

| | | *TLN-05220 $GI_{50}$ (μM)* | |
|---|---|---|---|
| *Cell lines* | *Tissue origin* | *EXP 1* | *EXP 2* |
| MCF7 | Breast | 0.59 | 0.22 |
| HCT 116 | Colon | 0.09 | 0.71 |
| PC-3 | Prostate | <0.01 | 0.04 |
| NCI-H460 | Lung | 0.28 | 1.22 |
| K-562 | Leukemia | 4.62 | 9.7 |

## Antitumor activity: *in vitro* studies

Human breast (MCF7), colon (HCT116), prostate (PC3), lung (NCI-H460) and leukemia (K562) tumor cell lines were purchased from the American Type Culture Collection (Manassas, VA, USA). Cells were grown in RPMI 1640 supplemented with 2 mM L-glutamine and 10% heat-inactivated fetal bovine serum (FBS; Cambrex, Verviers, Belgium) and maintained in a humidified atmosphere at 37 °C with 5% $CO_2$. Exponentially growing tumor cells (5 000–10 000 cells per well depending on their doubling time; cell number was determined with a hemocytometer) were seeded in 96-well flat-bottom microtiter plates. The following day, cells were exposed to six different concentrations of TLN-05220 (20, 10, 5, 1, 0.1 and 0.01 μM) in a final volume of 200 μl of RPMI 10% FBS and 0.1% DMSO for 96 h. The *in vitro* cytotoxic activity was determined by a standard 3-(4,5-Dimethylthiazol-2-yl)-2,5-diphenyltetrazolium bromide (MTT) assay.[16] All measurements were done in quadruplicate and each experiment was performed twice. A control plate, in which MTT was added to the cells after the overnight incubation period before compound addition, was used to determine day 1 absorbance reading (0 h). The dose response inhibition of proliferation (GI) for each concentration was determined following the formula:

$$GI = \frac{OD_{\text{drug-exposed wells (96h)}} - OD_{\text{drug-free wells (0h)}}}{OD_{\text{drug-free wells (96h)}} - OD_{\text{drug-free wells (0h)}}}$$

The $GI_{50}$ was estimated from individual inhibition curves and represents the concentration of drug that inhibits 50% of the cell growth as compared with

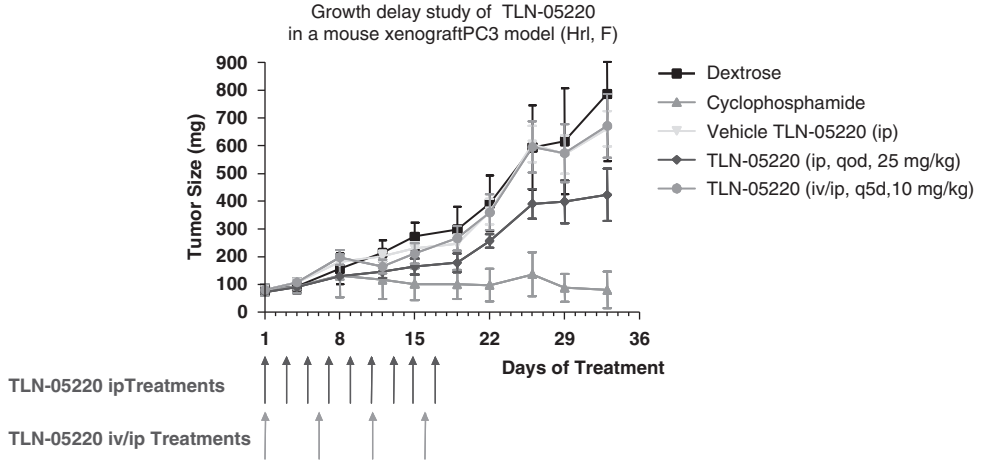


**Figure 2** Growth delay study of TLN-05220 in a mouse xenograft PC3 model (Hrl, F).

non-treated control cells (calculated with the PrismPad computer program (GraphPad software, San Diego, CA, USA)).

### *In vivo* studies

The human PC-3 prostate carcinoma line used for these studies was maintained in athymic nude mice by serial engraftment. The study was performed at Piedmont Research Center (Morrisville, NC, USA), which is accredited by AAALAC International. A tumor fragment (1 $mm^3$) was implanted SC into the right flank of male Nude-Foxn1nu/Foxn1+ mice (8–9 weeks old; Harlan, Indianapolis, IN, USA). When tumor volumes reached 80–120 $mm^3$, mice were randomized (10 mice per group) and treatment began (day 1 of study=19 days after tumor fragment inoculation). Group 1 received drug-free vehicle (5% ethanol, 4.5% glycocholate, 6% ethanolic polysorbate 80 and 84.5% dextrose-5%), i.p., once daily on alternate days for nine doses (qod $\times 9$). Group 2 (positive control group), received cyclophosphamide i.p. at 100 mg $kg^{-1}$, once daily on days 1–5 (qd $\times 5$). Group 3 received TLN-05220 i.p. at 25 mg $kg^{-1}$, once daily on alternate days for nine doses (qod $\times 9$). Group 4 received TLN-05220 i.v. (first dose) and i.p. (remaining three doses) at 10 mg $kg^{-1}$, on days 1, 6, 11 and 16 (q5d $\times 4$). Tumor growth was followed every other day by measuring tumor length ($L$) and width ($W$) using a caliper. Measurements were converted to tumor volumes (TV; $mm^3$) using the standard formula, $TV=(L\times W^2)/2$.

## ACKNOWLEDGEMENTS

We thank Professor André B. Charette of the Université de Montréal for the use of his polarimeter.

1 Alarco, A. M., Banskota, A., McAlpine, J., Farnet, C., Falardeau, P. & Zazopoulos, E. Profiling of new antitumor natural products discovered using a genomics/cheminformatics-based drug discovery platform. *Proc. Am. Assoc. Cancer Res.* **47,** A1992 (2006).

2 Gross, H. Genome mining—a concept for the discovery of new natural products. *Curr. Opin. Drug Discov. Devel.* **12,** 207–219 (2009).

3 Zazopoulos, E. *et al.* A genomics-guided approach for discovering and expressing cryptic metabolic pathways. *Nat. Biotechnol.* **21,** 187–190 (2003).

4 Zazopoulos, E. & Farnet, C. M. Improving drug discovery from microorganisms. *Natural Products: Drug Discovery and Therapeutic Medicine* (eds Zhang, L. and Demain, A. L.) 95–106 (Humana Press Inc., Totowa, NJ, USA, 2005).

5 McAlpine, J. B. *et al.* Microbial genomics as a guide to drug discovery and structural elucidation: ECO-02301, a novel antifungal agent, as an example. *J. Nat. Prod.* **68,** 493–496 (2005).

6 Banskota, A. H. *et al.* Isolation and identification of three new 5-Alkenyl-3,3(*2H*)-furanones from two Streptomyces species using a genomic screening approach. *J. Antibiot.* **59,** 168–176 (2006).

7 Waitz, J. A., Marquez, J. A., Patel, M. G. & Horan, A. C. Broad spectrum antibiotic complex produced by a novel micromonospora. US 4,440,751, April 3 (2001).

8 Sørensen, D., McAlpine, J. B., Piraee, M., Farnet, C. M. & Zazopoulos, E. Genome scanning technology reveals an antibacterial compound (ECO-0501) of a new structural class from the vancomycin-producer *Amycolatopsis orientalis* 44th ICAAC: no. F-720a, Washington, DC (2004).

9 McAlpine, J. B. *et al.* The power of genomic analysis in the discovery of novel secondary metabolites 46th Annual Meeting of American Society of Pharmacognosy: no. O-21, Corvallis, OR, USA (2005).

10 Gurevich, A. I. *et al.* The structure of albofungin. *Tet. Lett.* **13,** 1751–1754 (1972).

11 Carter, G. T., Goodman, J. J., Torrey, M. J., Borders, D. B. & Gould, S. J. Biosynthetic origin of the carbon skeleton of sisaomicin A, a hexacyclic xanthone antibiotic. *J. Org. Chem.* **54,** 4321–4323 (1989).

12 He, H., Yang, H. Y., Luckman, S. W. & Bernam, V. S. Antibiotic P175-A and semisynthetic derivatives thereof US Patent Application. US 2004/0220195 Nov. 4, (2004).

13 He, H. *et al.* Echinosporamicin, a new antibiotic produced by *Micromonospora echinospora* ssp. *echinospora, LL*-P175. *Helv Chim. Acta* **87,** 1385–1391 (2004).

14 Shu, Y-Z., Chen, J., Lam, K. S., Veitch, J. A. & Brown, D. Antibiotic Bravomicins US Patent 5, 994, 543, Nov. 30, (1999).

15 Methods for Dilution Antimicrobial Susceptibility Tests for Bacteria That Grow Aerobically; Approved Standard-Fifth Edition (NCCLS document M7-A5, ISBN 1-56238-394-9 Pennsylvania, USA).

16 Plumb, J. A., Milroy, R. & Kaye, S. B. Effects of the pH dependence of 3-(4,5-dimethylthiazol-2-yl)-2,5-diphenyl-tetrazolium bromide-formazan absorption on chemosensitivity determined by a novel tetrazolium-based assay. *Cancer Res.* **49,** 4435–4440 (1989).

The Journal of Antibiotics (2009) 62, 571–574

www.nature.com/ja

ORIGINAL ARTICLE

# LL-Z1272α epoxide, a precursor of ascochlorin produced by a mutant of *Ascochyta viciae*

Kuniaki Hosono[1], Jun Ogihara[1], Takamichi Ohdake[1] and Setsuko Masuda[2]

**A novel metabolite, LL-Z1272α epoxide, structurally related to ascochlorin, was isolated from the cultured mycelium of *Ascochyta viciae* J-29, a mutant derived from *A. viciae* Libert. The structure was elucidated on the basis of spectroscopic data. The epoxide is proposed to be enzymatically formed from LL-Z1272α and is a precursor of ascochlorin, an antiviral and antitumor antibiotic. The conversion of the epoxide to ascochlorin by cyclization of its farnesyl chain to a cyclohexanone ring is similar to that of squalene 2, 3-oxide to sterols. Unlike ascochlorin, the new metabolite had no growth inhibitory activity against *Candida albicans* in the paper-disc agar diffusion assay.**
*The Journal of Antibiotics* (2009) **62,** 571–574; doi:10.1038/ja.2009.80; published online 14 August 2009

**Keywords:** ascochlorin precursor; fungal metabolite; LL-Z1272α epoxide; prenylphenol antibiotic

## INTRODUCTION

Ascochlorin was originally isolated as an antiviral agent from the filter cake of the fermented broth of *Ascochyta viciae* Libert[1] (Figure 1), and ascofuranone was similarly isolated as an antiviral compound from the same strain.[2] Subsequently, many structurally related compounds have been isolated from various fungi such as an unclassified *Fusarium* species LL-Z1272,[3] *Cylindrocladium* sp.,[4] *Cylindrocladium ilicicola* MFC-870,[5] *Nectria coccinea*,[6] *Colletotrichum nicotianae*,[7] *Acremonium luzulae*,[8] *Cephalosporium diospyri*,[9] *Verticillium* sp. FO-2787,[10] *Cylindrocarpon lucidum*,[11] *Nigrosabulum globosum*[12] and the insect pathogenic fungus *Verticillium hemipterigenum* BCC 2370.[13]

Ascochlorin and its derivatives exhibit a large variety of physiological activities, including hypolipidemic activity,[14] suppression of hypertension,[15] amelioration of type I and II diabetes,[16] antitumor activity[17] and immunomodulation.[18]

Although ascochlorin and structurally related compounds have been isolated from diverse fungi and have been reported to have wide biological activities, their biosynthetic pathway has been uncertain. It has been proposed that the farnesyl chain of LL-Z1272α (Figure 1) is epoxidized, cyclized to a cyclohexanone ring and converted to ascochlorin just as in the case of the enzymatic conversion of squalene 2, 3-oxide to lanosterol and cholesterol.[3] However, this epoxide, the expected intermediate to which the farnesyl chain with a terminal double bond is converted, has not been isolated hitherto.

By screening metabolites produced by more than 2000 mutants of *A. viciae*, we found a new compound related to ascochlorin. The structure was elucidated to be LL-Z1272α epoxide on the basis of spectroscopic data. In this report, we describe the isolation and structure of this epoxide (Figure 1) and discuss the biosynthesis of ascochlorin.

## RESULTS

### Physico-chemical properties of LL-Z1272α epoxide

LL-Z1272α epoxides are crystals with a pale yellow color; Mp: 38–39 °C; $[\alpha]^{25.4}_{D}$=+6.6 (*c* 0.5, $CHCl_3$); high resolution fast atom bombardment mass spectrum (HRFAB-MS) *m/z* 407.1941 $[M+H]^+$ (calculated for $C_{23}H_{32}ClO_4$, 407.1989); UV (MeOH) $\lambda_{max}$ (ε) 227 (17 000) and 293 (12 900) nm; IR (KBr) $\nu_{max}$ 3384, 2984–2834, 1617, 1279, 1243 $cm^{-1}$. The $^1$H-NMR and $^{13}$C-NMR assignments of LL-Z1272α epoxide are listed in Table 1.

### Structure elucidation

The LL-Z1272α epoxide was obtained as crystals with a pale yellow color. Its formula was determined to be $C_{23}H_{31}ClO_4$ on the basis of HRFAB-MS at *m/z* 407.1941 $[M+H]^+$ (calculated for $C_{23}H_{32}ClO_4$, 407.1989). IR absorptions at 3384 (OH), 2984–2834 (methyl, methylene and methine), 1617 (CO), 1279 (CO) and 1243 (CO) $cm^{-1}$ were observed. UV spectral absorptions at $\lambda_{max}$ (ε) 227 (17 000) and 293 (12 900) nm were obtained. The $^{13}$C-NMR spectrum ($CDCl_3$) showed 23 resolved peaks, which were classified into 5 $sp^3$ methyls ($\delta_c$ 14.5, 16.2, 16.0, 23.4 and 26.5), 5 $sp^3$ methylenes ($\delta_c$ 22.1, 39.6, 26.2, 36.8 and 36.8), 1 $sp^3$ methine ($\delta_c$ 78.3), 2 $sp^2$ methines ($\delta_c$ 121.3 and 125.0), 1 $sp^3$ oxygenated quarternary carbon atom ($\delta_c$ 73.1), 8 $sp^2$ quarternary carbon atoms ($\delta_c$ 113.7, 162.2, 114.5, 156.5, 113.4, 137.7, 136.5 and 135.0) and 1 carbonyl group ($\delta_c$ 193.3). Its $^1$H-NMR spectral data revealed the signal of one aldehyde proton (1-CHO, $\delta_H$ 10.13), one $sp^3$ methyl attached to the aromatic ring (6-$CH_3$, $\delta_H$ 2.59), four $sp^3$ methyl groups ($\delta_H$ 1.77, 1.59, 1.15 and 1.19), one $sp^3$ methine ($\delta_H$ 3.35), two $sp^2$ methines ($\delta_H$ 5.19 and 5.15) and five $sp^3$ methylenes ($\delta_H$ 3.39, 2.01, 2.09, 2.06 and 2.19).

[1]Department of Applied Biological Science, College of Bioresource Sciences, Nihon University, Kameino, Fujisawa, Japan and [2]NRL Pharma, KSP, Takatsu-ku, Kawasaki, Japan
Correspondence: Dr K Hosono, Department of Applied Biological Science, College of Bioresource Sciences, Nihon University, Kameino 1866, Fujisawa, Kanagawa 252-8510, Japan.
E-mail: khosono@brs.nihon-u.ac.jp
Received 1 June 2009; revised and accepted 22 July 2009; published online 14 August 2009

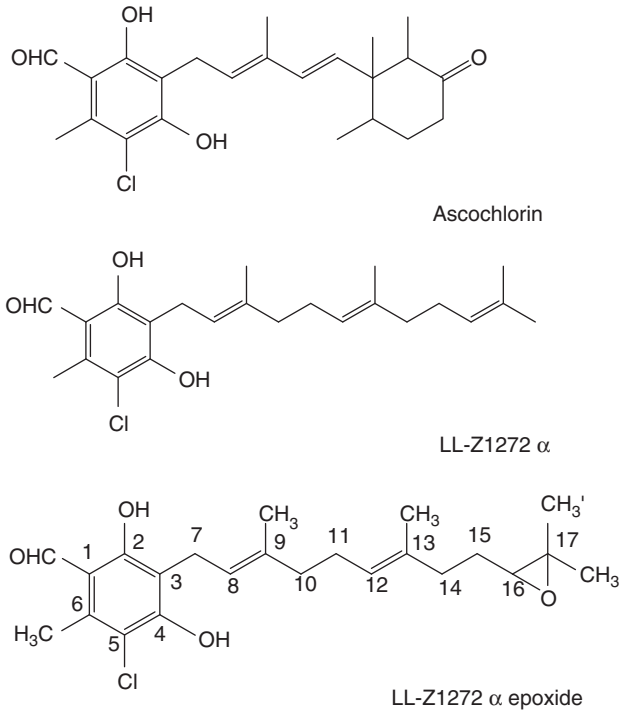


**Figure 1** Structures of ascochlorin, LL-Z1272α, and LL-Z1272α epoxide.

**Table 1 NMR spectral data on LL-Z1272α epoxide in $CDCl_3$**

| *No.* | $\delta_H$ (*J in Hz*) | $\delta_C$ (*Hz*) | *HMBC* |
|---|---|---|---|
| 1 | | 113.7 | |
| 2 | | 162.2 | |
| 3 | | 114.5 | |
| 4 | | 156.5 | |
| 5 | | 113.4 | |
| 6 | | 137.7 | |
| 7 | 3.39 (2H, d, *J*=6.9) | 22.1 | 2, 3, 4, 8, 9 |
| 8 | 5.19 (1H, t, *J*=6.9) | 121.3 | 7, 10, 9-$CH_3$ |
| 9 | | 136.5 | |
| 10 | 2.01 (2H, m) | 39.6 | 9, 11, 12 |
| 11 | 2.09 (2H, m) | 26.2 | 10, 12,13 |
| 12 | 5.15 (1H, t, *J*=6.5) | 125.0 | 14 |
| 13 | | 135.0 | |
| 14 | 2.06 (2H, m) | 36.8 | |
| 15 | 2.19 (2H, m) | 36.8 | |
| 16 | 3.35 (1H, d, *J*=10.3) | 78.3 | |
| 17 | | 73.1 | |
| 1-CHO | 10.13 (1H, s) | 193.3 | 1, 2, 3 |
| 6-CH3 | 2.59 (3H, s) | 14.5 | 1, 5, 6 |
| 9-$CH_3$ | 1.77 (3H, s) | 16.2 | 8, 9, 10 |
| 13-$CH_3$ | 1.59 (3H, s) | 16.0 | 12, 13, 14 |
| 17-$CH_3$ | 1.15 (3H, s) | 23.4 | 16, 17, 17-$CH_3'$ |
| 17-$CH_{3'}$ | 1.19 (3H, s) | 26.5 | 16, 17, 17-$CH_3$ |

Alignments of vicinal protons and carbons were determined by carrying out $^1H$–$^1H$ COSY and heteronuclear multiple bond correlation (HMBC) experiments. $^1H$–$^1H$ COSY experiments revealed correlations from 7-H to 9-$CH_3$ through to 8-H, and from 10-H to 16-H through to 11-H, 12-H, 13-$CH_3$, 14-H and 15-H, as indicated by the bold-faced lines in Figure 2. Assignments of the signals for nine quaternary carbons (C-1, C-2, C-3, C-4, C-5, C-6, C-9, C-13 and C-17) were revealed by HMBC experiments. The long-range couplings from the aldehyde proton 1-CHO to C-1, C-2 and C-3; from the methyl proton 6-$CH_3$ to C-1, C-5 and C-6; from the methylene proton 7-H to C-2, C-3, C-4, C-8 and C-9; from the methine proton 8-H to C-7, 9-$CH_3$ and C-10; from the methyl proton 9-$CH_3$ to C-8, C-9 and C-10; from the methylene proton 10-H to C-9, C-11 and C-12; from the methylene proton 11-H to C-10, C-12 and C-13; from the methine proton 12-H to C-14; from the methyl proton 13-$CH_3$ to C-12, C-13 and C-14; from the methyl proton 17-$CH_3$ to C-16, C-17 and 17-$CH_3'$; and from the methyl proton 17-$CH_3'$ to C-16, C-17 and 17-$CH_3$ were confirmed from HMBC spectra (Table 1).

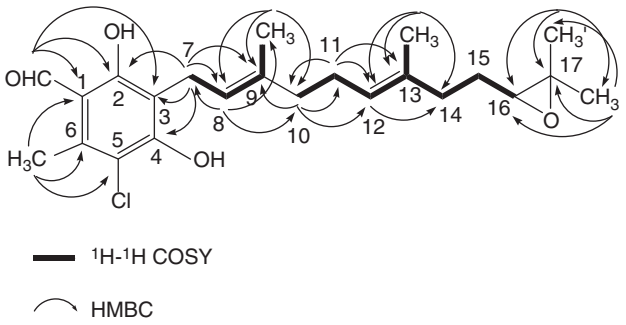


**Figure 2** Selected $^1H$–$^1H$ COSY and heteronuclear multiple bond correlation (HMBC) correlations for LL-Z1272α epoxide.

In differential NOE experiments, the correlations among 8-H, 7-H and 10-H, and among 7-H, 9-$CH_3$ and 13-$CH_3$ were observed, and the stereochemistry of the double bond at C-8 was deduced to be *E*. Similarly, the correlations among 12-H, 11-H and 14-H, and among 9-$CH_3$, 13-$CH_3$ and 17-$CH_{3'}$, established the stereochemistry of the double bond at C-12 to be *E*. The presence of a chlorine was shown using HRFAB-MS analysis, and the connection of its atom to C-5 was reasonable from its chemical shift ($\delta_c$ 113.4).

### Biological activity

It is reported that ascochlorin inhibits the growth of yeast *C. albicans*, in addition to having antiviral activity.[1] Ascochlorin at a concentration of 5 mg ml$^{-1}$ (12.4 mM) caused a clear growth inhibitory zone ($\varphi$ 14 mm) when tested against *C. albicans* NBRC 1386 in the paper-disc agar diffusion assay, but no such zone appeared with LL-Z1272α epoxide at a concentration of 12.3 mM. The diameter of the paper disc was 8 mm.

## DISCUSSION

The parent strain, *A. viciae* Libert, concurrently produces both ascochlorin and ascofuranone.[2] There are many structurally related compounds with various biological activities (see Introduction), but studies on their biosyntheses have not been reported yet. We obtained mutants that produced LL-Z1272α and/or LL-Z1272α epoxide, which is likely to be a precursor of ascochlorin. Mutant J-15 produced LL-Z1272α only (unpublished data), whereas mutant J-29 produced LL-Z1272α epoxide, together with ascofuranone (in this report). Both ascochlorin and LL-Z1272α have been isolated together from *Fusarium* species,[3] *Nectria coccinea*[6] and *Verticillium* sp.[10] Ellestad *et al.*[3] proposed that the farnesyl chain of LL-Z1272α was epoxidized, cyclized to a cyclohexanone ring and converted to ascochlorin

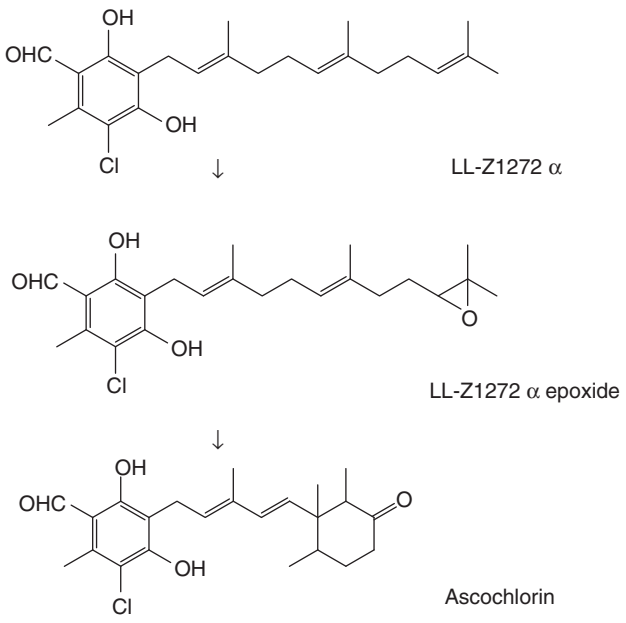


**Figure 3** Pathway for the biosynthesis of ascochlorin.

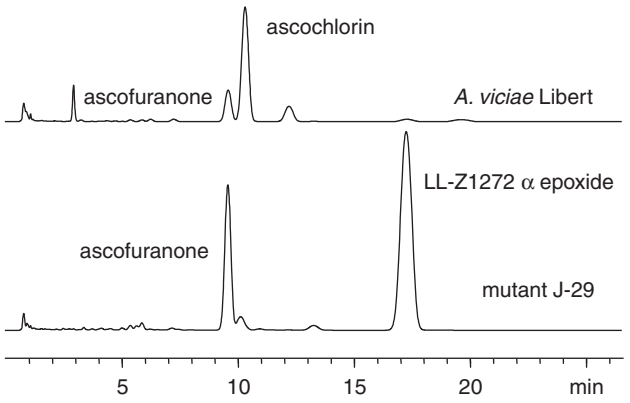


**Figure 4** HPLC profiles of metabolites produced by *A. viciae* Libert and mutant J-29 monitored at 295 nm.

(Figure 3), just as in the case of the enzymatic conversion of squalene 2, 3-oxide to lanosterol and cholesterol.[19] However, the epoxide, the expected intermediate to which the farnesyl chain with a terminal double bond was converted, had not been previously isolated. The isolation of LL-Z1272α epoxide supports the hypothesis of Ellestad *et al*., with the epoxide being converted into ascochlorin similarly as squalene oxide is converted into sterols. Thus, we are convinced that LL-Z1272α epoxide is a precursor of ascochlorin. Mutant J-29 produced the epoxide along with ascofuranone in an amount that was approximately one-half of that of the epoxide, suggesting that the activity of converting the epoxide to ascochlorin was severely blocked in the mutant and that the conversion into ascofuranone was less obstructed in it. If there were these branching pathways from the LL-Z1272α epoxide, the yield amounts of ascochlorin and ascofuranone might roughly correspond to the activity of each of the converting enzymes. In the future, it will be necessary to verify whether LL-Z1272α is converted into its epoxide by a specific enzyme and then to investigate whether the epoxide is converted into ascochlorin and ascofuranone separately by different branches of the biosynthetic pathway.

## METHODS

### Mutation and isolation of mutants

*A. viciae* Libert isolated from soil[1] was used as the parent strain and was maintained on a malt extract-yeast extract (MY) agar medium composed of glucose 1%, polypeptone 0.5%, yeast extract 0.3% and malt extract 0.3% at pH 6 in agar 1.8%. The strain grown on the MY agar medium at 28 °C for 7 days was harvested by centrifugation at 7300 *g* for 10 min and was washed once with 0.9% (w/v) NaCl solution. The short mycelial cells were suspended in the saline containing *N*-methyl-*N*′-nitro-*N*-nitrosoguanidine (NTG) at a final concentration of 10, 30 or 100 μg $l^{-1}$. After each cell suspension had been incubated with one of the above concentrations of NTG for 60 min at 28 °C, the cell was harvested by centrifugation, washed twice with saline, suspended in MY medium and incubated at 28 °C with gentle shaking for 2 h. Each cell suspension was appropriately diluted with saline and spread on the MY agar medium. After incubation at 28 °C for 7 days, a single colony from the colonies that appeared on the medium was transferred to the MY agar medium and maintained. About 400 mutant colonies were isolated with a certain concentration of NTG. For screening, the isolated fungal mutant was cultured in a thick test tube (φ 25 mm×20 cm) containing 20 ml of production medium (see following part), and the mycelium of each mutant strain was extracted with four volumes of MeOH to analyze for the presence of new metabolites. The production of new metabolites was monitored by HPLC. Each mutant that produced new ascochlorin-related compounds was repeatedly treated with different concentrations of NTG to generate further mutants that produced larger quantities of the new metabolites. The mutant J-29 was finally obtained after the parent strain had been mutated with successive concentrations of 10, 100, 100, 30 and 100 μg $l^{-1}$ NTG. Therefore, the mutant J-29 was selected from more than 2000 colonies.

### Fermentation of *A. viciae* mutant J-29

For production of LL-Z1272 α epoxide, the mutant J-29 was cultured in production medium composed of glucose 7.0%, polypeptone 0.3%, yeast extract 0.2%, $KH_2PO_4$ 0.05%, $MgSO_4{\cdot}7H_2O$ 0.05%, corn steep liquor 0.1%, $(NH_4)_2SO_4$ 0.1%, $CaCl_2{\cdot}2H_2O$ 0.2%, $CH_3COONa$ 0.5%, $CaCO_3$ 0.1% and one drop of Adekanol LG-109 (anti-foaming agent; Adeka, Tokyo, Japan). The fungus was aerobically cultured at 28 °C for 7 days in a 500-ml Erlenmeyer flask containing 50 ml of the production medium.

### HPLC analysis

To analyze the fungal products of isolated mutant strains, we cultured each mutant at 28 °C for 7 days in a 500-ml Erlenmeyer flask containing 50 ml of production medium. The mycelium of each mutant was harvested by centrifugation at 7300 *g* for 10 min and extracted with four volumes of MeOH. The extract was concentrated under reduced pressure and dissolved in a small amount of MeOH for analysis of products using a Shimadzu HPLC system, Model LC-VP (Shimadzu, Kyoto, Japan), equipped with an ODS column (YMC-Pack ODS-A302; 150×4.6 mm i.d.; YMC, Kyoto, Japan). The column was maintained at 40 °C and eluted isocratically with a mixture of acetonitrile–isopropyl alcohol–$H_2O$–acetic acid (350:200:450:2, v/v) at a flow rate of 2.0 ml $min^{-1}$. A small portion of the MeOH extract was subjected to HPLC using an automatic injection system, and separation was monitored at 295 nm. Representative HPLC chromatograms are shown in Figure 4. Ascochlorin and ascofuranone were determined by comparison with authentic compounds.

### Isolation and purification of LL-Z1272α epoxide

The mutant J-29 was cultured in production medium (4500 ml) and its mycelium was extracted with four volumes of MeOH. The extract was concentrated *in vacuo* and dissolved in brine. Thereafter, ascochlorin and its structurally related compounds were extracted with EtOAc and concentrated *in vacuo*. The extract (3.52 g) was passed through a silica gel 60 column (φ 35 mm×13 cm) with a mixture of EtOAc and *n*-hexane (1:5, v/v). The

fraction eluted with the mixture of solvents (2.56 g) was passed again through another silica gel 60 column ($\varphi$ 50 mm×26 cm), and four fractions, 1.35 g, 0.11 g, 0.74 g and 0.23 g, in the order eluted, were separated by the same mixture of EtOAc and *n*-hexane (1:5, v/v). The first fraction (1.35 g) was purified repeatedly by silica gel 60 column chromatography and was crystallized with difficulty. Finally, crystals with a pale yellow color (1.1 g) were obtained. From $^{1}$H-NMR and $^{13}$C-NMR analyses, the substance was elucidated to be LL-Z1272α epoxide. The second and fourth fractions were not analyzed further. The third fraction (0.74 g) was identical to ascofuranone on the basis of comparison of $^{1}$H-NMR spectra and the retention time of authentic ascofuranone on the HPLC chromatogram. After the fractions had been separated by silica gel 60 thin-layer chromatography with a mixture of EtOAc and *n*-hexane (1:5, v/v), the Rf values for ascochlorin, ascofuranone and LL-Z1272α epoxide were calculated to be 0.19, 0.25 and 0.31, respectively.

### Spectroscopic measurements

NMR spectra were recorded on a Jeol JNM-ECA 500 FT NMR system (Jeol, Tokyo, Japan), with $^{1}$HNMR at 500 MHz and $^{13}$C–NMR at 125 MHz, using deuterated solvent ($CDCl_3$). The melting point value was uncorrected. UV spectra were recorded on a Shimadzu UV-160A spectrophotometer, and IR spectra were measured with a Jasco FT/IR-7300 spectrometer linked to a WS/IR-7300 workstation (Jasco, Tokyo, Japan). Mass spectra were recorded with a Jeol SX-102A spectrometer in the FAB mode by using glycerol as matrix and polyethylene glycol as the internal standard. Optical rotation values were recorded with a Jasco DIP-1000 polarimeter.

### Inhibitory activity against *Candida albicans*

For determination of the inhibitory activity against *C. albicans* NBRC 1386, each solution of ascochlorin and LL-Z1272α epoxide, with the same concentration of 5 mg ml$^{-1}$, was applied to a paper disc ($\varphi$ 8 mm), and each paper disc was then placed onto YPD agar medium onto which *C. albicans* had been spread. The YPD medium was composed of yeast extract 1%, peptone 2% and glucose 2% at pH 7.2 in agar 1.8%.

## ACKNOWLEDGEMENTS

We are very grateful to Dr K Ando for providing *A. viciae* Libert and authentic compounds, ascochlorin and ascofuranone. We also thank Dr H Kondo (NRL Pharma) for discussion on the isolation of the epoxide. This work was partially supported by a grant from the New Energy and Industrial Technology Development Organization (NEDO), Japan.

1 Tamura, G., Suzuki, S., Takatsuki, A., Ando, K. & Arima, K. Ascochlorin, a new antibiotic, found by paper-disc agar-diffusion method. I. Isolation, biological and chemical properties of ascochlorin (Studies on antiviral and antitumor antibiotics. I). *J. Antibiot.* **21,** 539–544 (1968).
2 Sasaki, H., Okutomi, T., Hosokawa, T., Nawata, Y. & Ando, K. Ascofuranone, a new antibiotic from *Ascochyta viciae*. *Tetrahedron Lett.* **25,** 2541–2544 (1972).
3 Ellestad, G. A., Evans, R. H. Jr & Kunstmann, M. P. Some new terpenoid metabolites from an unidentified Fusarium species. *Tetrahedron* **25,** 1323–1334 (1969).
4 Kato, A., Ando, K., Tamura, G. & Arima, K. Cylindrochlorin, a new antibiotic produced by *Cylindrocladium*. *J. Antibiot.* **23,** 168–169 (1970).
5 Hayakawa, S., Minato, H. & Katagiri, K. The ilicicolins, antibiotics from *Cylindrocladium ilicicola*. *J. Antibiot.* **24,** 653–654 (1971).
6 Aldridge, D. C. *et al.* Metabolites of *Nectria coccinea*. *J. Chem. Soc.* [*Perkin I*] **17,** 2136–2141 (1972).
7 Kosuge, Y., Suzuki, A., Hirata, S. & Tamura, S. Structure of colletochlorin from *Colletotrichum nicotianae*. *Agric. Biol. Chem.* **37,** 455–456 (1973).
8 Cagnoli-Bellavita, N., Ceccherelli, P., Fringuelli, R. & Ribaldi, M. Ascochlorin: a terpenoid metabolite from *Acremonium luzulae*. *Phytochemistry* **14,** 807 (1975).
9 Kawagishi, H., Sato, H., Sakamura, S., Kobayashi, K. & Ui, T. Isolation and structure of a new diprenyl phenol, colletorin B produced by *Cephalosporium diospyri*. *Agric. Biol. Chem.* **48,** 1903–1904 (1984).
10 Takamatsu, S. *et al.* A novel testosterone 5α-reductase inhibitor, 8′,9′-dehydroascochlorin produced by *Verticillium* sp. FO-2787. *Chem. Pharm. Bull* **42,** 953–956 (1994).
11 Singh, S. B. *et al.* Chemistry and biology of cylindrols: novel inhibitors of Ras farnesyl-protein transferase from *Cylindrocarpon lucidum*. *J. Org. Chem.* **61,** 7727–7737 (1996).
12 Che, Y., Swenson, D. C., Gloer, J. B., Koster, B. & Malloch, D. Pseudodestruxins A and B: new cyclic depsipeptides from the coprophilous fungus *Nigrosabulum globosum*. *J. Nat. Prod.* **64,** 555–558 (2001).
13 Seephonkai, P., Isaka, M., Kittakoop, P., Boonudomlap, U. & Thebtaranonth, Y. A novel ascochlorin glycoside from the insect pathogenic fungus *Verticillium hemipterigenum* BCC 2370. *J. Antibiot.* **57,** 10–16 (2004).
14 Hosokawa, T., Sawada, M., Ando, K. & Tamura, G. Enhanced excretion of fecal neutral sterols and the hypocholesterolemic property of 4-*O*-methylascochlorin in mice. *Agric. Biol. Chem.* **44,** 2461–2468 (1980).
15 Hosokawa, T., Okutomi, T., Sawada, M., Ando, K. & Tamura, G. Unusual concentration of urine and prevention of polydipsia by fungal prenylphenols in DOCA hypertensive rats. *Eur. J. Pharmacol.* **69,** 429–438 (1981).
16 Hosokawa, T., Ando, K. & Tamura, G. An ascochlorin derivative, AS-6, potentiates insulin action in streptozotocin diabetic mice and rats. *Agric. Biol. Chem.* **46,** 2865–2869 (1982).
17 Magae, J., Hosokawa, T., Ando, K., Nagai, K. & Tamura, G. Antitumor protective property of an isoprenoid antibiotic, ascofuranone. *J. Antibiot.* **35,** 1547–1552 (1982).
18 Magae, J. *et al.* Antitumor and antimetastatic activity of an antibiotic, ascofuranone, and activation of phagocytes. *J. Antibiot.* **41,** 959–965 (1988).
19 Willett, J. D., Sharpless, K. B., Lord, K. E., van Tamelen, E. E. & Clayton, R. B. Squalene-2,3-oxide, an intermediate in the enzymatic conversion of squalene to lanosterol and cholesterol. *J. Biol. Chem.* **242,** 4182–4191 (1967).

The Journal of Antibiotics (2009) 62, 575–580

www.nature.com/ja

ORIGINAL ARTICLE

# A novel isoquinoline alkaloid, DD-carboxypeptidase inhibitor, with antibacterial activity isolated from *Streptomyces* sp. 8812. Part I: Taxonomy, fermentation, isolation and biological activities

Jolanta Solecka[1], Aleksandra Rajnisz[1] and Agnieszka E Laudy[2]

**A novel isoquinoline alkaloid of molecular formula $C_{10}H_9NO_4$, labeled JS-1, was isolated from the culture broth of *Streptomyces* sp. 8812. It was purified by acetone protein precipitation from the culture supernatant, followed by anion exchange and C18 RP HPLC columns. JS-1 is an inhibitor of exocellular DD-carboxypeptidases/transpeptidases (DD-peptidases) 64-575 II from *Saccharopolyspora erythraea* 64-575 II, and R39 from *Actinomadura* R39. JS-1 exhibits activity against Gram-negative bacteria, such as *Bordetella bronchiseptica*, *Stenotrophomonas maltophilia*, *Proteus vulgaris*, *P. mirabilis*, *Burkholderia cepacia* and *Acinetobacter baumanii*, with MIC values 10–160 μg ml$^{-1}$, and against Gram-positive bacteria, such as *Staphylococcus aureus*, with MIC values 40–206 μg ml$^{-1}$.**
*The Journal of Antibiotics* (2009) **62,** 575–580; doi:10.1038/ja.2009.85; published online 28 August 2009

**Keywords:** antibacterial agent; DD-carboxypeptidase inhibitor; isoquinoline alkaloid; JS-1

## INTRODUCTION

The increasing bacterial resistance to antibiotics is at present a serious therapeutic problem. Multiresistant pathogenic bacteria occur very frequently.[1] Hence, there is a necessity for the discovery of new classes of antibiotics for the treatment of drug-resistant bacterial infections. Apart from combinatorial chemistry, rational drug design and computer-assisted design technology, one of the solutions to bacterial resistance involves screening for microorganisms producing novel antimicrobial drugs.[2,3] Currently, the majority of antibacterial agents in clinical use are either microbial natural products or one of their analogs.[4] Streptomycetes are well-known producers of antibiotics and other bioactive metabolites. More than half (56%) of all bacterial metabolites consist of derivatives of amino acids, peptides, peptolides and polypeptides.[5] The purpose of this study was to search for novel antimicrobial agents, specifically inhibitors of DD-peptidases (EC 3.4.16.4). DD-carboxypeptidases/transpeptidases are the enzymes involved in peptide cross-linking during the last stage of bacterial cell wall peptidoglycan biosynthesis.[6,7] Enzymes participating in cell wall biosynthesis have proved to be excellent targets for antibacterial agents because the cell wall pathway is conserved among bacterial pathogens and is absent in mammalian cells. β-Lactam antibiotics are the most important class of DD-peptidases/penicillin-binding proteins inhibitors and antimicrobial agents.[6] However, resistance mechanisms of pathogenic bacteria, for example, changes in penicillin-binding proteins and production of β-lactamases, render the β-lactam antibiotics ineffective. In our screening program for novel inhibitors of DD-peptidases from microbial secondary metabolites, we used DD-peptidase 64-575 II[8,9] from our collection of streptomycetes strains. A novel compound having antibacterial activity, DD-peptidase inhibitor, labeled JS-1, a member of isoquinoline alkaloids, was isolated from the culture broth of *Streptomyces* sp. 8812. In this paper, we describe the taxonomy and fermentation of *Streptomyces* sp. 8812 and the isolation procedure of JS-1. We also characterize the biological properties of this compound.[10] The physico-chemical properties and structure elucidation of JS-1 are described in the following paper of this issue.[11] The structure of the discovered alkaloid is shown below (Figure 1).

## RESULTS AND DISCUSSION

### Taxonomy of the producing strain

The strain *Streptomyces* sp. 8812 forms well-developed and branching substrate mycelium and aeral mycelium. The culture characteristics and carbon utilization of sp. 8812 are shown in Table 1. Good growth was observed on inorganic salts–starch agar, on glycerol–asparagine agar and Czapek's agar. The best culture medium for this strain was yeast extract–malt extract agar and tyrosine agar on which it grew

[1]Independent Laboratory of Streptomycetes and Fungi Imperfecti, National Institute of Public Health—National Institute of Hygiene, Warsaw, Poland and [2]Department of Pharmaceutical Microbiology, Medical University of Warsaw, Warsaw, Poland
Correspondence: Dr J Solecka, Independent Laboratory of Streptomycetes and Fungi Imperfecti, National Institute of Public Health—National Institute of Hygiene, Chocimska 24, Warsaw 00-791, Poland.
E-mail: jsolecka@pzh.gov.pl
Received 6 May 2009; revised 24 July 2009; accepted 3 August 2009; published online 28 August 2009

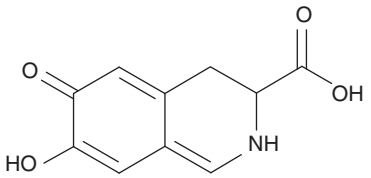


**Figure 1** The structure of the alkaloid, JS-1.

**Table 1 Cultural characteristics and carbon utilization of *Streptomyces* sp. 8812**

| *Medium* | *Growth* | *Aerial mycelium* | *Reverse side color* | *Melanin* |
|---|---|---|---|---|
| Yeast extract–malt extract agar | Abundant | R7a, R6a | Or3r | – |
| Inorganic salts–starch agar | Good | Oc7m | O4b | – |
| Glycerol–asparagine agar | Good | Oc7a | Oc7a | – |
| Tyrosine agar | Abundant | R5a | R7s | + |
| Czapek's agar | Good | Coo7c | Coo7c | – |
| *Carbon utilization* | | | | |
| D-Glucose | ++ | | | |
| D-Xylose | + | | | |
| L-Arabinose | ++ | | | |
| L-Rhamnose | – | | | |
| D-Fructose | ++ | | | |
| D-Mannitol | ++ | | | |
| D-Sucrose | – | | | |
| Raffinose | + | | | |
| I-Inositol | – | | | |
| Cellulose | – | | | |


**Figure 2** Scanning electron micrograph of the spore chain of *Streptomyces* sp. 8812 grown on yeast–malt agar for 14 days. Bar represents 2.0 µm.

abundantly. Substrate and aeral mycelium color were medium dependent. Spore chains were of the open loop (*Retinaculum apertum*) type with smooth surface and spore dimensions of 0.65–0.8 µm×1.3–1.5 µm (Figure 2).

From the characteristics stated above, the strain 8812 was identified as *Streptomyces* sp. This strain was deposited in the Polish Collection of Microorganism, Wroclaw, under the name of *Streptomyces* sp. 8812, with an accession number B/00017.

Culture broth (5 L)
|
Supernatant
| Protein precipitation with acetone
BioLogic System, IRA-400 (AcO-)
| 0-2 M AcOH
BioLogic System, Atlantis dC18
| 9-11 % phase B [phase B, $CH_3CN$ - 0.1 % TFA,
| 30 : 70 (v/v)]; phase A, 0.05 % TFA
HPLC, Atlantis dC18
| 2 % phase B [phase B, $CH_3CN$ - 0.05 % TFA,
| 20 : 80 (v/v)]; phase A, 0.05 % TFA
JS-1

**Figure 3** Isolation and purification of JS-1 under guidance of DD-peptidase 64-575 II inhibition reaction.

The culture broth was centrifuged (8000 *g* for 60 min at 4 °C; Beckman Coulter, Sykesville, MD, USA) to obtain the supernatant, followed by acetone precipitation of proteins (Figure 3). The precipitated proteins were centrifuged (8000 *g* for 30 min at 4 °C; Beckman) and discarded. The acetone solution was evaporated under reduced pressure to afford an aqueous solution, which was frozen and lyophilized (24 h, Beta 1-8, Christ, Osterode, Germany).

The crude material (22 g) was dissolved in deionized water (200 ml), applied to an anion exchange resin IRA-400 ($AcO^-$) (Supelco, Bellefonte, PA, USA) column 5×25 cm and washed with deionized water (1.5 l). Chromatography was performed using the BioLogic system (Bio-Rad, Hercules, CA, USA) at flow rates of 9.9 ml $min^{-1}$ and detection by UV absorption at 254 nm. Elution was performed with a stepwise gradient of aqueous acetic acid (0.5, 1, 2 M, 1 l each) and 6 ml fractions were collected. The active compound (fractions exhibiting an inhibitory effect on DD-peptidase activity) was eluted with ~0.5 M aqueous acetic acid and lyophilized to yield the partially purified material (140 mg). This procedure was repeated 4 times and 560 mg of the material was obtained.

Further purification of JS-1 was carried out by the BioLogic System (Bio-Rad) on a semi-preparative modified reversed-phase column (Atlantis, dC18, 10×250 mm, 10 µm, Waters, Milford, MA, USA); UV detection at 214 nm; flow rate of 4.7 ml $min^{-1}$; mobile phase: isocratic phase A: 0.05% trifluoroacetic acid (10 ml), and linear gradient from 0 to 19% of phase B (phase B was $CH_3CN$–0.1% trifluoroacetic acid, 30:70 (v/v)), 175 ml. The most active fractions obtained at 9–11% of phase B, exhibiting 100% inhibition of DD-peptidase activity, were collected. The fractions eluted in 22 repeated runs were pooled and lyophilized to yield 40 mg of powder.

This was then subjected to HPLC (Atlantis, dC18, 4.6×250 mm, 5 µm, Waters); detection by UV at 214 nm; flow rate of 1 ml $min^{-1}$; mobile phase: 2% phase B (B: $CH_3CN$–0.05% trifluoroacetic acid, 20:80 (v/v)), phase A (0.05% trifluoroacetic acid). Under these conditions, JS-1 was eluted at a retention time of 30.4 min. The fractions eluted in 80 repeated runs were pooled and lyophilized to yield 7 mg of yellow powder.

Further purification of JS-1 was carried out by the same procedure as described previously, namely, the detection by diode array detection (Figure 4). JS-1 of 5 mg was obtained.

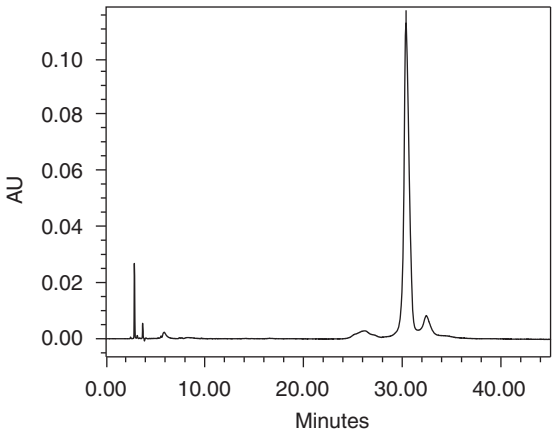


**Figure 4** HPLC profile of the purified JS-1 compound.

### Inhibitory effect of JS-1 on DD-peptidases

JS-1 exhibited inhibitory effects on DD-peptidases 64-575 II and R39. The concentrations of the compound necessary to inhibit DD-carboxypeptidases by 50% ($IC_{50}$) were calculated. The $IC_{50}$ values of JS-1 for these enzymes were 4.7 and 6.0 μM, respectively. The $IC_{50}$ values of β-lactam antibiotics for DD-carboxypeptidase 64-575 II were compared with the $IC_{50}$ value of JS-1 for DD-carboxypeptidase 64-575 II, for example, the $IC_{50}$ values of carbenicillin, cephalothin and imipenem for DD-carboxypeptidase 64-575 II were 1.4, 1.1 μM and 58 nM, respectively.[9] The $IC_{50}$ value of 6-aminopenicillanic acid for DD-carboxypeptidase R39 was comparable with the $IC_{50}$ value of JS-1 for this enzyme.[12] The $IC_{50}$ values of β-lactam antibiotics such as 6-aminopenicillanic acid, carbenicillin and cephalothin for DD-carboxypeptidase R39 were 5.7, 1.95 μM and 42 nM, respectively.[12] Until today, there have not been any described inhibitors of DD-peptidases from the group of isoquinoline alkaloids. It is assumed that JS-1 may inhibit cell wall biosynthesis by disturbing the cross-linking of peptidoglycan, analogous to the mechanism of action of β-lactam antibiotics.

### Inhibitory effect of JS-1 on β-lactamase

As the examined alkaloid has been shown to inhibit DD-peptidase 64-575 II activity, similar to clavulanic acid,[9] which is a known inhibitor of β-lactamases, an inhibition test was carried out for this enzyme. JS-1 did not show inhibitory activity against β-lactamase from *Bacillus cereus*.

### Inhibitory effect of JS-1 on common proteolytic enzymes

To examine the specificity of the JS-1 compound, inhibition assays were performed for a range of common proteolytic enzymes. It was determined that at a concentration of 65 μM, the JS-1 alkaloid causes a 100% inhibition of DD-peptidase 64-575 II and DD-peptidase R39, whereas the rest of the enzymes remained active even in a twofold higher concentration. Only pepsin lost 10% of its activity, whereas the activity of papain, a proteolytic enzyme with a disulfide bond in its active center, was inhibited by 7%. The obtained results on the examination of the JS-1 alkaloid implied it to be a specific inhibitor of DD-peptidases.

### Hemolytic activity

No hemolytic activity was observed on human erythrocyte.

**Table 2 MICs and MBCs of alkaloid JS-1 against Gram(+), Gram(−) bacteria and yeast[a]**

| *Microorganism* | *MIC, (μg ml$^{-1}$)* | *MBC, (μg ml$^{-1}$)* |
|---|---|---|
| *S. aureus* ATCC 25923 | 80 | 80 |
| *S. aureus* ATCC 43300 | 40 | 80 |
| *E. faecalis* ATCC 29219 | >320 | >320 |
| *B. bronchiseptica* ATCC 4617 | 10 | 20 |
| *A. baumanii* ATCC 19606 | 160 | 160 |
| *K. pneumoniae* ATCC 13882 | >320 | >320 |
| *B. cepacia* ATCC 25416 | 160 | 160 |
| *P. aeruginosa* ATCC 27853 | >320 | >320 |
| *S. maltophilia* ATCC 13637 | 160 | 160 |
| *P. vulgaris* ATCC 6896 | 160 | 160 |
| *P. mirabilis* ATCC 12453 | 160 | 160 |
| *E. coli* ATCC 25922 | >320 | >320 |
| *E. coli* ATCC BAA-198 | >320 | >320 |
| *B. subtilis* ATCC 6633 | >206 | >206 |
| *B. stearothermophilus* ATCC 7953 | >206 | >206 |
| *C. albicans* ATCC 90028 | >320 | >320 |
| *C. parapsilosis* ATCC 22019 | 206 | >206 |
| *C. krusei* ATCC 6258 | 206 | >206 |

[a]MIC's of the reference compounds: penicillin G against *S. aureus* ATCC 43300, 5.0 μg ml$^{-1}$; polimyxin B against *P. aeruginosa* ATCC 27853, 1.2 μg ml$^{-1}$; amphotericin against *C. krusei*, 1 μg ml$^{-1}$.

### Genotoxicity

*Bacillus subtilis* M45 (rec$^-$) is devoid of the recombinant-based DNA repair mechanism and, therefore, is much more susceptible to genotoxic damage than its rec$^+$ counterpart, which is evidenced by a wider zone of growth inhibition for this strain around the reference genotoxin (4-nitroquinoline *N*-oxide)-carrying discs. The diameter of the zone of growth inhibition reached 24 mm for the rec$^-$ strain and 12 mm for the rec$^+$ strain. The examined JS-1 alkaloid did not inhibit the growth of the tested *B. subtilis* strains and, hence, was determined as nongenotoxic. The lack of genotoxic features of JS-1 allows the consideration of potential modifications of the naturally isolated molecule to increase its antibacterial and antifungial activity.

### Antimicrobial activity

JS-1 was tested against three Gram-positive bacteria, reference bacteria (*Staphylococcus aureus* subsp. *aureus* ATCC 25923; *S. aureus* subsp. *aureus* ATCC 43300 resistant to methicillin; and *Enterococcus faecalis*), 12 Gram-negative bacteria (*Bordetella bronchiseptica*; *Stenotrophomonas maltophilia*; *Proteus vulgaris* and *P. mirabilis*; *Burkholderia cepacia; Acinetobacter baumanii; Klebsiella pneumoniae; Pseudomonas aeruginosa; Escherichia coli* ATCC 25922; *E. coli* ATCC BAA-198-producing extended spectrum β-lactamase ESBL TEM-26; *Bacillus subtilis; B. stearothermophilus*) and three yeasts (*Candida albicans; C. parapsilosis* and *C. krusei*) by the broth microdilution method. MIC and MBC are presented in Table 2. JS-1 exhibited the highest activity against *B. bronchiseptica* (MIC 10 μg ml$^{-1}$) and *S. aureus* strains, including methicillin-resistant *S. aureus* (MIC 40–80 μg ml$^{-1}$). Bacteria *E. faecalis, K. pneumoniae, E. coli* and *P. aeruginosa,* and the yeast *C. albicans* proved insensitive (MIC >320 μg ml$^{-1}$).

Antibiotic resistance has reached a crisis point in many hospitals around the world. The problem is related to methicillin-resistant *S. aureus* and to many multidrug-resistant Gram-negatives.[13–15] Therefore, new classes of potent antimicrobial agents, including natural products, are needed to resolve this problem.

**Table 3 MICs of alkaloid JS-1 against clinical isolates of *S. aureus***

| *Strains* | *MIC, ($\mu g\,ml^{-1}$)* | *Number of strains* |
|---|---|---|
| *S. aureus* (methicillin-resistant *S. aureus*) | 80 | 4 |
| | 103 | 6 |
| | 206 | 12 |
| | >206 | 5 |
| *S. aureus* (methicillin-sensitive *S. aureus*) | 103 | 1 |
| | 206 | 2 |
| | >206 | 1 |

In addition, the activity of JS-1 alkaloid on 31 clinical isolates of *S. aureus*, including 27 *S. aureus* methicillin-resistant *S. aureus* strains, was examined. MIC values are presented in Table 3. Of the clinical isolates, 30% exhibited sensitivity to the new compound (MIC 80–103 $\mu g\,ml^{-1}$). The obtained MIC values of JS-1 alkaloid for the clinical strains were similar to the MIC values determined for the *S. aureus* ATCC 25923 reference strain (MIC 80 $\mu g\,ml^{-1}$). No differences between the sensitivity of clinical methicillin-resistant *S. aureus* and methicillin-sensitive *S. aureus* strains toward JS-1 alkaloid have been observed.

On the contrary, the relatively poor MIC values of JS-1 in comparison with the good inhibitory activity of DD-peptidases was most probably associated with the weak permeability of the bacterial cell envelopes to the examined alkaloid. The inhibitory activity of JS-1 on DD-peptidases is comparable with the activity of certain β-lactam antibiotics.[9] Yet, in bacteria, DD-peptidases are known to occur in the periplasmic space. Hence, most probably the structure of JS-1 (Figure 1), which suggests low lipophility of the molecule, impedes its transport to the periplasmic space.

JS-1, the novel DD-carboxypeptidases inhibitor isolated from the culture broth of *Streptomyces* sp. 8812, belongs to isoquinoline alkaloids, some of which exhibit antibacterial activity (for example, plant origin products such as berberine, canadaline, canadine, (+)-*N*-(methoxycarbonyl)-*N*-norboline).[16,17] Some of them show an activity toward *S. aureus*, which is analogous to JS-1. Iwasa *et al.*[18] described antimicrobial, antimalarial, cytotoxic and anti-HIV activities of simple, natural and synthetic isoquinoline and benzylisoquinoline alkaloids. Some simple alkaloids were significantly active in each assay; especially those with a quaternary nitrogen atom of isoquinolinum or dihydroisoquinolinum type may contribute to enhanced potency in the first three types of activites.[18]

This study reports the discovery of a simple isoquinoline alkaloid, JS-1, and its biological activity.

Specific inhibition of DD-peptidase activity (occurring solely in *Prokaryota*) by JS-1 alkaloid implies the directed action of this compound and its derivatives on bacteria. Moreover, the demonstrated lack of both genotoxic and hemolytic activities toward human blood cells suggests the possible application of the JS-1 alkaloid as an initial compound in the search of a potentially new drug group. The active compound JS-1 must be studied further to determine its possible biological activity and toxicity thereof, and to resolve the mode of antibacterial action of isoquinoline alkaloids. Moreover, a synthetic modification of the natural molecule may generate new compounds with improved antibacterial activity.

## METHODS

### Taxonomy

The JS-1-producing actinomycetes strain, *Streptomyces* sp. 8812, was isolated from soil in Brasil. The strain, *Streptomyces* sp. 8812, was grown at 28 °C for 14 days on inorganic salts–starch agar, glycerol–asparagine agar, yeast extract–malt extract agar, tyrosine agar and on Czapek's medium and was examined visually to determine substrate mycelium pigmentation and spore color. Colors were determined by using the H. Prauser Code.[19] Morphological characteristics were observed with a scanning electron microscope (Jeol JSM-35, Tokyo, Japan). Standard biochemical properties of this strain were tested according to the methods of Williams *et al.*[20] All carbon sources for carbon utilization tests were tested at the concentrations recommended by Shirling and Gottlieb[21] and Williams *et al.*[20]

### Fermentation

A slant culture of strain 8812 was inoculated into a 500-ml Erlenmeyer flask containing 40 ml of liquid medium consisting of tryptone (Difco, Sparks, MD, USA) 17 g, peptone (Difco) 4 g, yeast extract (Difco) 5 g, corn steep liquor (Cerestar, Milan, Italy) 10 g, lactose 10 g, $CaCO_3$ 3 g, $K_2HPO_4$ 4 g, $KH_2PO_4$ 2 g and $MgSO_4{\cdot}7H_2O$ 0.5 g in 1.0 l of tap water, pH 6.7. The inoculated flasks were incubated for 24 h on a rotary shaker (220 r.p.m.) at 28 °C. A volume of 4 ml of the seed culture was transferred into 500 ml flasks containing 36 ml of the same medium, and incubated on a rotary shaker (220 r.p.m.) at 28 °C. Fermentation was carried out for 22 h. The production of JS-1 was analyzed by testing for DD-carboxypeptidase 64-575 II inhibition. After 22 h of fermentation, the amount of JS-1 in the broth filtrate reached a maximum (100% inhibition of DD-peptidase 64-575 II activity).

### Assay of DD-carboxypeptidase activity

Enzyme activity was measured as described previously.[22] Samples for assay of DD-carboxypeptidase activity consisted of 10 µl of exocellular DD-carboxypeptidase 64-575 II (50 µM) from *Saccharopolyspora erythraea* 64-575 II (Polish Collection of Microorganism, Wroclaw, accession number B/00018),[9,23] 10 µl of the substrate solution containing 2.98 $mg\,ml^{-1}$ $N^{\alpha}$,$N^{\varepsilon}$-diacetyl-L-lysyl-D-alanyl-D-alanine in 0.1 M phosphate buffer, pH 8.0, and 20 µl of 0.1 M phosphate buffer, pH 8.0. Standard sample contained 20 µl of D-alanine in distilled water. Samples were incubated for 30 min at 37 °C and then boiled for 2 min. After cooling, 77 µl of the reaction mixture was added, and all samples were incubated for 10 min at 37 °C. Reaction mixture for assay of DD-carboxypeptidase activity consisted of 60 µl of 0.05 $mg\,ml^{-1}$ flavin adenine dinucleotide in 0.1 M phosphate buffer, pH 8.0, 10 µl of 0.2 $mg\,ml^{-1}$ horseradish peroxidase (250–330 $U\,mg^{-1}$) in distilled water, 5 µl of 5 $mg\,ml^{-1}$ of *o*-dianisidine–HCl in distilled water and 2 µl of 11.9 $mg\,ml^{-1}$ of D-amino acid oxidase from hog kidney (20.7 $U\,mg^{-1}$) in 0.1 M phosphate buffer, pH 8.0. Finally, 350 µl of a mixture consisting of methanol, distilled water and sulfuric acid (5:5:6 by volume) was added to each sample. Absorbance of the resulting solution was measured spectrophotometrically at 540 nm (Jasco V-630, Tokyo, Japan).

### Assay of JS-1 inhibitory activity on DD-peptidases

Inhibition of DD-peptidase 64-575 II by the JS-1 compound was evaluated as follows. To detect the active compound during cultivation of strain 8812 and in subsequent stages of JS-1 purification, the DD-peptidase 64-575 II inhibition test was carried out. Mixtures of 10 µl of DD-peptidase 64-575 II (50 µM), 10 µl of the supernatant (or aliquots of concentrated fractions during purification steps) and 10 µl of 0.1 M phosphate buffer pH 8.0 were incubated for 30 min at 37 °C. After incubation, 10 µl of the substrate solution was added to 30 µl of each sample and the resulting mixtures were incubated again. The rest of the procedure was performed as mentioned above. To determine the inhibitory activity of the purified JS-1 alkaloid on DD-peptidase 64-575 II, the assay was performed as described above with the only exception being that the enzyme was incubated with JS-1 at different concentrations ranging from 0.1 mM to 0.1 µM (instead of the supernatant). The inhibition of DD-peptidase was expressed as $IC_{50}$ values, molar concentrations of JS-1 necessary to inhibit the DD-peptidase activity by 50%.

The inhibition of exocellular DD-peptidase R39 from *Actinomadura* R39[24] by JS-1 was performed as described previously. DD-peptidase R39 of 10 µl (Penzym test, UCB Bioproducts, Braine-l'Alleud, Belgium)[25] was used in the reaction mixtures.

### Assay of the universal protease activity

Pancreatic elastase (type IV) from porcine pancreas (0.017 U ml$^{-1}$) was assayed by monitoring the release of p-nitroanilide at 410 nm from 0.3 mM *N*-succinyl-Ala-Ala-Val-Ala p-nitroanilide in 0.1 M Tris buffer, pH 8.0, at 25 °C.[26]

Carboxypeptidase A from bovine pancreas (0.4 U ml$^{-1}$) was assayed by examining hydrolysis at 254 nm of 1 mM Hippuryl-L-Phe in 0.025 M Tris buffer with 0.5 M NaCl, pH 7.5, at 25 °C.[27]

Thrombin from bovine plasma (3.7 U ml$^{-1}$) was assayed by monitoring the release of p-nitroanilide at 410 nm from 1 mM *N*-Benzoyl-L-Arg p-nitroanilide in 10 mM HEPES, 10 mM Tris buffer, with 0.1 M NaCl, 0.1% $PEG_{6000}$ and 1% dimethylsulfoxide, pH 7.8, at 25 °C.[28]

Trypsin from porcine pancreas (73 U ml$^{-1}$) was assayed by monitoring the release of p-nitroanilide at 410 nm from 1 mM *N*-Benzoyl-D,L-Arg p-nitroanilide in 0.1 M Tris buffer with 20 mM $CaCl_2$, 1% dimethylsulfoxide, pH 8.0, at 25 °C.[29,30]

Papain from Papaya latex (2.5 U ml$^{-1}$) was assayed by examining the release at 410 nm of p-nitroanilide from 1 mM *N*-Benzoyl-L-Arg p-nitroanilide in 0.1 M phosphate buffer with 2 mM Cys, 2 mM EDTA, 1% dimethylsulfoxide, pH 7.0, at 25 °C.[31] Earlier, papain was activated by incubation at room temperature in the same buffer without dimethylsulfoxide for 1.5 h.

Endoproteinase Glu-C from *S. aureus* V8 (6.7 U ml$^{-1}$) was assayed by monitoring the release of p-nitroanilide from 1 mM Ac-Glu-p-nitroanilide in 0.1 M Tris buffer, pH 8.0, containing 2% dimethyl formamide and 2 mM $CaCl_2$, at 37 °C.[32]

The activity of pepsin from porcine gastric mucosa (30.3 U ml$^{-1}$) was assayed using 2.5% bovine hemoglobin as substrate, at acidic pH and at 37 °C. After 10 min of incubation, the reaction was stopped by the addition of 5% trichloroacetic acid. The samples were centrifuged and the resulting supernatant was analyzed at 280 nm.[33]

All enzyme assays were performed using a spectrophotometer (Jasco V-630).

Assessment of the inhibition of the above-listed proteolytic enzymes was carried out by preincubating the enzymes with JS-1 at a concentration of 65 μM, which causes 100% inhibition of DD-peptidase 64-575 II activity and, additionally, at a concentration twofold greater.

### Assay of β-lactamase activity

Inhibition of penicillinase (Penase, $5\times10^6$ IU ml$^{-1}$) by the JS-1 compound was evaluated on the basis of the method described in literature.[34] A mixture of β-lactamase and JS-1 in 0.1 M phosphate buffer, pH 7.0, was incubated for 30 min at 37 °C; thereafter, nitrocephin was added and the mixture was incubated for an additional 10 min at 37 °C. Subsequently, absorbance was measured at 482 nm.

### Antimicrobial activity

The antimicrobial spectrum of JS-1 was evaluated by the MIC method using the serial twofold dilution method under standard conditions as described in the Committee Laboratory Standards (CLSI) reference method M7-A7.[35] Test reference bacterial strains are presented in Table 2. The organisms were cultivated according to ATCC recommendation. Thirty-one clinical isolates of *S. aureus*, including 27 methicillin-resistant *S. aureus* strains, were cultivated on tryptic soy agar. All strains were incubated for 24 h at 37 °C.

The reference method (broth microdilution susceptibility test) was as follows: The compound JS-1 was dissolved in double-distilled water. A series of the twofold JS-1 alkaloid dilutions were diluted with cation-adjusted Mueller–Hinton broth. Aliquots of 95 μl were dispensed into microdilution sterile plates (Mar-Four). Then, 5 μl of bacteria inoculum, containing $5\times10^4$ CFU ml$^{-1}$, was added. The final concentration of the JS-1 compound ranged from 320 to 5 μg ml$^{-1}$ (or 206–12.9 μg ml$^{-1}$), all in twofold dilution steps. The experiments for each sample were conducted in triplicate. Polymyxin B and penicillin G were used as controls (from 8 to 0.15 μg ml$^{-1}$). The plates were incubated at 37 °C (35 °C) for 18–24 h depending on the bacterial strain. MIC was defined as the lowest drug concentration that reduced growth by 100%. For the MBC assay, aliquots (10 μl) of each culture without visible growth were transferred onto tryptic soy agar and incubated during 24 h at 37 °C.

Reference yeasts were presented in Table 2. *Candida* sp. was cultivated according to ATCC references. The broth microdilution susceptibility test was performed as described in Clinical and Laboratory Standards Institute, reference method M27-A2 (1).[36]

### Hemolysis test

The hemolysis test was evaluated following the literature method.[37] Red blood cells prepared in phosphate-buffered saline were suspended to correspond to a hematocrit of 1% in JS-1 alkaloid at final concentrations of 0.6 and 2.4 mM and were incubated for 30, 60, 90, 120 and 180 min at 23 °C.

### Genotoxicity

For genotoxicity research, two genetically modified *B. subtilis* strains, M45 rec$^-$ and H17 rec$^+$, obtained from Dr Sadaie were studied.[38–40] The JS-1 alkaloid was examined by the disc-diffusion method according to Kada's procedure.[38,39] Sterile filter paper discs (9 mm diameter, Whatman no. 3, Maidstone, UK) were dripped with tested JS-1 solution to load 206 μg of the compound per disc. As a standard, 4-nitroquinoline *N*-oxide (2 μg per disc) was used. Results of the genotoxicity test were read after 18 h of incubation of the discs at 35 °C.

## ACKNOWLEDGEMENTS

We are grateful to Professor Jean-Maria Ghuysen (Centre for Protein Engineering and Laboratoire d'Enzymologie, Université de Liège, Belgium) for kindly providing us with DD-peptidase R39. We thank Professor Stefan Tyski (Department of Pharmaceutical Microbiology, Medical University of Warsaw, Warsaw, Poland) for obtaining clinical strains of *S. aureus*.

1 Walsh, C. T. *Antibiotics: Actions, Origin, Resistance* (ASM Press, Washington, DC, 2003).
2 Baker, D. D., Chu, M., Oza, U. & Rajgarhia, V. The value of natural products to future pharmaceutical discovery. *Nat. Prod. Rep.* **24,** 1225–1244 (2007).
3 Imanaka, H. Screening microbial products for medicine. *Actinomycetologica* **14,** 22–26 (2001).
4 Singh, M. P. & Greenstein, M. Antibacterial leads from microbial natural products discovery. *Curr. Opin. Drug Disc. Develop.* **3,** 167–176 (2000).
5 Berdy, J. Bioactive microbial metabolites. *J. Antibiot.* **58,** 1–26 (2005).
6 Waxman, D. J. & Strominger, J. L. Penicillin-binding proteins and the mechanism of action of β-lactam antibiotics. *Ann. Rev. Biochem.* **52,** 825–969 (1983).
7 Ghuysen, J.-M. Bacterial active-site serine penicillin-interactive proteins and domains: mechanism, structure, and evolution. *Rev. Infect. Dis.* **10,** 726–732 (1988).
8 Kurzatkowski, W., Solecka, J., Filipek, J., Kurzatkowski, J. D. & Kurylowicz, W. Streptomycetes excreting DD-carboxypeptidases. *Appl. Microbiol. Biotechnol.* **33,** 452–454 (1990).
9 Solecka, J. & Kurzatkowski, W. Affinity of exocellular DD-carboxypeptidase/transpeptidase from *Saccharopolyspora erythraea* PZH 64-575 to beta-lactam compounds. *Med. Dosw. Mikrobiol.* **51,** 151–165 (1999).
10 Solecka, J. & Kozerski, L. A new inhibitor of DD-peptidase and its use as antibiotic or anticancer drug. PCT/WO 2009/028972 A1, 5 March (2009).
11 Solecka, J. *et al.* A novel isoquinoline alkaloid, DD-carboxypeptidase inhibitor, with antimicrobial activity isolated from *Streptomyces* sp. 8812. Part II: Physico-chemical properties and structure elucidation. *J. Antibiot.* (e-pub ahead of print 28 August 2009; doi:10.1038/ja.2009.86).
12 Dusart, J. *et al.* DD-Carboxypeptidase-transpeptidase and killing site of β-lactam antibiotics in *Streptomyces* strains R39, R61, and K11. *Antimicrob. Ag. Chemother.* **3,** 181–187 (1973).
13 Gould, I. M. The epidemiology of antibiotic resistance. *Int. J Antimicrob. Agents* **32S,** S2–S9 (2008).
14 Casey, A. L., Lambert, P. A. & Elliott, T. S. J. Staphylococci. *Int. J Antimicrob. Agents* **29** (Suppl. 3), S23–S32 (2007).
15 Denton, M. Enterobacteriaceae. *Int. J Antimicrob. Agents* **29**(Suppl. 3), S9–S22 (2007).
16 Scazzocchio, F., Cometa, M. F., Tomassini, L. & Palmery, M. Antibacterial activity of *Hydrastis canadensis* extract and its major isolated alkaloids. *Planta Med.* **67,** 561–564 (2001).
17 Feng, T., Xu, Y., Cai, X.-H., Du, Z.-Z. & Luo, X.-D. Antimicrobially active isoquinoline alkaloids from *Litsea cubeba*. *Planta Med.* **75,** 76–79 (2009).
18 Iwasa, K. *et al.* Simple isoquinoline and benzylisoquinoline alkaloids as potential antimicrobial, antimalarial, cytotoxic, and anti-HIV agents. *Bioorg. Med. Chem.* **9,** 2871–2884 (2001).
19 Prauser, H. Aptness and application of colour codes for exact description of colours of streptomycetes. *Z. Allg. Mikrobiologie* **4,** 95–98 (1964).
20 Williams, S. T., Goodfellow, M. & Alderson, G. Genus *Streptomyces* Waksman and Henrici 1943. in *Bergey's Manual of Systematic Bacteriology*, Vol. 4 (ed. Williams, S. T.) 2452–2492 (Williams & Wilkins, Baltimore, 1989).
21 Shirling, E. B. & Gottlieb, D. Methods for characterization of *Streptomyces* species. *Int. J. Syst. Bacteriol.* **16,** 313–340 (1966).

22 Frère, J. M., Leyh-Bouille, M., Ghuysen, J. M., Nieto, M. & Perkins, H. R. Exocellular DD-carboxypeptidases/transpeptidases from Streptomyces. *Methods Enzymol.* **45,** 610–636 (1976).
23 Solecka, J., Łysek, R., Furman, B., Chmielewski, M. & Kurzątkowski, W. Practical use of DD-peptidase 64-575 for assay inhibition activity of natural and synthetic β-lactam compounds. *Acta. Poloniae Pharmaceutica* **60,** 115–118 (2003).
24 Frère, J.-M. *et al*. Molecular weight, amino acid composition and physicochemical properties of the exocellular DD-carboxypeptidase-transpeptidase of *Streptomyces* R39. *Biochem. J.* **143,** 233–240 (1974).
25 Sternesjo, A. & Gustavsson, E. Biosensor analysis of [beta]-lactams I milk using the carboxypeptidase activity of a bacterial penicillin binding protein. *J. AOAC Int.* **89,** 832–837 (2006).
26 Bieth, J., Spiess, B. & Wermuth, C. G. Synthesis and analytical use of highly sensitive an convenient substrate of elastase. *Biochem. Medicine* **11,** 350–357 (1974).
27 Hass, G. M. & Ryan, C. A. Carboxypeptidase inhibitor from potatoes. *Methods Enzymol.* **80,** 778–791 (1981).
28 Bezeaud, A. & Guillin, M.-C. Enzymatic and nonenzymic properties of human β-thrombin. *J. Biol. Chem.* **263,** 3576–3581 (1988).
29 Erlanger, B. F., Edel, F. & Cooper, A. G. The action of chymotrypsin on two new chromogenic substrates. *Arch. Biochem. Biophys.* **210,** 206–210 (1966).
30 Kassell, B. Bovine trypsin-kallikrein inhibitor (kunits inhibitor, basic pancreatic inhibitor, polyvalent inhibitor from bovine organs). *Methods Enzymol.* **19,** 844–852 (1970).
31 Mole, J. & Horton, H. R. Kinetics of papain-catalyzed hydrolysis of α-*N*-benzoyl-L-arginine-p-nitroanilide. *Biochemistry* **12,** 816–822 (1973).
32 Kakudo, S. *et al*. Purification, characterization, cloning, and expressin of a glutamic acid-specific protease from *Bacillus licheniformis* ATCC 14580. *J. Biol. Chem.* **267,** 23782–23788 (1992).
33 Anson, M. L. The estimation of pepsin, trypsin, papain, and cathepsin with hemoglobin. *J. Gen. Physiol.* **22,** 79–89 (1938).
34 O'Callaghan, C. H., Morris, A., Kirby, S. M. & Shingler, A. H. Novel method for detection of β-lactamases by using a chromogenic cephalosporin substrate. *Antimicrob. Ag. Chemother.* **1,** 283–288 (1972).
35 CLSI. Method for Dilution Antimicrobial Susceptibility Test for Bacteria That Grow Aerobically; Approved Standard-Seventh Edition. M7-A7 [ISBN 1-56238-587-9]. CLSI, 940 West Valley Road, Suite 1400, Wayne, Pennsylvania 19087-1898, USA (2006).
36 CLSI. Reference Method for Broth Dilution Antifungal Susceptibility Testing of Yeast; Approved Standard—Second Edition. M27-A2, CLSI, Wayne, PA, USA (2002).
37 Dehghan-Noudeh, G., Housaindokht, M. & Bazzaz,, B. S. F. Isolation, characterization, and investigation of surface and hemolytic activites of a lipopeptide biosurfactant produced by *Bacillus subtilis* ATCC 6633. *J. Microbiol.* **43,** 272–276 (2005).
38 Kada, T., Moriya, M. & Shirasu, Y. Screening of pesticides for DNA interactions by 'rec-assay' and mutagenesis testing, and frameshift mutagens detected. *Mutat. Res.* **26,** 243–248 (1974).
39 Kada, T., Hirano, K. & Shirasu, Y. *Bacillus subtilis* rec-assay test. in *Chemical Mutagenesis* Vol. 6 (eds de Sevres, F. E. & Hollaender, A.) 149 (Plenum Press, New York, 1980).
40 Sadaie, T. & Kada, T. Recombination-deficient mutants of *Bacillus subtilis*. *J. Bacteriol.* **125,** 489–500 (1976).

The Journal of Antibiotics (2009) 62, 581–585

www.nature.com/ja

ORIGINAL ARTICLE

# A novel isoquinoline alkaloid, DD-carboxypeptidase inhibitor, with antibacterial activity isolated from *Streptomyces* sp. 8812. Part II: Physicochemical properties and structure elucidation

Jolanta Solecka[1], Jerzy Sitkowski[2,3], Wojciech Bocian[2,3], Elżbieta Bednarek[2], Robert Kawęcki[3] and Lech Kozerski[2,3]

**A novel antimicrobial agent labeled JS-1, being a member of isoquinoline alkaloids, of molecular formula $C_{10}H_9NO_4$ was isolated from the culture broth of *Streptomyces* sp. 8812. In this study, we present the structure based on physicochemical and spectroscopic NMR investigations and on quantum chemical structure modeling. The structure of a molecule suggests the biosynthetic path starting from 3′-hydroxy tyrosine. The synthesis was undertaken and it resulted in NMR data that fully agree with the presented analysis.**

*The Journal of Antibiotics* (2009) **62,** 581–585; doi:10.1038/ja.2009.86; published online 28 August 2009

**Keywords:** antibacterial activity; DD-peptidase inhibitor; isoquinoline alkaloid; JS-1 structure; NMR

## INTRODUCTION

The increasing bacterial resistance to antibiotics causes a great therapeutic problem because of the widespread presence of multiresistant pathogenic bacteria. The solution of this problem involves screening for microorganisms producing novel antimicrobial drugs. Streptomycetes are well-known producers of antibiotic and other bioactive metabolites.[1] The purpose of this work was the investigation of novel antimicrobial agents, inhibitors of DD-carboxypeptidase/transpeptidase (DD-peptidase). In our screening program for new inhibitors of DD-peptidase 64–575 II (EC 3.4.16.4)[2–4] from microbial secondary metabolites, a novel isoquinoline alkaloid with documented antibacterial activity, JS-1, was isolated from the culture broth of *Streptomyces* sp. 8812.[5] In a recent paper,[6] we have described the taxonomy, fermentation of producing strain and isolation, as well as the purification and biological activity of novel isoquinoline alkaloid. In this study, we present the structure based on physicochemical and spectroscopic NMR investigations, quantum chemical structure modeling and synthesis protocol, which confirmed an established structure and chirality.

## RESULTS AND DISCUSSION

The physicochemical properties of a compound are shown in Table 1.

JS-1 is soluble in water (phosphate buffer pH 7.2), and insoluble in $CHCl_3$ or acetonitrile. It is soluble, but degrading, in methanol and dimethylosulfoxide.

The molecular formula of **JS-1** was determined to be $C_{10}H_9NO_4$ on a basis of high resolution ESI-MS [$(M+H)^+$, 208.06043 *m/z* (−0.03 mmu error)], thus requiring 7 degrees of unsaturation. The IR spectrum of **JS-1** showed a broad hydroxyl band at 3436 $cm^{-1}$, and the multiple bands in a region of 1600–1700 $cm^{-1}$ may indicate the presence of an aromatic carbonyl group, a C=N double bond at 1681 $cm^{-1}$, a carboxylate group as well as a carbonyl group conjugated to a double bond, or an enamine at the C-N bond at 1636 $cm^{-1}$. The UV absorption maximum at 321 nm suggests the presence of a conjugated system.

JS led us to suggest an isoquinoline structure shown in Figure 1.

It is essential to know which tautomeric form has the biological activity and therefore all spectroscopic investigations were carried out in physiological conditions, that is, pH 7.2 in phosphate buffer. The tautomeric equilibrium, if present, is fast in the NMR timescale and therefore only one set of sharp signals is observed at room temperature in buffered water solution. In Table 2, NMR data are presented that allow the confirmation of a structure.

A deceptively simple $^1H$ NMR spectrum, consisting of only three singlets, at 6.53, 7.04 and 8.23 p.p.m., and an ABM system, at 4.39, 3.29 and 3.18 p.p.m., with 5 heteroatoms present makes structure assignment ambiguous and requires a detailed recourse to $^1H \sim {}^1H$ and $^1H \sim {}^{13}C$ correlations in heteronuclear single quantum coherence (HSQC), heteronuclear multiple bond correlation (HMBC) and

[1]Independent Laboratory of Streptomycetes and Fungi Imperfecti, National Institute of Public Health—National Institute of Hygiene, Warsaw, Poland; [2]National Medicines Institute, Warsaw, Poland and [3]Institute of Organic Chemistry, Polish Academy of Sciences, Warsaw, Poland
Correspondence: Dr J Solecka, Independent Laboratory of Streptomycetes and Fungi Imperfecti, National Institute of Public Health—National Institute of Hygiene, Chocimska 24, Warsaw 00-791, Poland.
E-mail: jsolecka@pzh.gov.pl
Received 7 May 2009; revised 9 June 2009; accepted 11 June 2009; published online 28 August 2009

double pulsed field gradient spin-echo NOE,[7] respectively. In addition, dynamic O**H**, COO**H** and N**H** protons are in fast exchange with bulk water, thus making impossible the assignment of nitrogen atom functionality in the latter case, by means of running the $^{1}H$-$^{15}N$ HSQC spectrum or drastically less sensitive $^{1}H$-$^{15}N$ HMBC correlation.

$^{13}C$ Chemical shifts of proton-bearing carbon atoms were established using the HSQC spectrum. It proved useful to distinguish two carbon atoms of the same chemical shifts, that is, C-5 and C-8, 117.1 p.p.m., and to assign the two geminal protons to carbon atom C-4 at 3.29 and 3.18 p.p.m. This latter observation brings about the important conclusion that the molecule has a stable stereogenic center giving rise to the nonequivalence of the geminal protons. The $^{3}J$ (H, H) coupling constants in the ABM system of 7.4 and 9.2 Hz indicate that the stereogenic center is in vicinal arrangement with the geminal protons. Figure 2 presents key correlations split for clarity into two projections. Only one tautomer, ketone, is shown for simplicity. The HMBC correlations in a left projection prove the connection of an AMX aliphatic system to aromatic carbon atom C-5. The NOE contacts also prove the spatial vicinity of 1-H and 8-H, both being distant from 5-H. Comparable NOE effects in both directions point to the isolated two-spin system, in agreement with the structural environment. The NOE contacts in the right projection in Figure 2 confirm the connectivity of 5-H with the ABM system. In addition, nearly equal NOEs from H-5 to H4$^{a}$ and H-4$^{b}$ suggest that they are nearly equidistant to 5-H. Three-bond HMBC correlations from 8-H to C-1 and C-6 and from 1-H to C-3 allow for the unambiguous assignment of $\delta_C$ 159.5 and 168.8 p.p.m. to their positions in a structure, C-1 and C-6, respectively. Our experience in an enamine carbon chemical shifts suggests that the same assignment as=C–N carbon atom with a formally single bond in a conjugated system of α,β-unsaturated ketones gives resonances up to 155 p.p.m. for an alkyl disubstituted nitrogen atom.[8]

In contrast, the C=N bonds in imines give carbon resonances at approximately 160 p.p.m.[9,10]

It is commonly recognized that aromatization leads to enhanced stability and defines the thermodynamically more stable species in equilibrium.

To address in more depth the position of tautomeric equilibrium, we have performed the theoretical calculations of the $^{1}H$, $^{13}C$ chemical shift and the geometry of all possible tautomers (see Supplementary Figure 2S) using the PCM protocol in the $H_2O$ box at the B3LYP/6-31/+6($2d_{18}$) basis set level. The chemical shift data are compiled in Supplementary Tables 1S–3S in the Supplementary materials along with the structures. Scarce data regarding the $^{13}C$ chemical shifts in a similar system are available in the literature.[12]

The calculated chemical shifts of conformers suggested for the equilibrium are shown in Figure 3. The protonated dihydroxy imine tautomer **4a** can also be considered as a species present in equilibrium.

**Table 1 Physicochemical properties of JS-1**

| *Appearance* | *Yellow powder* |
|---|---|
| $[\alpha]_D^{23}$ | 21.1° (*c*=0.185, $H_2O$) |
| Molecular formula | $C_{10}H_9NO_4$ |
| LR ESI-MS (*m/z*) | |
| Positive | 208 $(M+H)^+$ |
| Negative | 206 $(M-H)^-$ |
| HRESI-MS (*m/z*) | |
| Calcd | 208.06043 |
| Found (M+H) $^+$ | 208.06040 |
| UV $\lambda_{max}$ nm (ε) ($H_2O$) | 397.92 (3475), 321.33 (943), 266.38 (2225) |
| IR (KBr) $\nu_{max}$ $cm^{-1}$ | 3436, 1681, 1636, 1131, 1075, 986, 984, 804, 724 |

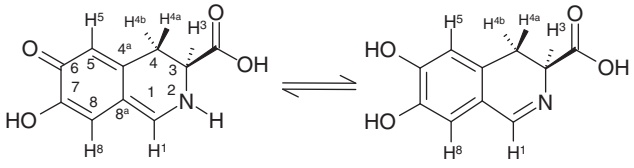


**Figure 1** Postulated structure of **JS-1**.

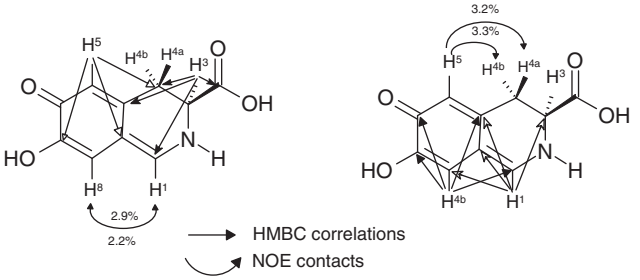


**Figure 2** Key HMBC correlations and NOE[11] contacts in **JS-1**. For clarity, only one tautomer is shown.

**Table 2 $^{13}C$ (176 MHz) and $^{1}H$ (500 MHz) NMR data for JS-1 in buffered water solution (pH 7.2)**

| | | *Proton spectral parameters, scalar, $^{1}H$–$^{13}C$, and dipolar, $^{1}H$–$^{1}H$, correlations* | | |
|---|---|---|---|---|
| *C* | $\delta_C$ | $\delta_H$ | *HMBC correlations* | *DPFGSE NOE contacts (%)* |
| 1 | 159.5 | 8.21(s) | C-3, C-4a, C-8, C8a | 8-H (2.9) |
| 3 | 55.8 | 4.39(dd,7.4, 9.2) | C-1, C-4,C-4a, C=O | 4-H$^{a}$(1.7); 4-H$^{b}$(1.1) |
| 4 | 29.2 | 3.29(dd, 7.4,16.7) 4-H$^{a}$ 3.18(dd, 9.2,16.7) 4-H$^{b}$ | C-3,C-4a,C-8a,C=O C-3, C-4a | 3-H(1.9); 5-H(1.5)* |
| 4a | 135.0 | | | |
| 5 | 117.1 | 6.53(s) | C-4, C-7, C-8a | 4-H$^{a}$(1.1); 4-H$^{b}$(1.2) |
| 6 | 168.8 | | | |
| 7 | 146.5 | | | |
| 8 | 117.1 | 7.04(s) | | 1-H(2.2) |
| 8$^{a}$ | 110.5 | | | |

Abbreviations: DPFGSE NOE, double pulsed field gradient spin-echo NOE; HMBC, heteronuclear multiple bond correlation.
*These values represent the effect of simultaneous irradiation of both 4-H$^{a}$ and 4-H$^{b}$ protons, which cannot be selectively irradiated due to strong coupling.

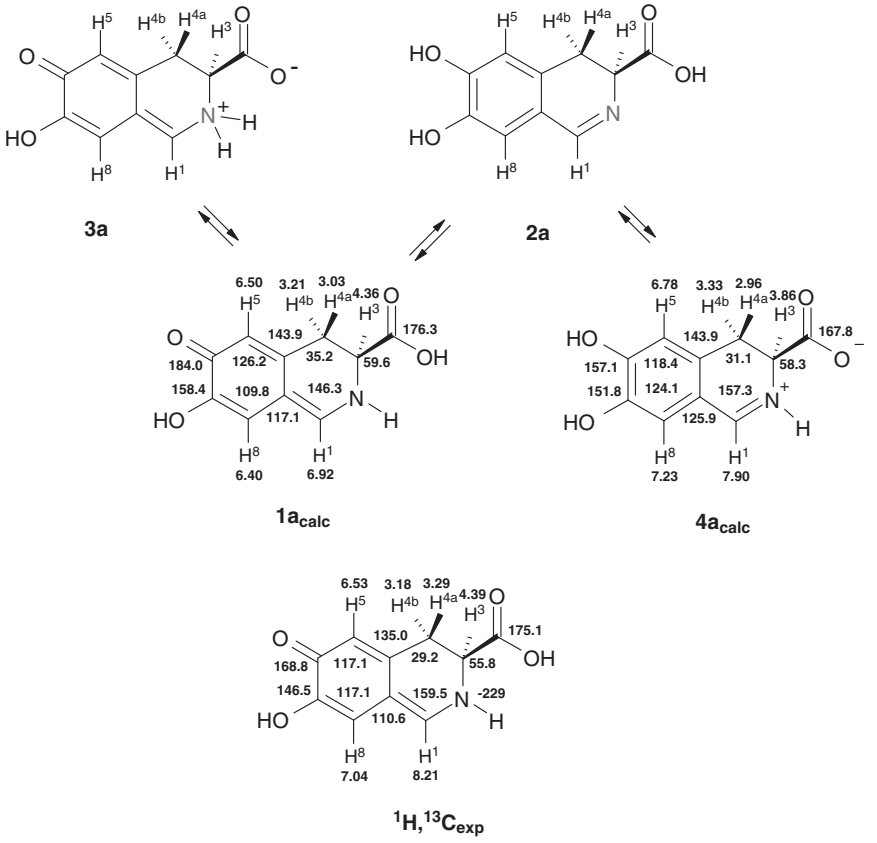


**Figure 3** Comparison of calculated, *in vacuo*, $^{1}$H and $^{13}$C chemical shift in tautomers **1a** and **4a** of **JS-1** with experimental ones, $^{1}$**H,**$^{13}$**C$_{exp}$**, assigned to specific carbon atoms using heteronuclear multiple bond correlation and double pulsed field gradient spin-echo NOE data. The hypothetical structures **2a** and **3a** are also shown (see text).

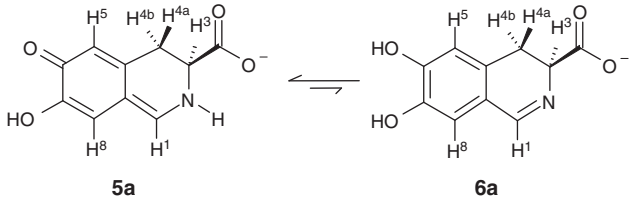


**Figure 4** Proposed equilibrium for JS-1 at basic conditions.

The predominance of the enamine tautomer in solution is further confirmed in $^{15}$N NMR, which gives the $\delta$ ($^{15}$N)=−229.0 p.p.m. (versus external $CH_3NO_2$), at pH 7.2. This chemical shift is representative both for nitrogen atoms in enamine, **1a** or **1b,** and protonated imine (zwitter ion) **4a**. A small amount of the form **2a** can be allowed in equilibrium with **1a**. The **3a** form cannot be considered on the basis of the observed $^{15}$N chemical shift as its nitrogen resonance appears at approximately −300 p.p.m. from nitromethane. The situation above applies to experimental conditions close to the isoelectric point.

Under more basic conditions, the carboxylate is deprotonated and the equilibrium shown in Figure 4 applies. As discussed above, the $^{15}$N chemical shift allows a small amount of imine in equilibrium.

It is worth noting that near the isoelectric point, pI=6.0, for this compound (see to Supplementary Materials), the molecule can be both neutral and ionized and therefore the species discussed in Figures 3 and 4 should be considered.

Figure 5 presents the possible species in tautomeric equilibrium in solution. Structures **1a** and **1b** are the conformers having planar ring B in **1a** and twisted in **1b.**

The calculations carried out also allow comparison of the geometry of both tautomers, relating it to experimental observables. The geometry of the N-$C_{sp3}$-$C_{sp3}$ motif is expected to be most sensitive to tautomerization because of the changes in nitrogen hybridization and bond length around it. The ABM system of investigated molecule offers an experimental check of the calculated geometry along the C4–C3 bond in both conformers shown in Figure 5.

It is shown in Figure 5 that the H-4$^{a}$ and H-4$^{b}$ protons in **1b** are both in synclinal positions with respect to the H-3 proton, having torsion angles of −69.9° and +47.0°, respectively. This spatial arrangement leads to $^{3}$J(H-3, H-4$^{a}$) and $^{3}$J(H-3,H-4$^{b}$) vicinal coupling constants 1.6 and 7.7. Hz, in disagreement with observed experimental observation, 7.4 and 9.2 Hz. On the contrary, in **1a**, H-4$^{b}$ is in synclinal and H-4$^{a}$ in anti-periplanar position to H-3 with torsion angles of −51.0° and –167.0° leading to 4.5 and 13.7 Hz, respectively, again in disagreement with experimental values. Averaging of the respective coupling constants in both forms results in agreement with the experiment and this fact gives strong evidence to the predominance of this tautomeric form in equilibrium in solution.

With respect to the above discussion, Lakhlifi *et al.*[13] report the $^{1}$H NMR spectrum of closely related 3,4-dihydro-6,7-dimethoxy-3-methylcarboxylate-isoquinoline. Unfortunately, the geminal nonequivalence of H-4$^{a}$ and H-4$^{b}$ was not observed and the reported splitting in the $A_2M$ system is 10.2 Hz.

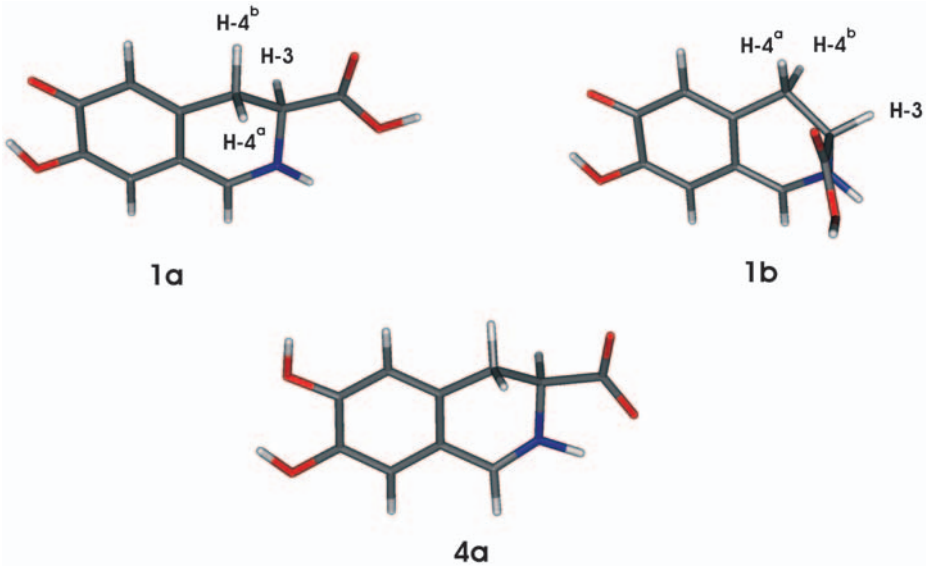


**Figure 5** Established structure of JS-1 based on a comparison of calculated and experimental $^{1}H$ and $^{13}C$ chemical shifts. Projection along the C4–C3 bond in both conformers 1a, 1b calculated using the PCM protocol.

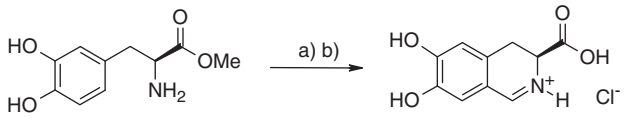


a) HCHO, $Ac_2O$ b) $POCl_3$

**Scheme 1**

Finally, the configuration of the C-3 carbon atom should be addressed. The structure of a molecule suggests the biosynthetic path starting from the 3′-hydroxy tyrosine. This defines the (S) C-3 configuration of natural L-amino acid. The verification of this hypothesis was performed by comparison of a specific rotation with the synthetic product.

The synthesis was undertaken and its product yielded NMR data that fully agree with the above analysis (Scheme 1). Spectrum 1S (Supplementary Information, Figure 1S) presents the heteronuclear multiple bond correlation trace of a synthetic product which verifies proper structure elucidation of **JS-1**.

## EXPERIMENTAL SECTION

IR spectrum was obtained on an FT-IR-1600 Perkin-Elmer spectrophotometer (Perkin-Elmer, Ramsey, MN, USA). UV spectrum was recorded on a Jasco V-630 UV-Visible spectrophotometer (Jasco, Tokyo, Japan). The pI was established using this facility for UV measurements and the Orion pH meter (Orion, Boston, MA, USA).

The optical rotation was measured with a Jasco P-2000 digital polarimeter. A low-resolution mass spectrum was recorded on an HPLC-MS (Hewlett-Packard 1100; API 365, PESCIEX) mass spectrometer (Hewlett-Packard, Santa Clara, CA, USA). A high-resolution mass spectrum was recorded on a Bruker APEX-Q (9.4T) spectrometer (ESI), positive-ion mode (Bruker, Leipzig, Germany).

The NMR spectra were recorded at 303 K on a Varian INOVA 500 spectrometer (Varian, Palo Alto, CA, USA) operated at 499.8, 125.7 and 50.51 MHz for $^{1}H$ and $^{13}C$, and 15 N, respectively. A 0.1 mg amount of compound was dissolved in 0.7 ml of $H_2O/D_2O$ (9:1), pH 7.2 and transferred to a 5 mm NMR tube. Chemical shifts, $\delta$ given in p.p.m., were referenced against internal reference (trimethylsily1)propanoic acid. The spectrometer was equipped with an inverse $^{1}H\{^{31}P–^{15}N\}$, the 5 mm Nalorac probe with an actively shielded z-gradient coil (ID-pulsed field gradients).

$^{1}H$ NMR was run using the standard method of presaturation of residual water implemented in Varian software.

*HSQCAD spectra:*[14] The Echo-antiecho phase-sensitive $^{1}H$-$^{13}C$ HSQC (adiabatic version) NMR spectra were obtained with a spectral width of 6 000 Hz, 2048 points in the $^{1}H$ dimension and 20 100 Hz, 400 increments in the $^{13}C$ dimension; 128 transients per $t_1$ increment, with a relaxation delay of 1.0 s and $^{1}J(C,H)=135$ Hz. The data were linearly predicted to 1600 points and zero-filled to 8192 points in $F_1$ before Fourier transformation.

The $^{1}H/^{13}C$-HMQC (heteronuclear multiple quantum coherence) technique with pulsed field gradients coherence selection using two pulsed field gradient pulses of relative amplitudes of $+(\gamma I+\gamma S)$: $-(\gamma I–\gamma S)$ and $-(\gamma I–\gamma S)$: $+(\gamma I+\gamma S)$, for heteronuclear echo and antiecho, respectively was used. The S-spin 90 degree pulse low-pass filter was used to suppress one-bond correlation. Such implementation enabled us to obtain a nearly pure absorption line shape along $F_1$, combined with an absolute value mode in $F_2$ dimension.[15,16] The $^{1}H$ $\{^{13}C\}$ HMQC spectra were recorded with the following experimental conditions: an acquisition time of 0.2 s, spectral windows of 5000 ($F_2$) and 25500 ($F_1$) Hz, 2048 data points in the $^{1}H$ dimension, 256 increments in the $^{13}C$ dimension, $^{n}J(C,H)=8$ Hz, a 1.3 s relaxation delay and 512 transients per increment. The data were zero filled to 4096 points in $F_1$ and processed using sine bell multiplication in $t_2$ and cosine window function in $t_1$ dimensions before Fourier transformation. The proton and carbon $\pi/2$ pulse lengths were 8.0 and 11.5 μs, respectively.

$^{1}H/^{15}N$-HMQC $^{1}N$ parameters: $F_2$, 5000 Hz; $F_1$, 10000; number of increments, 80; 512 scans/increment; delay, 120 ms. A low-pass filter (see above) was not used.

Double pulsed field gradient spin-echo NOE experiments were run using a pulse sequence published by Stott *et al.*[17] using shaped selective pi soft pulses generated by a standard Varian program. The rsnob pi pulse was calibrated for each individual multiplet.

*(S)-6,7-dihydroxy-3,4-dihydroisoquinolin-3-carboxylic acid synthesis:* To a warm solution of *N*-formyl-(L)-DOPA[18] (70 mg, 0.31 mmol) in acetonitrile (13 ml) was added phosphorus oxychloride (342 mg, 2.24 mmol) and the mixture was heated under reflux for 1 h. The precipitate was separated and the filtrate was evaporated to give brown oil. The product was purified by preparative HPLC on an RP C18 column (Nucleosil, Duren, Germany) using first 0.1% TFA in water as eluent and then 10% acetonitrile in 0.1% aqueous TFA. Spectral data is identical as for JS-1.

HRESI-MS calculated for $C_{10}H_{10}NO_4$ $(M+H)^+$, 208.06043. Found 208.06093.

## ACKNOWLEDGEMENTS

We gratefully acknowledge running the $^1H/^{13}C$-HMBC spectrum at 176 MHz on the limited amount of a sample (0.03 mg) by Prof W Koźmiński, Department of Chemistry, Warsaw University. We also thank Associate Prof Vladimir Havliček, Institute of Microbiology, Laboratory of Molecular Structure Characterization, Prague Czech Republic, for HRESI-MS data.

1 Bérdy, J. Bioactive microbial metabolites. *J. Antibiot.* **58,** 1–26 (2005).
2 Kurzątkowski, W., Solecka, J., Filipek, J., Kurzatkowski, J. D. & Kurylowicz, W. Streptomycetes excreting DD-carboxypeptidases. *Appl. Microbiol. Biotechnol.* **33,** 452–454 (1990).
3 Solecka, J. & Kurzatkowski, W. Affinity of exocellular DD-carboxypeptidase/transpeptidase from *Saccharopolyspora erythraea* PZH 64-575 to beta-lactam compounds. *Med. Dosw. Mikrobiol.* **51,** 151–165 (1999).
4 Solecka, J., Łysek, R., Furman, B., Chmielewski, M. & Kurzątkowski, W. Practical use of DD-peptidase 64-575 for assay inhibition activity of natural and synthetic β-lactam compounds. *Acta. Poloniae. Pharmaceutica.* **60,** 115–118 (2003).
5 Solecka, J. & Kozerski, L. A new inhibitor of DD-peptidase and its use as antibiotic or anticancer drug. PCT/WO 2009/028972 A1. 5 March (2009).
6 Solecka, J., Rajnisz, A. & Laudy, A. E. A novel isoquinoline alkaloid, DD-carboxypeptidase inhibitor with antimicrobial activity isolated from *Streptomyces* sp. 8812. Part I Taxonomy, fermentation, isolation and biological activities. *J. Antibiot.* (2009) (e-pub ahead of print 28 August 2009; doi:10.1038/ja.2009.85).
7 Stott, K., Stonehouse, J., Keeler, J., Hwang, T.-L. & Shaka, A. J. Excitation sculpting in high resolution nuclear magnetic resonance spectroscopy: application to selective NOE experiments. *J. Am. Chem. Soc.* **117,** 4199–4200 (1995).
8 Dąbrowski, J., Kamieńska-Trela, K. & Kozerski, L. Conformational studies by NMR. Part VII. The direct observation of rotational isomerism in some enamino carbonyl compounds and their thione derivatives by CMR. *Org. Mag. Reson.* **6,** 499 (1974).
9 Kozerski, L. & von Philipsborn, W. Solvent induced deuterium effects in $^{13}C$ and $^{15}N$ NMR spectra of enaminones. *Helv. Chim. Acta* **65,** 2077 (1982).
10 Kozerski, L. *et al.* The tautomeric equilibrium and stereochemistry of β-sulfonylenamines. *N. J. Chem.* **26,** 1060–1069 (2002).
11 Neuhaus, D. & Williamson, M. P. *Nuclear Overhauser Effect in Conformational and Structural Analysis. A Guide for Chemists* (Viley-VCH Publisher, Inc New York, 1995).
12 Haraguchi, Y., Kozima, S. & Yamaguchi, R. An efficient assymetric synthesis of *allo*- and pseudo-7,8-dimethoxyberbane systems through Tin-mediated three component coupling. *Tetrahedron: Asymmetry* **7,** 443–449 (1996).
13 Lakhlifi, T., Sedqui, A., Laude, B., Dinh An, N. & Verbel, J. Cycloaddition d'ylures d'azométhine derives de la 3,4-dihydro-6,7-diméthoxycarbonyl-isoquinoléine. *Can. J. Chem.* **69,** 1156–1160 (1991).
14 Summers, M. F., Marzilli, L. G. & Bax, A. Complete proton and carbon-13 assignments of coenzyme B12 through the use of new two-dimensional NMR experiments. *J. Am. Chem. Soc.* **108,** 4285–4294 (1986).
15 Meissner, A. & Sørensen, O. W. Economizing spectrometer time and broadband excitation in small-molecule heteronuclear NMR correlation spectroscopy. Broadband HMBC. *Magn. Res. Chem.* **38,** 981–984 (2000).
16 KoŸmiñski, W., Bednarek, E., Bocian, W., Sitkowski, J. & Kozerski, L. J. The new HMQC-based technique for the quantitative determination of heteronuclear coupling constans. Application for the measurement of $^3J(\mathbf{H'}_i, \mathbf{P}_{i+1})$ in DNA oligomers. *Magn. Reson.* **160,** 120 (2003).
17 Stott, K., Stonehouse, J., Keeler, J., Hwang, T.-L. & Shaka, A. J. Excitation sculpting in high resolution nuclear magnetic resonance spectroscopy: application to selective NOE experiments. *J. Am. Chem. Soc.* **117,** 4199–4200 (1995).
18 Dickner, T. & Laschat, S. *Pictet-Spengler* cyclization *vs.* aminal formation: competing reaction pathway of Benzo[*b*][1,7]napthyridines controlled by the configuration. *Helv. Chim. Acta* **84,** 2064–2070 (2001).

Supplementary Information accompanies the paper on The Journal of Antibiotics website (http://www.nature.com/ja)

The Journal of Antibiotics (2009) 62, 587–591

www.nature.com/ja

NOTE

# New β-class milbemycin compound from *Streptomyces avermitilis* NEAU1069: fermentation, isolation and structure elucidation

Ming Wang[1], Xiao-Hu Yang[2], Ji-Dong Wang[2], Xiang-Jing Wang[1], Zheng-Jie Chen[2] and Wen-Sheng Xiang[1]

*The Journal of Antibiotics* (2009) **62,** 587–591; doi:10.1038/ja.2009.78; published online 14 August 2009

**Keywords:** *Streptomyces avermitilis* NEAU1069; β-class milbemycins; structure elucidation

Microbial metabolites attract increasing attention as potential pesticides. They are expected to overcome the resistance and pollution that have accompanied the use of synthetic pesticides.[1,2] Our experiments were conducted as part of a program to screen new antibiotics for pesticides and antiparasitic veterinary drugs, or as semisynthetic intermediates. As a result, a new compound **1**, two known milbemycins (compounds **2** and **3**, Figure 1) and avermectin $B_{1a}$ were isolated from the fermentation broth of *Streptomyces avermitilis* NEAU1069 strain, which was newly obtained from a soil sample. The structures of compounds **1**, **2** and **3** were elucidated by UV, IR, electrospray ionization (ESI)-MS, high-resolution ESI (HRESI)-MS, extensive 1D and 2D NMR analyses, and a comparison with data reported in literature. Their structures are similar to milbemycin β3,[3–6] β4,[7,8] β13,[9] β14[9] and aromatic S541 analogs,[10] which are generated by the nemadectin-producing strains *S. thermoarchaensis* NCIB 12015 and NCIB 12212. However, there are differences among them at positions C-23 and C-25. β-Class milbemycins have not been previously reported as being from *S. avermitilis*.[3–10] This paper describes the fermentation, isolation and identification of compounds **1**, **2** and **3**. Moreover, the spectroscopic data of compounds **2** and **3** are reported for the first time (although the structures of compounds **2** and **3** could be searched in SciFinder Scholar (Chemical Abstract Service, ACS; http://www.cas.org/products/sfacad/index.html), no reference was cited. Furthermore, they were not reported). The discovery of these three compounds possibly has an important role in understanding and perfecting the proposed pathways of avermectins and milbemycins. In addition, it is significant that they are useful intermediates in the preparation of other derivatives.[11]

## MATERIALS AND METHODS

### Screening, isolation and identification of the producing organism

The agar plate dilution method was used to separate the microorganism reported in this paper. A sample soil of 0.5 kg obtained from Harbin city, China, was taken in a sterilized test tube and sterilized water was added thereto. After 10 min of setting, supernatant was obtained. The supernatant thus obtained was 100-fold diluted using sterilized water, and 0.1 ml of the diluted solution was distributed onto a yeast–malt extract (yeast extract 4 g $l^{-1}$, malt extract 10 g $l^{-1}$, glucose 4 g $l^{-1}$, agar 20 g $l^{-1}$ and distilled water 1 l, pH 7.0–7.2) taken in a petri dish and cultured at 28 °C for 15 days. Colonies formed on the yeast–malt extract agar, from which a single colony was isolated using a sterilized needle. The obtained colony was transferred to a fresh yeast–malt extract agar at regular intervals for 10 days, followed by submerged fermentation. Metabolites were extracted by adding 4 ml methanol to 2 ml whole broth and mixing intermittently for 3 h. The extracts were examined on two-spotted spider mites to determine whether they have acaricidal activity. Then, the metabolites with acaricidal activity were purified and their structures were determined.

To identify the isolated strain with acaricidal activity in the metabolites, morphological properties of cells, cultural characteristics of cells, morphological characteristics of colonies, physiological characteristics, utilization of a carbon source and 16S rDNA (Accession No: DQ768097 in National Center for Biological Information, Bethesda, MD, USA) were investigated. The strain was named *S. avermitilis* NEAU1069. It has been deposited at the China General Microbiology Culture Collection Center, Beijing, China (Accession No: CGMCC 2943).

### Fermentation

The strain was maintained on a YMS (yeast extract–malt extract-soluble starch) medium containing soluble starch (Beijing Ao Bo Xing, Beijing, China) 10 g, yeast extract (Beijing Ao Bo Xing) 2 g, $KNO_3$ 1 g and agar 20 g in 1.0 l tap water, pH 7.0. The seed medium consisted of glucose (Beijing Ao Bo Xing) 20 g, soybean flour (Comwin, Beijing, China) 15 g and yeast autolysate (Beijing Ao Bo Xing) 5.0 g in 1.0 l water, pH 7.0. Both the media were sterilized at 121 °C for 20 min. Slant cultures were incubated for 6–8 days at 28 °C.

A total of 10 ml of sterile water was added to the slant of the YMS medium. The spores were scraped and transferred onto a sterile tube containing glass beads; the spore suspension was then filtered through six layers of a sterile filter cheesecloth and adjusted to $10^7$–$10^8$ c.f.u $ml^{-1}$. A 2.0 ml of the spore suspension was inoculated into a 250-ml flask containing 25 ml of seed medium and incubated at 28 °C for 24 h, shaken at 250 r.p.m. Then, 8 ml of the culture was

[1]Department of Biochemical Engineering, School of Life Science, Northeast Agricultural University, Harbin, China and [2]Zhejiang Hisun Pharmaceutical, Taizhou, Zhejiang, China
Correspondence: Professor W-S Xiang, School of Life Science, Northeast Agricultural University, Harbin 150030, China.
E-mail: xiangwensheng@yahoo.com.cn
Received 26 April 2009; revised 14 July 2009; accepted 15 July 2009; published online 14 August 2009

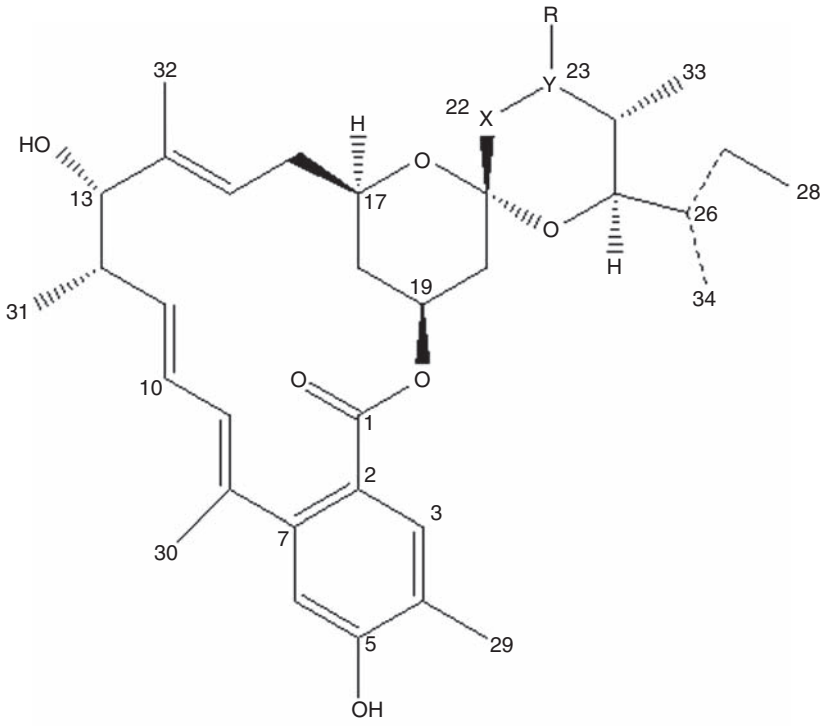


| | X-Y | Y-R |
|---|---|---|
| Compound 1 | $CH_2$=C | C=O |
| Compound 2 | CH=CH | |
| Compound 3 | $CH_2$=CH | CH---OH |

The structures of compound 1, 2 and 3

**Figure 1** The structures of compounds **1**, **2** and **3**.

transferred into a 1-l Erlenmeyer flask containing 100 ml of the producing medium consisting of corn starch (Comwin) 10%, soybean powder 1%, cotton flour (Comwin) 1%, α-Amylase (Beijing Ao Bo Xing) 0.02%, NaCl 0.1%, $K_2HPO_4$ 0.2%, $MgSO_4 \cdot 7H_2O$ 0.1%, $CaCO_3 \cdot 0.7\%$ and pH 7.0, before sterilization. Fermentation was carried out at 28 °C for 12–13 days on a rotary shaker at 250 r.p.m.

## Isolation and purification

A total of 31 of broth from 40 producing fermentations was filtered. The resulting cake was washed with water (31), and both filtrate and wash were discarded. Methanol (11) was used to extract the washed cake. The MeOH extract was evaporated under reduced pressure to approximately 0.21 at 45 °C and the resulting concentrate was extracted three times using an equal volume of EtOAc. The combined EtOAc phase was concentrated under reduced pressure to yield 5 g of oily substances. The residual oily substance was chromatographed on silica gel (Qingdao Haiyang Chemical Group, Qingdao, Shandong, China; 100–200 mesh) and eluted with a petroleum (60 °C −90 °C)–acetone mixture (95:5, 75:25 and 50:50, v/v). The fractions eluted with the petroleum–acetone mixture (95:5–75:25, v/v) were combined and evaporated to obtain a crude mixture. The crude mixture was applied to a silica gel column and eluted with a petroleum–EtOAc mixture (95:5, 85:25, 75:25, 65:35 and 50:50, v/v) to give five fractions.

Semipreparative HPLC (Agilent 1100, Zorbax SB-C18, 5 μm, 250×9.4 mm i.d.; Agilent, Palo Alto, CA, USA) and preparative HPLC (Shimadzu LC-8A, Shimadzu-C18, 5 μm, 250×20 mm i.d.; Shimadzu, Kyoto, Japan) were further performed to obtain pure compounds. The eluates were monitored using a photodiode array detected at 220 nm, and the flow rates were 1.5 ml $min^{-1}$ for the semipreparative HPLC and 20 ml $min^{-1}$ for the preparative HPLC at room temperature. Fraction one was purified by semipreparative HPLC using a solvent containing a $CH_3OH$–$H_2O$ mixture (97:3, v/v) to obtain **2** ($t_R$ 10.6 min, 13 mg). Fraction two was also subjected to silica gel elution using petroleum–EtOAc mixture (85:15 and 75:25, v/v) to obtain two subfractions. Subfraction one was further separated by semipreparative HPLC elution using $CH_3OH$–$H_2O$ mixture (92:8, v/v) to afford compound **1** ($t_R$ 12.3 min, 11 mg). Subfraction two was purified by preparative HPLC using $CH_3OH$–$H_2O$ mixture (8:2, v/v) to obtain **3** ($t_R$ 17.1 min, 24 mg).

## General

Melting points were measured using a Fisher–Johns micro-melting point apparatus (corrected; Fisher–Johns, Pittsburgh, PA, USA); UV spectra were obtained on a Varian CARY 300 BIO spectrophotometer (Varian, Palo Alto, CA, USA); IR spectra were recorded on a Nicolet Magna FT-IR 750 spectrometer (Nicolet Magna, Madison, WI, USA); $^1H$ and $^{13}C$-NMR spectra were measured using a Bruker DRX-400 (400 MHz for $^1H$ and 100 MHz for $^{13}C$) spectrometer (Bruker, Rheinstetten, Germany); chemical shifts are reported in p.p.m (δ) using the residual $CHCl_3$ ($\delta_H$ 7.26; $\delta_C$ 77.0) as an internal standard, and coupling constant (*J*) in Hz. $^1H$ and $^{13}C$-NMR assignments were supported by $^1H$-$^1H$ COSY, heteronuclear multiple quantum coherence and heteronuclear multiple bond correlation (HMBC) experiments. The ESI-MS and HRESI-MS spectra were taken on a Q-TOF Micro LC-MS-MS mass spectrometer (Waters,

**Table 1** $^{1}H$ and $^{13}C$-NMR data of compounds 1–3 (coupling constants in parenthesis)

| | *Proton* | | | *Carbon* | | |
|---|---|---|---|---|---|---|
| *Position* | ***1*** | ***2*** | ***3*** | ***1*** | ***2*** | ***3*** |
| 1 | | | | 168.9 s[a] | 169.1 s | 169.0 s |
| 2 | | | | 123.6 s | 123.8 s | 123.3 s |
| 3 | 7.41 s | 7.39 s | 7.39 s | 132.3 d | 132.1 d | 132.2 d |
| 4 | | | | 122.5 s | 122.4 s | 122.7 s |
| 5 | | | | 155.8 s | 155.6 s | 156.1 s |
| 6 | 6.61 s | 6.61 s | 6.61 s | 114.3 d | 114.2 d | 114.2 d |
| 7 | | | | 144.5 s | 144.3 s | 144.3 s |
| 8 | | | | 135.0 s | 135.0 s | 135.1 s |
| 9 | 5.70 d (10.8) | 5.73 d (10.8) | 5.68 dd (1.1, 10.9) | 128.5 d | 128.5 d | 128.4 d |
| 10 | 6.16 dd (10.8, 15.0) | 6.17 dd (10.9, 15.1) | 6.16 dd (10.9, 15.1) | 127.3 d | 127.4 d | 127.3 d |
| 11 | 5.45 dd (9.6, 15.2) | 5.45 dd (9.6, 14.5) | 5.45 dd (9.6, 15.1) | 134.5 d | 134.3 d | 134.3 d |
| 12 | 2.64 m | 2.62 m | 2.61 m | 40.7 d | 40.6 d | 40.6 d |
| 13 | 4.02 br s | 4.02 br s | 4.02 br s | 79.1 d | 79.1 d | 79.1 d |
| 14 | | | | 138.3 s | 137.8 s | 138.3 s |
| 15 | 5.17 br d (8.6) | 5.21 br d (8.7) | 5.20 d (8.9) | 117.4 d | 117.7 d | 117.2 d |
| 16 | 2.28 m | 2.32 m | 2.34 m | 33.1 t | 33.7 t | 33.4 t |
| | | 2.39 m | | | | |
| 17 | 3.76 m | 3.98 m | 3.84 m | 68.6 d | 68.6 d | 68.7 d |
| 18 | 0.78 q (12.0) | 0.79 q (12.1) | 0.79 q (12.4) | 36.1 t | 36.6 t | 36.3 t |
| | 1.97 m | 1.97 m | 1.97 m | | | |
| 19 | 5.43 m | 5.43 m | 5.37 m | 67.4 d | 67.9 d | 67.2 d |
| 20 | 1.47 t (12.0) | 1.54 m | 1.47 t (6.9) | 40.8 t | 40.7 t | 41.0 t |
| | 2.20 m | 1.98 m | 1.98 m | | | |
| 21 | | | | 100.8 s | 96.0 s | 99.9 s |
| 22 | 2.47 br s | 5.55 dd (2.6, 9.8) | 1.67 dd (3.0, 14.1) | 51.6 t | 128.1 d | 41.3 t |
| | | | 1.96 m | | | |
| 23 | | 5.74 dd (1.7, 9.8) | 3.83 br s | 207.4 s | 136.1 d | 70.2 d |
| 24 | 2.45 m | 2.27 m | 1.64 m | 46.6 d | 30.6 d | 35.8 d |
| 25 | 3.51 d (10.4) | 3.48 dd (1.7, 10.0) | 3.55 dd (1.2, 10.7) | 76.8 d | 75.2 d | 71.3 d |
| 26 | 1.58 m | 1.58 m | 1.53 m | 36.1 d | 35.3 d | 35.2 d |
| 27 | 1.52 m | 1.50 m | 1.49 m | 27.4 t | 27.6 t | 27.4 t |
| 28 | 0.96 t (7.6) | 0.93 t (7.4) | 0.95 t (7.3) | 12.4 q | 12.1 q | 12.5 q |
| 29 | 2.23 br s | 2.24 br s | 2.21 br s | 15.3 q | 15.3 q | 15.3 q |
| 30 | 2.07 br s | 2.08 br s | 2.06 d (1.1) | 18.3 q | 18.2 q | 18.2 q |
| 31 | 1.21 d (6.9) | 1.21 d (6.9) | 1.21 d (6.9) | 18.4 q | 18.3 q | 18.4 q |
| 32 | 1.62 br s | 1.63 br s | 1.63 br s | 15.1 q | 15.1 q | 15.1 q |
| 33 | 0.97 d (6.7) | 0.91 d (7.1) | 0.91 d (6.9) | 8.8 q | 16.4 q | 13.8 q |
| 34 | 0.97 d (6.7) | 0.92 d (6.6) | 0.86 d (6.4) | 11.4 q | 12.8 q | 11.5 q |

[a]By DEPT sequence.

Milford, MA, USA). Optical rotation was measured on a Perkin-Elmer 341 Polarimeter (Perkin-Elmer, Fremont, CA, USA).

Compound (**1**, Figure 1) $C_{34}H_{46}O_7$, white amorphous powder; mp. 98–100 °C; $[\alpha]_D^{25}$ +74° (*c* 0.031, EtOH); UV (EtOH) $\lambda_{max}$ nm (log ε): 200 (4.57), 243 (4.25); IR (KBr), $\nu_{max}$ $cm^{-1}$: 3448, 1701, 2927, 1457, 1379, 1277, 1235, 1151, 989; $^{1}H$-NMR (400 MHz, $CDCl_3$) and $^{13}C$-NMR (100 MHz, $CDCl_3$), for data see Table 1; ESI-MS *m/z* 565 $[M-H]^-$; HRESI-MS *m/z* 589.3093 $[M+Na]^+$; calculated for $C_{36}H_{48}O_7Na$ 589.3136.

Compound (**2**, Figure 1) $C_{34}H_{46}O_6$, white amorphous powder; mp. 124–126 °C; $[\alpha]_D^{25}$ +166° (*c* 0.060, EtOH); UV (EtOH) $\lambda_{max}$ nm (log ε): 200 (4.88), 246 (4.57); IR (KBr), $\nu_{max}$ $cm^{-1}$: 3448, 1700, 2926, 1457, 1378, 1280, 1159, 997; $^{1}H$-NMR (400 MHz, $CDCl_3$) and $^{13}C$-NMR (100 MHz, $CDCl_3$) for data see Table 1; ESI-MS *m/z* 551 $[M+H]^+$; HRESI-MS *m/z* 573.3180 $[M+Na]^+$; calculated for $C_{36}H_{48}O_6Na$ 573.3187.

Compound (**3**, Figure 1) $C_{34}H_{48}O_7$, white amorphous powder; mp. 150–153 °C; $[\alpha]_D^{25}$ +113° (*c* 0.135, EtOH); UV (EtOH) $\lambda_{max}$ nm (log ε): 201 (4.66), 247 (4.40); IR (KBr), $\nu_{max}$ $cm^{-1}$: 3446, 1701, 2928, 1456, 1381, 1280, 1164, 997; $^{1}H$-NMR (400 MHz, $CDCl_3$) and $^{13}C$-NMR (100 MHz, $CDCl_3$), for data see Table 1; ESI-MS *m/z* 567 $[M-H]^-$; HRESI-MS *m/z* 591.3315 $[M+Na]^+$; calculated for $C_{36}H_{50}O_7Na$ 591.3292.

Compound **1** was isolated as a white amorphous powder. Its molecular formula was determined to be $C_{34}H_{46}O_7$ on the basis of HRESI-MS at *m/z* 589.3093 $[M+Na]^+$ (calculated as 589.3136 for $C_{34}H_{46}NaO_7$) and $^{13}C$-NMR data (Table 1). The IR spectrum of **1** showed hydroxyl absorption at 3448 $cm^{-1}$. $^{1}H$-NMR data of **1** indicated one triplet aliphatic methyl signal at δ 0.96; three doublet aliphatic methyl signals at δ 0.97, 0.97, 1.21; three olefinic or aromatic methyl signals at δ 1.62, 2.07, 2.23; and two downfield singlet proton signals at δ 7.41 and 6.61. Its $^{13}C$-NMR spectrum displayed 34 carbon

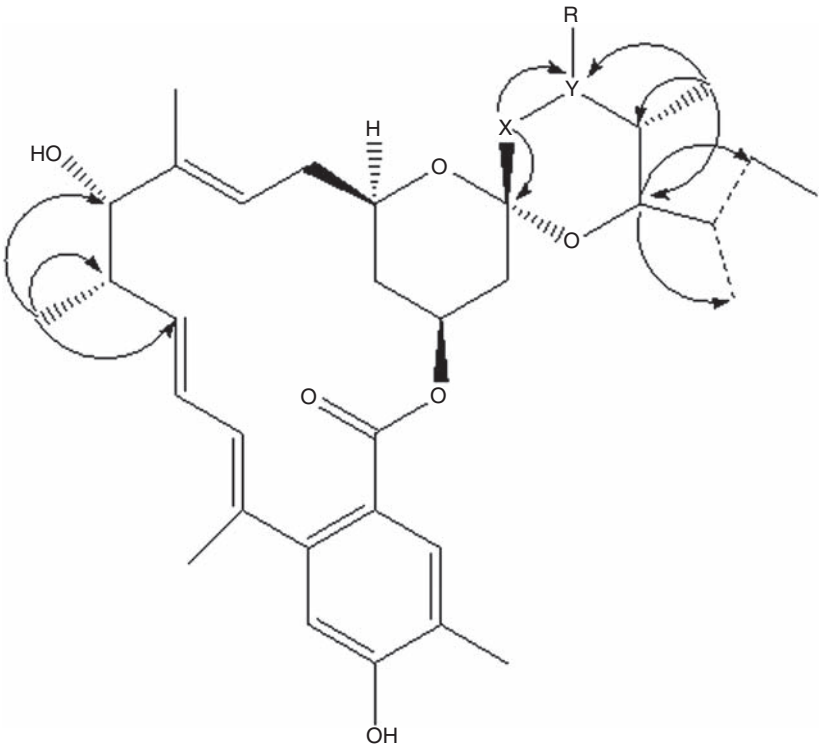


The key HMBC correlations of compound 1, 2 and 3

**Figure 2** The key heteronuclear multiple bond correlations (HMBC) of compounds **1**, **2** and **3**.

signals, including 1 carbonyl, 1 ester carbonyl, 12 $sp^2$ carbons, 7 methyls, 5 methylenes and 7 aliphatic methines (including 4 oxygenated and 1 ketal carbon). Comparing the $^1$H and $^{13}$C-NMR data with those of avermectin[12] suggested that compound **1** may be a derivative of avermectin aglycone. By a detailed comparison of the NMR data of **1** with those of milbemycin β3,[3–6] β4,[7,8] β13 and[9] β14[9] isolated from the milbemycin-producing strain, it was revealed that compound **1** was similar to milbemycin β3 except for the differences observed in C-13, C-23 and C-25 positions. In the HMBC spectrum, the observed correlation between $\delta_H$ 1.21 and $\delta_C$ 134.5, 40.7, 79.1 showed that C-13 was substituted by a hydroxyl group (Figure 2). Both the HMBC correlated signals of $\delta_H$ 0.97, $\delta_C$ 76.8, 46.6, 207.4 and the HMBC correlated signals of $\delta_H$ 2.47, $\delta_C$ 100.8, 207.4 indicated that the carbonyl group was in C-23 (Figure 2). The remaining one aliphatic methylene, one aliphatic methine, one doublet aliphatic methyl and one triplet aliphatic methyl showed the presence of an isopropyl group. The three bonds' correlation signals between $\delta_H$ 3.51 and $\delta_C$ 11.4, 27.4 assigned the second butyl group at C-25 similar to that of avermectin $B_{1a}$. The relative stereochemistry of **1** was assigned by concurring with that of avermectin B.[12]

Compound **2** was obtained as a white amorphous powder. Its $^1$H and $^{13}$C-NMR data were very similar to those of compound **1**, except for the presence of another double bond and the absence of one carbonyl and one methylene group. The $^1$H-$^1$H COSY correlation of $\delta_H$ 5.55 and $\delta_H$ 5.74, and the HMBC correlations between $\delta_H$ 0.91 and $\delta_C$ 136.1, indicated that the C-23 carbonyl and C-22 methylene (Figure 2) in **1** were replaced by one double bond in compound **2**. Thus, the structure of compound **2** was established.

Compound **3** was also isolated as a white amorphous powder. Comparison of the $^1$H and $^{13}$C-NMR data with those of compound **1** exhibited that the difference between compound **3** and compound **1** was only in the C-23 position, in which one carbonyl in compound **1** was replaced by a hydroxyl in compound **3**. The crossing peaks of $\delta_H$ 0.91 and $\delta_C$ 70.2 in the HMBC spectrum confirmed the hydroxyl group substituted at C-23 in compound **3** (Figure 2). Consequently, the structure of compound **3** was elucidated.

We have determined the 16S rDNA sequence of the strain (DQ768097), which produces compounds **1, 2** and **3**. It shared 99.05, 99.93 and 99.93% identity with the 16S rDNA sequences of *S. avermitilis* strains NBRC 14893 (AB184632), MA-4680 (AB078897) and AF145223, respectively, thereby characterizing strain NEAU1069 as *S. avermitilis*. We also isolated avermectin $B_{1a}$ from the *S. avermitilis* NEAU1069 fermentation broth. Furthermore, compounds **1**, **2** and **3** produced by *S. avermitilis* NEAU1069 had the same isopropyl group at C-25 as avermectin. Although compounds **1**, **2** and **3** are analogs of milbemycin β13 and β14[9] produced by *S. bingchenggensis*, the 16S rDNA sequence of *S. avermitilis* NEAU1069 only shared 94.84% identity compared with that of *S. bingchenggensis* (DQ449953). β-Class milbemycin compounds isolated from *S. avermitilis* were not reported.

## ACKNOWLEDGEMENTS

This study was supported by the National Natural Science Foundation of China (No. 30571234 and 30771427), the National Key Technology R&D Program (No. 2006BAD31B) and the Program for New Century Excellent Talents in University.

1 Dayan, F. E., Cantrell, C. L. & Duke, S. O. Natural products in crop protection. *Bioorg. Med. Chem.* **17,** 4022–4034 (2009).
2 Copping, L. G. & Duke, S. O Natural products that have been used commercially as crop protection agents. *Pest. Manag. Sci.* **63,** 524–554 (2007).

3 Davies, H. G. & Green, R. H. Avermectins and milbemycins, part I. *Chem. Soc. Rev.* **20,** 211–269 (1991).
4 Aoki, A., Fukuda, R. & Nakayabu, T. Antibiotic substances. US. 3,950,360, April 13 (1976).
5 Smith, A. B., Schow, S. R., Bloom, J. D., Thompson, A. S. & Winzenberg, K. N Total synthesis of milbemycin β3. *J. Am. Chem. Soc.* **104,** 4015–4018 (1982).
6 Schow, S. R., Bloom, J. D., Thompson , A. S., Winzenberg, K. N. & Smith, A. B. Total synthesis of milbemycin β3 and its C(12) epimer. *J. Am. Chem. Soc.* **108,** 2662–2674 (1986).
7 Nonaka, K. *et al.* New milbemycins from *Streptomyces hygroscopicus* subsp. *aureolacrimosus*: fermentation, isolation and structure elucidation. *J. Antibiot.* **53,** 694–704 (2000).
8 Hood, J. D. *et al.* A novel series of milbemycin antibiotics from *Streptomyces* strain E225. I. Discovery, fermentation and anthelmintic activity. *J. Antibiot.* **42,** 1593–1598 (1989).
9 Xiang, W. S., Wang, J. D., Wang, X. J. & Zhang, J. Two new β-Class milbemycins from *Streptomyces bingchenggensis*: fermentation, isolation, structure elucidation and biological properties. *J. Antibiot.* **60,** 351–356 (2007).
10 Rudd, B. A. M. Macrolide compounds. E.P. 0,242,052, Oct 21 (1987).
11 Tsukiyama, T., Kajino, H. & Tsukamoto, Y. Synthesis of novel 26-substituted milbemycin A(4) derivatives and their acaricidal activities. *J. Antibiot.* **57,** 446–455 (2004).
12 Springer, J. P., Arison, B. H., Hirshfield, J. M. & Hoogston, K. The absolute stereochemistry and conformation of avermectin $B_{2a}$ aglycon and avermectin $B_{1a}$. *J. Am. Chem. Soc.* **103,** 4221–4224 (1981).

The Journal of Antibiotics (2009) 62, 593–595

www.nature.com/ja

NOTE

# JBIR-52, a new antimycin-like compound, from *Streptomyces* sp. ML55

Ikuko Kozone[1], Jun-ya Ueda[1], Motoki Takagi[1] and Kazuo Shin-ya[2]

*The Journal of Antibiotics* (2009) **62,** 593–595; doi:10.1038/ja.2009.79; published online 7 August 2009

**Keywords:** antimycin; GRP78; JBIR-06; molecular chaperone; *Streptomyces*

GRP78/Bip is a molecular chaperone in the endoplasmic reticulum (ER) induced by ER stress that promotes protein folding and has an important role as a survival factor in solid tumors by providing resistance to both chemotherapy and hypoglycemic stress.[1] Thus, specific downregulators of GRP78 expression can reasonably be expected to become promising drugs in cancer chemotherapy.[2] In the course of our screening program for downregulators of GRP78 expression, we have isolated versipelostatin A-F,[3–11] prunustatin A,[12,13] JBIR-04, -05[14] and JBIR-06.[15] Further screening resulted in the isolation of a new inhibitor designated as JBIR-52 (**1**, Figure 1) from culture of a JBIR-06 producer, *Streptomyces* sp. ML55.[15,16] In this paper, we report the isolation, structure elucidation and brief biological activity of a new member of antimycin, **1**.

*Streptomyces* sp. ML55 was cultured on a rotary shaker (220 r.p.m.) at 27 °C for 5 days in 500-ml Erlenmeyer flasks containing 100 ml of a production medium consisting of 2% glycerol (Nacalai Tesque, Kyoto, Japan), 1% molasses (Dai-Nippon Meiji Sugar, Tokyo, Japan), 0.5% casein (Kanto Chemical, Tokyo, Japan), 0.1% polypepton (Nihon Pharmaceutical, Tokyo, Japan), 0.4% $CaCO_3$ (Kozaki Pharmaceutical, Tokyo, Japan) (pH 7.2 before sterilization). The mycelium from the culture broth (2 l) was extracted with $Me_2CO$ (400 ml). After concentration *in vacuo*, the residue was extracted twice with EtOAc. The organic layer was dried over anhydrous $Na_2SO_4$, and concentrated *in vacuo*. The dried residue (1.99 g) was applied to normal-phase MPLC (Purif-Pack SI-60, size:60, Moritex, Tokyo, Japan) and developed with a *n*-hexane–EtOAc linear gradient system (0–100% EtOAc), and peak detection was carried out by UV absorption at 254 nm. The 60–75% EtOAc eluate (470 mg) was further chromatographed on normal-phase MPLC (Purif-Pack SI-60, size:20, Moritex) with *n*-hexane–EtOAc (80:20). A portion (44.5 mg) of the fraction (388 mg) including both **1** and JBIR-06 was finally purified by preparative reversed-phase HPLC using an L-column2 ODS (20 i.d.×150 mm, Chemical Evaluation Research Institute, Tokyo, Japan) with 60% $CH_3CN$–$H_2O$ containing 0.1% formic acid (flow rate, 9.5 ml $min^{-1}$) to yield **1** (1.7 mg, retention time (Rt) 28.0 min) and JBIR-06 (2.3 mg, Rt 37.0 min).

Compound **1** was obtained as a white powder ($[\alpha]_D$ +40.0, *c* 0.07, 29 °C in MeOH, UV (MeOH) $\lambda_{max}$ ($\varepsilon$) 225 (22 500), 336 nm (4050)). The IR spectrum of **1** revealed the characteristic absorptions of esters ($\nu_{max}$ 1750, 1280 $cm^{-1}$), amide ($\nu_{max}$ 1645 $cm^{-1}$), hydroxyl and/or amide NH ($\nu_{max}$ 3400 $cm^{-1}$) groups. The HR electron spray ionization MS spectrum of **1** gave the $(M+H)^+$ ion at *m/z* 549.2429 (calcd. for $C_{27}H_{37}N_2O_{10}$, 549.2448) consistent with a molecular formula of $C_{27}H_{36}N_2O_{10}$. Direct connectivity between protons and carbons was established by the heteronuclear single quantum coherence spectrum and the $^{13}C$ and $^1H$ NMR spectral data for **1** are shown in Table 1. The observed double-quantum-filtered (DQF)-COSY and constant time heteronuclear multiple bond correlation (HMBC)[17] spectra established four partial structures.

The sequence from an oxymethine proton 2-H ($\delta_H$ 5.46) to 11-H ($\delta_H$ 1.64), which in turn coupled to two methyl protons 12-H ($\delta_H$ 0.95) and 13-H ($\delta_H$ 0.94), through 10-H ($\delta_H$ 1.84, 1.72) in the DQF-COSY spectrum established a 3-methyl-1-oxybutyl moiety. A doublet methyl proton 27-H ($\delta_H$ 1.33) and a low-field shifted methine proton 9-H ($\delta_H$ 3.32), which were spin–spin coupled to each other, were each long-range coupled to an ester carbonyl carbon C-8 ($\delta_C$ 170.2) and a ketone carbonyl carbon C-1 ($\delta_C$ 202.1), which in turn long-range coupled to 2-H and 10-H. These HMBC correlations indicated the successive connectivity of C-2, C-1, C-9 and C-8 as shown in Figure 1b. Thus, a 2,6-dimethyl-3-oxo-4-oxyheptanoic acid moiety was elucidated as a partial structure of **1** (Figure 1b).

The proton sequence between the aromatic protons 22-H ($\delta_H$ 8.58), 23-H ($\delta_H$ 6.97) and 24-H ($\delta_H$ 7.36) indicated the presence of a 1,2, 3-trisubstituted benzene ring moiety. An amide proton 21-NH ($\delta_H$ 7.97) was coupled to an aldehyde proton 25-H ($\delta_H$ 8.52), which was

[1]Biomedicinal Information Research Center (BIRC), Japan Biological Informatics Consortium (JBIC), Koto-ku, Tokyo, Japan and [2]Biomedicinal Information Research Center (BIRC), National Institute of Advanced Industrial Science and Technology (AIST), Koto-ku, Tokyo, Japan
Correspondence: Dr M Takagi, Biomedicinal Information Research Center (BIRC), Japan Biological Informatics Consortium (JBIC), 2-42 Aomi, Koto-ku, Tokyo 135-0064, Japan.
E-mail: motoki-takagi@aist.go.jp or Dr K Shin-ya, Biomedicinal Information Research Center (BIRC), National Institute of Advanced Industrial Science and Technology (AIST), 2-42 Aomi, Koto-ku, Tokyo 135-0064, Japan.
E-mail: k-shinya@aist.go.jp
Received 9 July 2009; revised 20 July 2009; accepted 21 July 2009; published online 7 August 2009

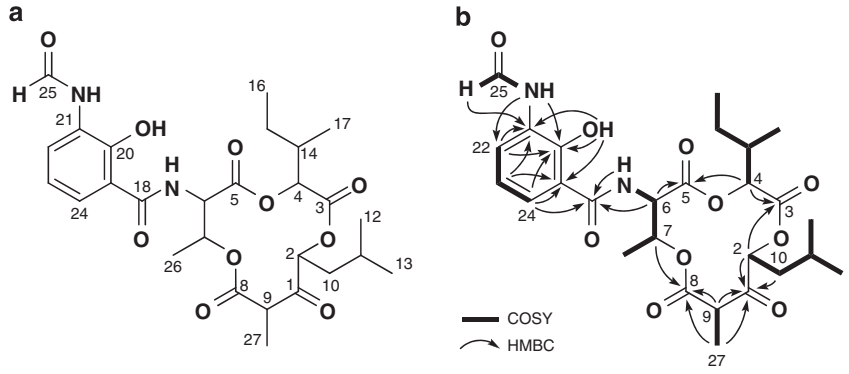


**Figure 1** (**a**) Structure of JBIR-52 (**1**) (**b**) correlations in DQF-COSY (bold line) and constant time heteronuclear multiple bond correlation (arrow) spectra of **1**.

**Table 1** $^{13}C$ and $^{1}H$ NMR data for **1**

| | $\delta_C$ | $\delta_H$ |
|---|---|---|
| 1 | 202.1 | |
| 2 | 79.1 | 5.46 (dd, 8.0, 4.5) |
| 3 | 167.7 | |
| 4 | 77.6 | 5.30 (d, 6.5) |
| 5 | 168.8 | |
| 6 | 55.4 | 5.29 (dd, 8.5, 3.5) |
| 7 | 73.1 | 5.60 (qd, 6.5, 3.5) |
| 8 | 170.2 | |
| 9 | 49.6 | 3.32 (q, 7.0) |
| 10 | 42.1 | 1.84 (ddd, 14.5, 9.0, 4.5); 1.72 (ddd, 14.5, 8.0, 4.5) |
| 11 | 24.5 | 1.64 (m) |
| 12 | 22.8 | 0.95 (d, 6.5) |
| 13 | 21.7 | 0.94 (d, 6.5) |
| 14 | 37.0 | 2.05 (m) |
| 15 | 24.6 | 1.57 (m); 1.31 (m) |
| 16 | 10.9 | 0.94 (t, 7.0) |
| 17 | 14.9 | 0.99 (d, 7.0) |
| 18 | 170.2 | |
| 19 | 112.7 | |
| 20 | 150.6 | |
| 21 | 127.2 | |
| 22 | 125.0 | 8.58 (dd, 8.0, 1.0) |
| 23 | 119.1 | 6.97 (t, 8.0) |
| 24 | 120.5 | 7.36 (dd, 8.0, 1.0) |
| 25 | 159.4 | 8.52 (d, 1.5) |
| 26 | 15.9 | 1.38 (d, 6.5) |
| 27 | 12.3 | 1.33 (d, 7.0) |
| 6-NH | | 7.10 (br d, 8.5) |
| 20-OH | | 12.58 (br s) |
| 21-NH | | 7.97 (br s) |

$^{13}C$ (150 MHz) and $^{1}H$ (600 MHz) NMR spectra were taken on a Varian NMR System 600 NB CL in $CDCl_3$, and the solvent peak was used as an internal standard ($\delta_C$ 77.0, $\delta_H$ 7.26 p.p.m.).

considered to connect directly with this amide nitrogen atom from its $^{13}C$ chemical shift ($\delta_C$ 159.4). The aldehyde proton and the aromatic proton 23-H were long-range coupled to an aromatic carbon C-21 ($\delta_C$ 127.2). These results suggested that a formamide group is substituted at the position of C-21. The aromatic proton 24-H was long-range coupled to a carbonyl carbon C-18 ($\delta_C$ 170.2) at the peri position, indicating that this carbonyl carbon is substituted at C-19 ($\delta_C$ 112.7). The aromatic protons 22-H and 24-H in addition to a phenolic hydroxyl proton 20-OH ($\delta_H$ 12.58) were long-range coupled to an aromatic carbon C-20 ($\delta_C$ 150.6). By taking into consideration these $^{13}C$ chemical shifts of aromatic carbons, an oxygen atom should be substituted at the C-20 position. Other $^{1}H$–$^{13}C$ long-range couplings (Figure 1b) and the UV spectrum of **1** also suggested the existence of the 3-(formylamino)-2-hydroxybenzoyl moiety, which is the same chromophore as those of the antimycin-related compounds.[12–15]

The sequence from an amide proton 6-NH ($\delta_H$ 7.10) to a methyl proton 26-H ($\delta_H$ 1.38) through an α-methine proton 6-H ($\delta_H$ 5.29) and an oxymethine proton 7-H ($\delta_H$ 5.60) was observed in the DQF-COSY spectrum of **1**. In addition to these correlations, the long-range couplings from the methine proton 6-H to a carbonyl carbon C-5 ($\delta_C$ 168.8) and the amide carbonyl carbon C-18 were observed. These results established a threonine residue and its connectivity with the chromophore moiety.

The remaining substructure was also determined by the interpretation of $^{1}H$–$^{1}H$ spin couplings and $^{1}H$–$^{13}C$ long-range couplings as follows. The long-range coupling between an oxymethine proton 4-H ($\delta_H$ 5.30) and an ester carbonyl carbon C-3 ($\delta_C$ 167.7) along with the sequence from 4-H to 16-H ($\delta_H$ 0.94) through 14-H ($\delta_H$ 2.05), which was additionally coupled to a methyl proton 17-H ($\delta_H$ 0.99), and 15-H ($\delta_H$ 1.57, 1.31), established a 3-methyl-2-oxypentanoic acid moiety (Figure 1b). The connectivity of these partial structures was elucidated by the long-range couplings between 2-H and C-3, 4-H and C-5 and 7-H and C-8. In this manner, the planar structure of **1** was determined as shown in Figure 1. JBIR-52 is structurally related to JBIR-06 in which the dimethyl residue is replaced by a methyl residue at the position of C-9.

To evaluate the inhibitory activity of **1** against GRP78 expression induced by 2-deoxyglucose as an ER stress, we used reporter gene assay system utilizing luciferase gene described previously.[5] The human fibrosarcoma HT1080 cells transformed with the luciferase reporter gene driven by the GRP78 promoter when treated with 10 mM of 2-deoxyglucose, produced four times more luciferase than did the untreated control. In this evaluation system, **1** reduced the expression of the reporter gene with an $IC_{50}$ value of 137 nM, which is almost the same as that of JBIR-06 ($IC_{50}$ value, 262 nM[14]). Contrary to the weak activity of 12-membered macrocyclic derivatives, 15-membered macrocyclic derivatives such as prunustatin A showed more potent activities ($IC_{50}$ values, 1.9 nM[12]). It has been reported that GRP78 protects epithelial cells from ATP depletion.[18] These results suggested that the coordinate action of ER and mitochondrial respiration exerts protective action against both ER and mitochondrial stress. Hence, the activities of GRP78 suppression by these compounds were considered to depend on respiratory inhibition due to salicylic

acid moiety.[14] These results provide us the interesting information that the size of macrocyclic structure determines the inhibitory activity of GRP78 expression by salicylic acid function. Studies in the detailed biological activities are now underway.

## ACKNOWLEDGEMENTS

This work was supported in part by the New Energy and Industrial Technology Development Organization of Japan (NEDO), and a Grant-in-Aid for Scientific Research (B) (20380070), the Ministry of Education, Culture, Sports, Science and Technology, Japan.

1 Katschinski, D. M., Jacobson, E. L., Wiedemann, G. J. & Robins, H. I. Modulation of VP-16 cytotoxicity by carboplatin and 41.8 °C hyperthermia. *J. Cancer Res. Clin. Oncol.* **127,** 425–432 (2001).
2 Imaizumi, K. *et al.* The unfolded protein response and Alzheimer's disease. *Biochem. Biophys. Acta.* **1536,** 85–96 (2001).
3 Park, H.-R., Furihata, K., Hayakawa, Y. & Shin-ya, K. Versipelostatin, a novel GRP78/Bip molecular chaperone down-regulator of microbial origin. *Tetrahedron Lett.* **43,** 6941–6945 (2002).
4 Chijiwa, S *et al.* Biosynthetic studies of versipelostatin, a novel 17-membered α-tetronic acid involved macrocyclic compound isolated from *Streptomyces versipellis*. *Tetrahedron Lett.* **44,** 5897–5900 (2003).
5 Park, H.-R. *et al.* Effect on tumor cells blocking survival response to glucose deprivation. *J. Natl. Cancer Inst.* **96,** 1300–1310 (2004).
6 Saito, S. *et al.* Chemical genomics identifies the unfolded protein response as a target for selective cancer cell killing during glucose deprivation. *Cancer Res.* **69,** 4225–4234 (2009).
7 Park, H.-R., Chijiwa, S., Furihata, K., Hayakawa, Y. & Shin-ya, K. Relative and absolute configuration of versipelostatin, a down-regulator of molecular chaperone GRP78 expression. *Org. Lett.* **9,** 1457–1460 (2007).
8 Ueda, J., Chijiwa, S., Takagi, M. & Shin-ya, K. A novel versipelostatin analogue, versipelostatin F isolated from *Streptomyces versipellis* 4083-SVS6. *J. Antibiot.* **61,** 752–755 (2008).
9 Matsuo, J. *et al.* Preventing the unfolded protein response via aberrant activation of 4E-binding protein 1 by versipelostatin. *Cancer Sci.* **100,** 327–333 (2009).
10 Zhao, P. *et al.* New glycosylated derivatives of versipelostatin, the GRP78/Bip molecular chaperone down-regulator, from *Streptomyces versipellis* 4083-SVS6. *Org. Biomol. Chem.* **7,** 1454–1460 (2009).
11 Tanaka, H. *et al.* Efficient synthesis of the deoxysugar part of versipelostatin by direct and stereoselective glycosylation and revision of the structure of the trisaccharide unit. *Chem. Asian J.* **4,** 1114–1125 (2009).
12 Umeda, Y. *et al.* Prunustatin A, a novel GRP78 molecular chaperone downregulator isolated form *Streptomyces violaceoniger. J. Antibiot.* **58,** 206–209 (2005).
13 Umeda, Y. *et al.* Absolute structure of prunustatin A, a novel GRP78 molecular chaperone down-regulator. *Org. Lett.* **9,** 4239–4242 (2007).
14 Izumikawa, M., Ueda, J., Chijiwa, S., Takagi, M. & Shin-ya, K. Novel GRP78 molecular chaperone expression down-regulators JBIR-04 and -05 isolated from *Streptomyces violaceoniger. J. Antibiot.* **60,** 640–644 (2007).
15 Ueda, J. *et al.* A novel antimycin-like compound, JBIR-06, from *Streptomyces* sp. ML55. *J. Antibiot.* **61,** 241–244 (2008).
16 Ueda, J. *et al.* A novel nuclear export inhibitor JBIR-02, a new piericidin discovered from *Streptomyces* sp. ML55. *J. Antibiot.* **60,** 459–462 (2007).
17 Furihata, K. & Seto, H. Constant time HMBC (CT-HMBC), a new HMBC technique useful for improving separation of cross peaks. *Tetrahedron Lett.* **39,** 7337–7340 (1998).
18 Bush, K. T., George, S. K., Zhang, P. L. & Nigam, S. K. Pretreatment with inducers of ER molecular chaperones protects epithelial cells subjected to ATP depletion. *Am. J. Physiol.* **277,** F211–F218 (1999).

The Journal of Antibiotics (2009) 62, 597–599

www.nature.com/ja

NOTE

# Gramicidin S analogs having six basic amino acid residues

Makoto Tamaki[1], Ichiro Sasaki[1], Yuki Nakao[1], Mitsuno Shindo[2], Masahiro Kimura[2] and Yoshiki Uchida[2]

*The Journal of Antibiotics* (2009) **62,** 597–599; doi:10.1038/ja.2009.81; published online 28 August 2009

**Keywords:** gramicidin S; polycation analog; antiparallel $\beta$-sheet conformation; structure–activity relationship

Gramicidin S (GS), cyclo(-Val$^{1,1'}$-Orn$^{2,2'}$-Leu$^{3,3'}$-D-Phe$^{4,4'}$-Pro$^{5,5'}$-)$_2$,[1–3] is a potent cyclopeptide antibiotic isolated from *Bacillus brevis*. Its secondary structure has been established as an antiparallel β-sheet conformation with amphiphilicity.[4,5] The conformation is characteristically featured with the orientation of side chains in such a way that the charged Orn side chains are situated on one side of the molecule and the hydrophobic Val and Leu side chains are situated on the other side. The side-chain arrangement is apparently held together by a rigid conformation containing two D-Phe-Pro type II′ β-turns. It has been proposed that the principal modes of antibiotic actions result from an interaction of GS with the cell membrane of the target microorganisms. GS then adopts an antiparallel β-sheet conformation with amphiphilicity, which disrupts cell membrane.[6] Thus, the hydrophobic Val and Leu residues have been considered to be essential for exhibiting the strong activity of GS. Therefore, syntheses of antimicrobially active analogs of GS containing amino acid residues with hydrophilic side chain in place of Val and Leu residues have not been reported yet.[2,3,7–9]

In this account, we designed and synthesized novel GS analogs, cyclo(-Orn$^{1,1'}$-Orn$^{2,2'}$-Orn$^{3,3'}$-D-Phe$^{4,4'}$-Pro$^{5,5'}$-)$_2$ (**1**) and cyclo (-Lys$^{1,1'}$-Orn$^{2,2'}$-Lys$^{3,3'}$-D-Phe$^{4,4'}$-Pro$^{5,5'}$-)$_2$ (**2**), which have four basic amino acid residues (Orn and Lys residues) in place of four hydrophobic amino acid residues (Val and Leu residues), to investigate the role of amphiphilic β-sheet structure of GS for the antibiotic activity.

Syntheses of **1** and **2** were performed by a solid-phase method using oxime resin.[10] The formation of the cyclic peptides by the dimerization–cyclization of H-D-Phe-Pro-X-Orn(Z)-X-oxime on resin (X=Orn(Z), and Lys(Z)) (Z-=benzyloxycarbonyl-) gave cyclo(-X$^{1,1'}$-Orn(Z)$^{2,2'}$-X$^{3,3'}$-D-Phe$^{4,4'}$-Pro$^{5,5'}$-)$_2$ in 83 and 92% yields, respectively. The removal of all the masking groups by 25% HBr/AcOH produced the corresponding antibiotics **1** and **2** in 53 and 67% yields, respectively. The homogeneities of **1** and **2** were confirmed by thin-layer chromatography, high performance liquid chromatography, FAB-MS and $^1$H NMR spectrometry.

To investigate the secondary structures of **1** and **2**, CD and $^1$H NMR spectra of **1** and **2** were measured. Compounds **1**, **2** and GS showed almost identical CD spectra in methanol (Figure 1), suggesting that **1** and **2** have a β-sheet structure similar to that of GS.

The $^1$H NMR (400 MHz) spectra of **1** and **2** were measured at 30 °C in DMSO-*d*6 (peptide concentration: ~17 mg ml$^{-1}$). All protons were assigned by means of H–H COSY (correlation spectroscopy), TOCSY (total correlation spectroscopy) and ROESY (rotating frame nuclear Overhauser enhancement spectroscopy). Only one $^{\alpha}$NH resonance appeared for X$^{1,1'}$, Orn$^{2,2'}$, X$^{3,3'}$ and D-Phe$^{4,4'}$ residues (**1**: X=Orn, **2**: X=Lys), indicating that **1** and **2** have conformations with $C_2$ symmetry in the NMR time average. In the $^1$H NMR spectrum of **1**, temperature coefficient values of $^{\alpha}$NH groups for Orn$^{1,1'}$, Orn$^{2,2'}$, Orn$^{3,3'}$ and D-Phe$^{4,4'}$ were 2.8, 6.3, 2.8 and 5.7 ppb K$^{-1}$, respectively. These results indicated that Orn$^{1,1'}$ $^{\alpha}$NH and Orn$^{3,3'}$ $^{\alpha}$NH are shielded from the solvent and involved in two stable intramolecular hydrogen bonds, whereas Orn$^{2,2'}$ $^{\alpha}$NH and D-Phe$^{4,4'}$ $^{\alpha}$NH are exposed to the solvent. The $J_{NH\text{-}^{\alpha}CH}$ values of Orn$^{1,1'}$, Orn$^{2,2'}$, Orn$^{3,3'}$ and D-Phe$^{4,4'}$ residues were 8.1, 8.8, 7.6 and 2.0 Hz, respectively. The $J_{NH\text{-}^{\alpha}CH}$ values observed for Orn$^{1,1'}$, Orn$^{2,2'}$ and Orn$^{3,3'}$ residues were strongly indicative of an extended β-sheet conformation.[11] On the other hand, $J_{NH\text{-}^{\alpha}CH}$ value of D-Phe residue was indicative of a β-turn conformation.[11] The chemical shift perturbation[12] ($\Delta\delta H_{\alpha}$=observed $\delta H_{\alpha}$−random coil $\delta H_{\alpha}$) of the $^{\alpha}$H of Orn$^{1,1'}$, Orn$^{2,2'}$ and Orn$^{3,3'}$ showed positive values (>0.1 p.p.m.). On the other hand, the D-Phe$^{4,4'}$ and Pro$^{5,5'}$ residues showed negative values. The chemical shift perturbation of the $^{\alpha}$H of **1** agreed well with those of GS.[13] The results suggested that Orn$^{1,1'}$-Orn$^{2,2'}$-Orn$^{3,3'}$ sequences in **1** have a similar β-sheet conformation to that of GS sequences. Next, for detailed analysis, the spatial ROE correlations were measured. (Figure 2) ROE spatial correlations between Pro$^{5,5'}$ $^{\alpha}$CH and Orn$^{1,1'}$ $^{\alpha}$NH, Orn$^{1,1'}$ $^{\alpha}$CH and Orn$^{2,2'}$ $^{\alpha}$NH, Orn$^{2,2'}$ $^{\alpha}$CH and Orn$^{3,3'}$ $^{\alpha}$NH, Orn$^{3,3'}$ $^{\alpha}$CH and D-Phe$^{4,4'}$ $^{\alpha}$NH, and D-Phe$^{4,4'}$ $^{\alpha}$CH and Pro$^{5,5'}$ $^{\delta}$CH$_2$ were observed. The results indicated that amide bonds in **1** are

[1]Department of Chemistry, Toho University, Funabashi, Chiba, Japan and [2]Department of Food Science and Nutrition, Osaka Shoin Women's University, Higashi-Osaka, Osaka, Japan
Correspondence: Dr M Tamaki, Department of Chemistry, Toho University, Miyama 2-2-1, Funabashi, Chiba 274-8510, Japan.
E-mail: tamaki@chem.sci.toho-u.ac.jp
Received 7 April 2009; revised 10 July 2009; accepted 13 July 2009; published online 28 August 2009

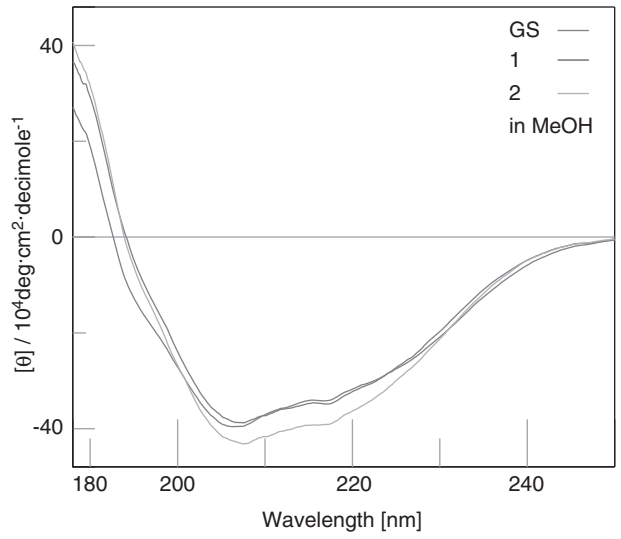


**Figure 1** CD spectra of **1**, **2** and GS in methanol.

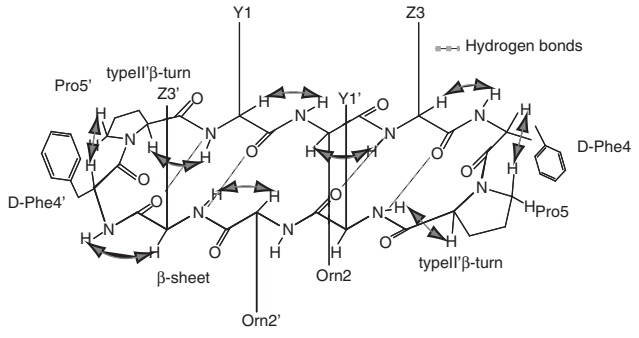


**Figure 2** Proposed secondary structures of **1** ($Y^{1,1'}$ and $Z^{3,3'}$=-$(CH_2)_3NH_2$), **2** ($Y^{1,1'}$ and $Z^{3,3'}$=-$(CH_2)_4NH_2$) and GS ($Y^{1,1'}$=-$CH(CH_3)_2$, $Z^{3,3'}$=-$CH_2CH(NH_3)_2$) with ROE spatial correlations.

all-*trans* conformation. The signal of D-Phe $^{\beta}CH_2$ was two multiplets, indicating that they are nonequivalent and fixed in certain arrangement. The chemical shifts of H resonances for the diastereotopic β-, γ- and δ-$CH_2$ of Pro residues were separated by 0.29, 0.00 and 0.83 p.p.m., respectively, suggesting that the aromatic ring of D-Phe residue orients in close proximity to Pro $^{\delta}CH$. Similar results were obtained from the NMR studies of **2**. The NMR data indicated that **1** and **2** have GS-like antiparallel β-sheet structures with a type II′ β-turn around D-Phe-Pro as shown in Figure 2, and that the hydrophobic side chains of Val and Leu residues are not necessary for holding the rigid β-sheet conformation of GS.

The antibiotic activities and hemolytic activities of **1**, **2** and GS were summarized in Table 1. The difference of antibiotic activities among **1**, **2** and GS reflects the characters of side chains of the amino acid residues at positions 1, 1′, 3 and 3′ because the antibiotics have similar β-sheet structure to each other. The antibiotic activities of **1** and **2** were 1/4 and 1/8 of GS against *Bacillus subtilis* NBRC 3513 and *Bacillus megaterium* ATCC 19213, respectively, and less against *Staphylococcus epidermidis* NBRC 12933 and *Staphylococcus aureus* NBRC 12732. On the other hand, **1** and **2** showed no activity against Gram-negative microorganisms tested. The results indicated that the presence of hydrophobic side chains of Val and Leu residues are important for exhibiting the strong activity of GS. In addition, it is interesting to note that **1** and **2** showed some selectivity against

**Table 1 Antibiotic activities[a] and hemolytic activity[b] of 1, 2 and GS**

| | *MIC μg ml$^{-1}$* | | | | | | *(%)* |
|---|---|---|---|---|---|---|---|
| *Peptides* | *A* | *B* | *C* | *D* | *E* | *F* | *G* |
| GS | 3.13 | 3.13 | 3.13 | 3.13 | 25 | 25 | 100 |
| 1 | 12.5 | 12.5 | 100 | 50 | >100 | >100 | 0.84 |
| 2 | 25 | 25 | 100 | 100 | >100 | >100 | 1.49 |

[a]MIC value in μg ml$^{-1}$. A: *Bacillus subtilis* NBRC 3513, B: *Bacillus megaterium* ATCC 19213, C: *Staphylococcus epidermidis* NBRC 12933, D: *Staphylococcus aureus* NBRC 12732, E: *Pseudomonas aeruginosa* NBRC 3080, F: *Escherichia coli* NBRC 12734.
[b]G is hemolytic percentage of the peptides (50 μM) in buffer solution against sheep erythrocytes.

different microorganisms. Then, **1** and **2** showed almost no hemolytic activity toward sheep red blood cells (Table 1),[14] indicating that the replacement of the Val and Leu hydrophobic side chains into the Orn and Lys basic side chains could result in substantial reduction of hemolytic activities.

In these studies, we reported the structure–activity relationship of GS analogs **1** and **2** containing Orn and Lys residues with basic side chains in place of four hydrophobic Val and Leu residues. Currently, we are investigating the design and syntheses of other antimicrobially active analogs of GS without the hydrophobic Val and Leu residues on one side of the molecule on the basis of these studies in order to find new types of drug candidates with high antimicrobial and low hemolytic activities.

## EXPERIMENTAL SECTION

Melting points were measured on Mel-Temp II melting point apparatus (Laboratory Devices, Cambridge, MA, USA) and are uncorrected. Low-resolution mass spectra (LR-MS) were obtained by using FAB mass spectrometry on a JEOL600H mass spectrometer (Jeol, Tokyo, Japan). CD spectra were recorded on a Jasco J-820 spectropolarimeter (Jasco, Tokyo, Japan) using a quarts cell of 0.5-mm pathlength. The CD spectra in methanol were measured at a peptide concentration of $1.10\times10^{-4}$ M at room temperature. $^1$H NMR spectra were measured in DMSO-$d_6$ at 30 °C (peptide concentration ca. 17 mg ml$^{-1}$) on a JEOL JNM-ECP400 spectrometer (Jeol) using standard pulse sequences and software. The chemical shifts were determined with respect to internal TMS (tetramethylsilane).

### cyclo(-Orn-Orn-Orn-D-Phe-Pro-)$_2$ 6HBr (1)

A protected linear precursor oxime, H-D-Phe-Pro-Orn(Z)-Orn(Z)-Orn(Z)-oxime, was prepared by using Boc-solid phase peptide synthesis on resin (Loading of oxime group: 0. 35 mmol g$^{-1}$ resins). The formation of the cyclic peptide by the dimerization–cyclization of H-D-Phe-Pro-Orn(Z)-Orn(Z)-Orn(Z)-oxime on resin was performed in 1,4-dioxane with two equiv. of triethylamine and acetic acid for 1 day at room temperature.[10] The cyclizations gave cyclo(-Orn(Z)-Orn(Z)-Orn(Z)-D-Phe-Pro-)$_2$ in yield of 83%. The removal of all the masking groups was performed by 25% HBr/acetic acid. The product was purified by gel filtration on a Sephadex LH-20 column (GE Healthcare Bio-Sciences AB, Uppsala, Sweden), and by reprecipitation from methanol–ether to give a white powder of **1** in 53% yield.

Mp 234–235 °C. LR-FAB-MS (matrix: *m*-NBA (*m*-nitro benzyl alcohol)) Calcd for $C_{58}H_{92}N_{16}O_{10}$ [M]$^+$=1173, Found *m/z* 1174 ([M+H]$^+$, 0.90%), 1196 ([M+Na]$^+$, 0.32%). $^1$H NMR (400 MHz, DMSO-$d_6$) $\delta$ 9.30 (d, 2H, $NH_{\alpha}$ D-Phe$^{4,4'}$, $^3J_{NH\text{-}H\alpha}$=2.0 Hz), 8.75 (d, 2H, $NH_{\alpha}$ Orn$^{2,2'}$, $^3J_{NH\text{-}H\alpha}$=8.8 Hz), 8.16 (d, 2H, $NH_{\alpha}$ Orn$^{3,3'}$, $^3J_{NH\text{-}H\alpha}$=7.6 Hz), 7.78 (m, 4H, $NH_{\delta}$ Orn$^{1,1'}$, m, 4H, $NH_{\delta}$ Orn$^{3,3'}$), 7.69 (m, 4H, $NH_{\delta}$ Orn$^{2,2'}$), 7.33–7.27 (m, 10H, $H_{ar}$ D-Phe$^{4,4'}$), 7.31 (d, 2H, $NH_{\alpha}$ Orn$^{1,1'}$, $^3J_{NH\text{-}H\alpha}$=8.1 Hz), 4.82 (m, 2H, $H_{\alpha}$ Orn$^{2,2'}$), 4.55 (m, 2H, $H_{\alpha}$ Orn$^{1,1'}$), 4.49 (m, 2H, $H_{\alpha}$ Orn$^{3,3'}$), 4.43 (m, 2H, $H_{\alpha}$ D-Phe$^{4,4'}$), 4.35 (m, 2H, $H_{\alpha}$ Pro$^{5,5'}$), 3.52 (m, 2H, $H_{\delta}$ Pro$^{5,5'}$), 3.00 (m, 2H $H_{\beta}$ D-Phe$^{4,4'}$), 2.87 (m, 2H $H_{\beta}$ D-Phe$^{4,4'}$), 2.80 (m, 4H, $H_{\delta}$ Orn$^{1,1'}$, m, 4H, $H_{\delta}$ Orn$^{2,2'}$, m, 4H, $H_{\delta}$ Orn$^{3,3'}$), 2.69 (m, 2H, $H_{\delta}$ Pro$^{5,5'}$), 1.97 (m, 2H, $H_{\beta}$ Pro$^{5,5'}$), 1.74 (m, 2H, $H_{\beta}$ Orn$^{1,1'}$), 1.70 (m, 2H, $H_{\beta}$ Orn$^{2,2'}$), 1.69 (m, 2H, $H_{\beta}$ Orn$^{1,1'}$), 1.61 (m, 2H, $H_{\beta}$ Orn$^{2,2'}$, m, 2H, $H_{\beta}$ Orn$^{3,3'}$, m, 2H, $H_{\beta}$ Pro$^{5,5'}$, m, 4H, $H_{\gamma}$ Pro$^{5,5'}$), 1.47 (m, 2H, $H_{\beta}$ Orn$^{3,3'}$, m, 4H, $H_{\gamma}$ Orn$^{3,3'}$), 1.45 (m, 4H, $H_{\gamma}$ Orn$^{1,1'}$, m, 4H, $H_{\gamma}$ Orn$^{2,2'}$).

**cyclo(-Lys-Orn-Lys-D-Phe-Pro-)$_2$ 6HBr (2)**

cyclo(-Lys(Z)-Orn(Z)-Lys(Z)-D-Phe-Pro-)$_2$ was synthesized in 92% yield as has been described for the preparation of cyclo(-Orn(Z)-Orn(Z)-Orn(Z)-D-Phe-Pro-)$_2$. The removal of all the masking groups by 25% HBr/acetic acid produced **2** in 67% yield.

Mp. 231.5–233.0 °C. LR-FAB-MS (matrix: *m*-NBA) Calcd for $C_{62}H_{100}N_{16}O_{10}$ $[M]^+$=1229, Found *m/z* 1230 ($[M+H]^+$, 1.01%), 1252 ($[M+Na]^+$, 0.33%). $^1$H NMR (400 MHz, DMSO-$d_6$) $\delta$ 9.22 (d, 2H, $NH_\alpha$ D-Phe$^{4,4'}$, $^3J_{NH\text{-}H\alpha}$=1.6 Hz), 8.69 (d, 2H, $NH_\alpha$ Orn$^{2,2'}$, $^3J_{NH\text{-}H\alpha}$=7.8 Hz), 8.16 (d, 2H, $NH_\alpha$ Lys$^{3,3'}$, $^3J_{NH\text{-}H\alpha}$=8.1 Hz), 7.84 (m, 4H, $NH_\varepsilon$ Lys$^{1,1'}$, m, 4H, $NH_\delta$ Orn$^{2,2'}$, m, 4H, $NH_\varepsilon$ Lys$^{3,3'}$), 7.32–7.27 (m, 10H, $H_{ar}$ D-Phe$^{4,4'}$), 7.28 (d, 2H, $NH_\alpha$ Lys$^{1,1'}$, $^3J_{NH\text{-}H\alpha}$=8.3 Hz), 4.79 (m, 2H, $H_\alpha$ Orn$^{2,2'}$), 4.50 (m, 2H, $H_\alpha$ Lys$^{1,1'}$), 4.47 (m, 2H, $H_\alpha$ Lys$^{3,3'}$), 4.41 (m, 2H, $H_\alpha$ D-Phe$^{4,4'}$), 4.32 (m, 2H, $H_\alpha$ Pro$^{5,5'}$), 3.59 (m, 2H, $H_\delta$ Pro$^{5,5'}$), 3.00 (m, 2H $H_\beta$ D-Phe$^{4,4'}$), 2.89 (m, 2H $H_\beta$ D-Phe$^{4,4'}$), 2.83 (m, 4H, $H_\delta$ Orn$^{2,2'}$), 2.74 (m, 4H, $H_\varepsilon$ Lys$^{3,3'}$), 2.68 (m, 4H, $H_\varepsilon$ Lys$^{1,1'}$), 2.52 (m, 2H, $H_\delta$ Pro$^{5,5'}$), 1.98 (m, 2H, $H_\beta$ Pro$^{5,5'}$), 1.74 (m, 2H, $H_\beta$ Orn$^{2,2'}$), 1.71 (m, 4H, $H_\beta$ Lys$^{1,1'}$), 1.69 (m, 2H, $H_\beta$ Orn$^{2,2'}$), 1.57 (m, 4H, $H_\gamma$ Lys$^{1,1'}$, m, 4H, $H_\gamma$ Orn$^{2,2'}$, m, 4H, $H_\beta$ Lys$^{3,3'}$, m, 2H, $H_\beta$ Pro$^{5,5'}$, m, 4H, $H_\gamma$ Pro$^{5,5'}$), 1.33 (m, 4H, $H_\gamma$ Lys$^{3,3'}$), 1.27 (m, 4H, $H_\delta$ Lys$^{1,1'}$), 1.19 (m, 4H, $H_\delta$ Lys$^{3,3'}$).

1 Gause, G. F. & Brazhnikova, M. G. Gramicidin S and its use in the treatment of infected wounds. *Nature* **154,** 703 (1944).

2 Izumiya, N., Kato, T., Aoyagi, H., Waki, M. & Kondo, M. *Synthetic Aspects of Biologically Active Cyclic Peptide-Gramicidin S and Tyrocidines* (Kodansha, Tokyo, and Halsted Press, New York, 1979).

3 Waki, M. & Izumiya, N. Biochemistry of peptide antibiotics (eds. Kleinkauf, H. & von Dohren, H.) *Fed Rep, Ger* 205–244 (de Gruyter, Berlin, 1990).

4 Hull, S. E., Karlson, R., Main, P., Woolfson, M. M. & Dodson, E. J. The crystal structure of a hydrated gramicidin S-urea complex. *Nature* **275,** 206–207 (1978).

5 Yamada, K. *et al.* Stereochemistry of protected ornithine side chains of gramicidin S derivatives: X-ray crystal structure of the bis-Boc-tetra-*N*-methyl derivative of gramicidine S. *J. Am. Chem. Soc.* **124,** 12684–12688 (2002).

6 Katsu, T. *et al.* Structure-activity relationship of gramicidin S analogues on membrance permeability. *Biochim. Biophys. Acta.* **899,** 159–170 (1987).

7 Arai, T. *et al.* Synthesis of [Hexafluorovalyl$^{1,1'}$]gramicidin S. *Bull. Chem. Soc. Jpn.* **69,** 1383–1389 (1996).

8 Mihara, H. *et al.* A pair of pyrene groups as a conformational probe for antiparallel β-sheet structure formed in cyclic peptides. *J. Chem. Soc., Perkin Trans.* **2,** 517–522 (1997).

9 Solanas, C. *et al.* Therapeutic Index of gramicidin S is strongly modulated by D-phenylalanine analogues at the β-turn. *J. Med. Chem.* **52,** 664–674 (2009).

10 Tamaki, M., Honda, K., Kikuchi, S. & Ishii, R. Biomimetic formation of gramicidin S by dimerization-cyclization pentapeptide precursor on solid support. *Tetrahedron Lett.* **47,** 8475–8478 (2006).

11 Pardi, A., Billeter, M. & Wüthrich, K. Calibration of the angular dependence of the amide proton-C$^\alpha$proton coupling constants, $^3$JHNα, in a globular protein. *J. Mol. Biol.* **180,** 741–751 (1984).

12 Wishart, D. S., Sykes, B. D. & Richards, F. M. The chemical shift index: a fast and simple method for assignment of protein secondary structures through NMR spectroscopy. *Biochemistry* **31,** 1647–1651 (1992).

13 Grotenbreg, G. M. *et al.* Synthesis and biological evalution of novel turn-modified gramicidine S analogues. *Bioorg. Med. Chem.* **11,** 2835–2841 (2003).

14 Tamaki, M. *et al.* Syntheses of low-hemolytic antimicrobial gratisin peptides. *Bioorg. Med. Chem. Lett.* **19,** 2856–2859 (2009).

The Journal of Antibiotics (2009) 62, 601–603

www.nature.com/ja

NOTE

# Novel siderophore, JBIR-16, isolated from *Nocardia tenerifensis* NBRC 101015

Akira Mukai[1], Hisayuki Komaki[2], Motoki Takagi[1] and Kazuo Shin-ya[3]

*The Journal of Antibiotics* (2009) **62,** 601–603; doi:10.1038/ja.2009.84; published online 21 August 2009

**Keywords:** *Nocardia tenerifensis*; siderophore; heterobactin; JBIR-16

*Nocardia* is the causative microorganism of a human infection called nocardiosis. It is also known to produce a variety of compounds with antitumor,[1,2] antimicrobial[3,4] and immunosuppressive activity.[5,6] To take up iron, which is an essential element for all organisms, into cells under iron-deficient conditions, microorganisms produce iron chelators, namely, siderophores. Five types of siderophores have been isolated: hydroxamates, catecholates, salicylates, nitrosophenols and carboxylates.[7] Some siderophores, such as brasilibactin A,[8] asterobactin,[9] nocobactin NA[10] and nocardamine,[11] are produced by *Nocardia* spp. In the course of our screening program for biologically active compounds of microbial origin, we isolated a novel heterobactin[12] analog, JBIR-16 (**1**), containing hydroxamate and catecholate, from the culture broth of *Nocardia tenerifensis* NBRC 101015 (Figure 1). In this paper, we report the production, isolation, structural determination, and briefly the biological activity of **1**.

The producing strain *N. tenerifensis* NBRC 101015 was cultured on a rotary shaker for 6 days in a 50-ml Erlenmeyer flask containing 10 ml of Brain Heart Infusion broth (Difco Lab., Detroit, MI, USA), including 2% glucose as a seed culture. The seed culture was transferred into 500-ml Erlenmeyer flasks containing 100 ml of a producing medium consisting of a twice concentrated nutrient broth (Difco Lab.), including 1% glucose and 1% glycerol, and incubated on a rotary shaker at 250 r.p.m. for 6 days.

After centrifugation of the culture broth, the supernatant (5 l) was applied on a HP-20 column (Mitsubishi Chemical, Tokyo, Japan), the column was washed with water and then eluted with 100% MeOH to obtain the fraction containing **1** (833 mg). The $R_f$ value of **1** showed 0.6 on a TLC analysis using chloroform–MeOH (10:1) as mobile phase. The eluate was evaporated to dryness, applied on a normal-phase medium-pressure liquid chromatography column (Purif-Pack SI-60, Moritex, Tokyo, Japan) and eluted with a chloroform–MeOH gradient (0–80% MeOH). The main fraction (43.8 mg) was finally separated by preparative HPLC using an XBridge Prep $C_{18}$ column (5 μm OBD, 20 i.d. ×150 mm, Waters, Milford, MA, USA: mobile phase; 35% aqueous MeOH, flow rate; 10 ml $min^{-1}$, detection; 254 nm) to obtain **1** (3.6 mg; retention time 22 min).

Compound **1** was obtained as a white powder ($[\alpha]_D^{25}$ −9.3, *c* 0.1, in MeOH, UV (MeOH) $\lambda_{max}$ ($\varepsilon$) 205 (50 800), 249 nm (15 085). The IR spectrum of **1** revealed the characteristic absorptions of amide carbonyl ($\nu_{max}$ 1643 $cm^{-1}$) and amide N–H ($\nu_{max}$ 1542 $cm^{-1}$) groups. The HR electron spray ionization-MS of **1** resulted in the $(M+H)^+$ ion at *m/z* 574.2149, consistent with a molecular formula of $C_{26}H_{32}N_5O_{10}$ (calculated for $C_{26}H_{32}N_5O_{10}$, 574.2133).

Although the partial and putative structure of **1** was elucidated by the analyses of a series of NMR techniques, such as constant time heteronuclear multibond correlation[13] and double-quantum filtered (DQF)–COSY, their connectivities could not be confirmed because of the lack of signals of exchangeable protons. Therefore, the structure of **1** was determined by spectral analyses of a pentamethylated derivative **2**, which was prepared by the treatment of **1** with methyl iodide. Compound **2** gave the $(M+H)^+$ ion at *m/z* 644 in the positive mode. In addition, $^1H$ and $^{13}C$ chemical shifts of these methyl residues (Table 1) indicated the presence of five hydroxyl groups in **2**. The direct C–H connectivity was established by heteronuclear single quantum coherence (see Table 1). The analyses of DQF–COSY and heteronuclear multibond correlation spectra of **2** established five substructures as follows: In the DQF spectrum, the sequence from methylene proton 1-$H_2$ ($\delta_H$ 3.52, 3.60) to an amide proton 4-NH ($\delta_H$ 7.00) through methylene protons 2-$H_2$ ($\delta_H$ 1.95, 2.01), 3-$H_2$ ($\delta_H$ 1.63, 2.37) and an α-methine proton 4-H ($\delta_H$ 4.30, $\delta_C$ 51.5)

[1]Biomedicinal Information Research Center (BIRC), Japan Biological Informatics Consortium (JBIC), Koto-ku, Tokyo, Japan; [2]NITE Biological Resource Center (NBRC), National Institute of Technology and Evaluation (NITE), Kisarazu, Chiba, Japan and [3]Biomedicinal Information Research Center (BIRC), National Institute of Advanced Industrial Science and Technology (AIST), Koto-ku, Tokyo, Japan
Correspondence: Dr M Takagi, Biomedicinal Information Research Center (BIRC), Japan Biological Informatics Consortium (JBIC), 2-42 Aomi, Koto-ku, Tokyo 135-0064, Japan.
E-mail: motoki-takagi@aist.go.jp or Dr K Shin-ya, Biomedicinal Information Research Center (BIRC), National Institute of Advanced Industrial Science and Technology (AIST), 2-42 Aomi, Koto-ku, Tokyo 135-0064, Japan.
E-mail: k-shinya@aist.go.jp
Received 9 June 2009; revised 28 July 2009; accepted 30 July 2009; published online 21 August 2009

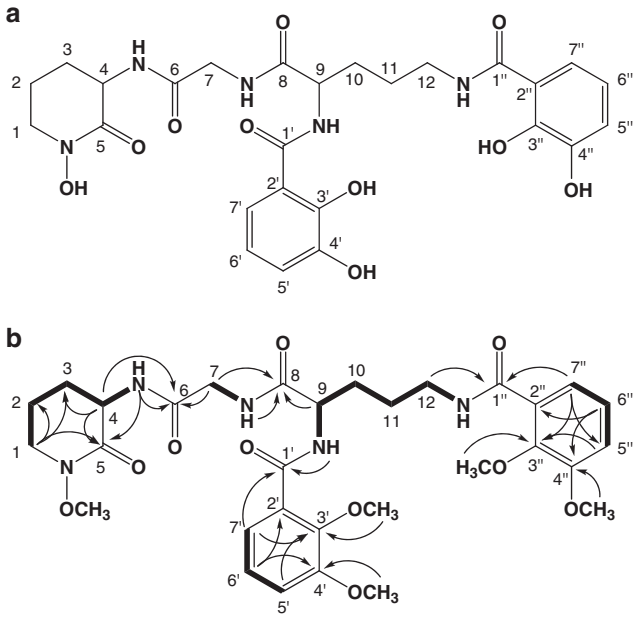


**Figure 1** Structure of **1** (**a**), and $^{1}H$–$^{1}H$ (bold lines) and main $^{1}H$–$^{13}C$ (arrows) correlations in the 2D NMR of **2** (**b**).

was observed. $^{1}H$–$^{13}C$ long-range couplings in heteronuclear multi-bond correlation spectrum from 1-$H_2$ and 4-H to a carbonyl carbon C-5 ($\delta_C$ 167.1), together with a $^{13}C$ chemical shift of C-1 ($\delta_C$ 49.7), revealed a 3-amino piperizin-2-one moiety. The proton spin coupling between an amide proton 7-NH ($\delta_H$ 7.31) and methylene proton 7-$H_2$ ($\delta_H$ 3.91, 4.08), which in turn $^{1}H$–$^{13}C$ long-range coupled to an amide carbonyl carbon C-6 ($\delta_C$ 169.2), established a glycine residue. The sequence from an amide proton 9-NH ($\delta_H$ 8.66) to another amide proton 12-NH ($\delta_H$ 8.13) through an α-methine proton 9-H ($\delta_H$ 4.82, $\delta_C$ 53.2), methylene protons 10-$H_2$ ($\delta_H$ 1.85, 2.06), 11-$H_2$ ($\delta_H$ 1.77) and 12-$H_2$ ($\delta_H$ 3.40, 3.80), and an $^{1}H$–$^{13}C$ long-range coupling from the α-methine proton 9-H to an amide carbonyl carbon C-8 ($\delta_C$ 172.5), revealed an ornithine moiety. An aromatic proton 5′-H ($\delta_H$ 7.03) was *ortho*- and *meta*- coupled to the aromatic protons 6′-H ($\delta_H$ 7.13) and 7′-H ($\delta_H$ 7.63), respectively, supporting the presence of a 1,2,3-trisubstituted benzene ring. In addition, $^{1}H$–$^{13}C$ long-range couplings from the methoxyl protons 3′-$OCH_3$ ($\delta_H$ 3.90) and 5′-H to an oxygenated aromatic quaternary carbon C-3′ ($\delta_C$ 147.7), from the methoxyl protons 4′-$OCH_3$ ($\delta_H$ 3.88) and 6′-H to an oxygenated aromatic quaternary carbon C-4′ ($\delta_C$ 152.8), and 7′-H to a carbonyl carbon C-1′ ($\delta_C$ 166.0) were observed. These results established a 2,3-dimethoxybenzoate moiety as shown in Figure 1. In the same manner, another 2,3-dimethoxybenzoate moiety was determined.

The connection of these substructures was elucidated by $^{1}H$–$^{13}C$ long-range couplings from 4-NH to C-6, from 7-NH to C-8, from 9-NH to C-1′ and from 12-H to C-1″ ($\delta_C$ 166.0), as shown in Figure 1b. In addition to the molecular formula of **2**, no cross signal was observed with the remaining methoxyl group 1-$NOCH_3$ ($\delta_H$ 3.68, $\delta_C$ 61.3), indicating that this methoxyl group is attached to the nitrogen of the piperidin-2-one moiety. Thus, the structure of **1** was established as shown in Figure 1a. A compound related with **1** is heterobactin A,[12] in which one 2,3-dihydrobenzoate moiety in **1** is replaced by a benzoxazole residue. In addition, rhodobactin,[14] which possesses both hydroxamate and biscatecholate moieties, has been

**Table 1** $^{1}H$- and $^{13}C$-NMR data of 1 and 2

| | ***1*** | | | | ***2*** | | |
|---|---|---|---|---|---|---|---|
| *Position* | $\delta_C$ | $\delta_H$ | | *Position* | $\delta_C$ | $\delta_H$ | |
| 1 | 52.5 | 3.58 | (m) | 1 | 49.7 | 3.52 | (m) |
| | | 3.64 | (m) | | | 3.60 | (m) |
| | | | | 1-$NOCH_3$ | 61.3 | 3.68 | (s) |
| 2 | 21.7 | 1.94 | (m) | 2 | 21.1 | 1.95 | (m) |
| | | 2.02 | (m) | | | 2.01 | (m) |
| 3 | 28.6 | 1.82 | (m) | 3 | 27.8 | 1.63 | (m) |
| | | 2.03 | (m) | | | 2.37 | (m) |
| 4 | 51.4 | 4.46 | (dd, 8.3, 5.6) | 4 | 51.5 | 4.30 | (m) |
| | | | | 4-NH | | 7.00 | (d, 6.4) |
| 5 | 167.2 | | | 5 | 167.1 | | |
| 6 | 171.6 | | | 6 | 169.2 | | |
| 7 | 43.6 | 3.90 | (d, 8.8) | 7 | 43.5 | 3.92 | (dd, 16.9, 5.6) |
| | | | | | | 4.08 | (dd, 16.9, 6.1) |
| | | | | 7-NH | | 7.31 | (t, 5.8, 5.8) |
| 8 | 174.0 | | | 8 | 172.5 | | |
| 9 | 55.4 | 4.54 | (dd, 10.3, 5.1) | 9 | 53.2 | 4.84 | (m) |
| | | | | 9-NH | | 8.66 | (d, 6.9) |
| 10 | 30.2 | 1.90 | (m) | 10 | 30.3 | 1.83 | (m) |
| | | 2.03 | (m) | | | 2.06 | (m) |
| 11 | 27.0 | 1.78 | (m) | 11 | 26.6 | 1.77 | (m) |
| 12 | 40.0 | 3.45 | (m) | 12 | 38.8 | 3.40 | (m) |
| | | | | | | 3.80 | (m) |
| | | | | 12-NH | | 8.13 | (t, 5.9, 5.9) |
| 1′ | 171.5 | | | 1′ | 166.0[a] | | |
| 2′ | 117.2 | | | 2′ | 127.0 | | |
| 3′ | 150.9 | | | 3′ | 147.7 | | |
| | | | | 3′-$OCH_3$ | 61.6 | 3.90 | (s) |
| 4′ | 147.5 | | | 4′ | 152.8 | | |
| | | | | 4′-$OCH_3$ | 56.3 | 3.88 | (s) |
| 5′ | 119.4 | 6.91 | (d, 7.3) | 5′ | 115.6 | 7.03 | (dd, 8.1, 1.5) |
| 6′ | 119.1 | 6.68 | (t, 7.8, 7.8) | 6′ | 124.6 | 7.13 | (t, 8.1, 8.1) |
| 7′ | 118.7 | 7.21 | (d, 8.5) | 7′ | 122.9 | 7.63 | (dd, 8.0, 1.5) |
| 1″ | 171.6 | | | 1″ | 166.0[a] | | |
| 2″ | 116.7 | | | 2″ | 126.1 | | |
| 3″ | 150.7 | | | 3″ | 148.1 | | |
| | | | | 3″-$OCH_3$ | 61.9 | 3.96 | (s) |
| 4″ | 147.6 | | | 4″ | 152.8 | | |
| | | | | 4″-$OCH_3$ | 56.4 | 3.88 | (s) |
| 5″ | 119.4 | 6.91 | (d, 6.8) | 5″ | 116.2 | 7.05 | (dd, 8.8, 1.71) |
| 6″ | 119.1 | 6.68 | (t, 8.1, 8.1) | 6″ | 124.6 | 7.13 | (t, 8.1, 8.1) |
| 7″ | 120.0 | 7.35 | (d, 8.1) | 7″ | 123.0 | 7.63 | (dd, 8.0, 1.5) |

The $^{13}C$ (125 Hz) and $^{1}H$ (500 Hz) NMR spectra were taken on an NMR system 500 NB CL (Varian, Palo Alto, CA, USA) in $CD_3OD$, and the solvent peak was used as an internal standard ($\delta_C$ 49.0 p.p.m., $\delta_H$ 3.30 p.p.m.).
[a]These assignments are exchangeable.

reported as a siderophore. To our knowledge, this is the first report with regard to secondary metabolites from *N. tenerifensis*.

Compound **1** showed a red color in 10% aqueous $FeCl_3$ and the ESI–MS of the complex resulted in the $(M+Fe+H)^+$ ion at *m/z* 627 in the positive mode. The formation of **1**–iron complex was also confirmed by the changes in UV spectrum (absorption maxima at 205 and 249 nm were changed to 245 and 364 nm, respectively). However, **2** did not form a complex with ferric ion. The hydroxamate involved in trichostatin A is known to chelate metal ions.[15] Mycobactin[16] and exochelin[16] have been reported as siderophores that lack catechol units. In contrast, azotochelin,[17] which possesses 2,3-dihydrobenzoate moieties but not hydroxamate functional groups, has

also been reported to show siderophore activity. Thus, both the hydoxamate and catechol functional groups in **1** are considered to have a significant role in chelating properties. The lack of the siderophore activity of **2**, by which hydroxamate and catechols are methylated, also supports the role of these functional groups. Further biological activities are under investigation.

## ACKNOWLEDGEMENTS

This work was supported by a grant from the New Energy and Industrial Technology Department Organization (NEDO) of Japan.

1 Tanaka, Y., Gräfe, U., Yazawa, K., Mikami, Y. & Ritzau, M. Nocardicyclins A and B: new anthracycline antibiotics produced by *Nocardia pseudobrasiliensis*. *J. Antibiot.* **50,** 822–827 (1997).
2 Tanaka, Y., Gräfe, U., Yazawa, K. & Mikami, Y. Production of nocardicyclins by clinical isolates of *Nocardia pseudobrasiliensis* and *in vivo* antitumor activity of the antibiotic. *J. Antibiot.* **5I,** 589–591 (1998).
3 Mikami, Y. *et al*. A new antifungal macrolide component, Brasilicardin B produced by *Nocardia brasiliensis*. *J. Antibiot.* **53,** 70–74 (2000).
4 Mukai, A. *et al.* Transvalencin Z, a new antimicrobial compound with salicylic acid residue from *Nocardia transvalensis* IFM 10065. *J. Antibiot.* **59,** 366–369 (2006).
5 Shigemori, H. *et al*. Brasilicardin A. A novel tricyclic metabolite with potent immunosuppressive activity from actinomycete *Nocardia brasiliensis*. *J. Org. Chem.* **63,** 6900–6904 (1998).
6 Mikami, Y. *et al*. A new antifungal macrolide component, Brasilicardin B produced by *Nocardia brasiliensis*. *J. Antibiot.* **53,** 70–74 (2000).
7 Drechsel, H. & Jung, G. Peptide siderophore. *J. Peptide Sci.* **4,** 147–181 (1998).
8 Tsuda, M. *et al*. Brasilibactin A, a cytotoxic compound from actinomycete *Nocardia brasiliensis*. *J. Nat. Prod.* **68,** 462–464 (2005).
9 Nemoto, A. *et al*. Asterobactin, a new siderophore group antibiotic from *Nocardia asteroides*. *J. Antibiot.* **55,** 593–597 (2002).
10 Ratledge, C. & Snow, G. A. Isolation and structure of nocobactin NA, a lipid-soluble iron-binding compound from *Nocardia asteroides*. *Biochem. J.* **139,** 407–413 (1974).
11 DeBoer, C. & Dietz, A. The description and antibiotic production of *Streptomyces hygroscopicus* var. *Geldanus*. *J. Antibiot.* **29,** 1182–1191 (1976).
12 Carran, C. J., Jordan, M., Drechsel, H., Schmid, D. G. & Winkelmann, G. Heterobactins. A new class of siderophores from *Rhodococcus erythropolis* IGTS8 containing both hydroxamate and catecholate donor groups. *Biometals* **14,** 119–125 (2001).
13 Furihata, K. & Seto, H. Constant time HMBC (CT-HMBC), a new HMBC technique useful for improving separation of cross peaks. *Tetrahedron Lett.* **39,** 7337–7340 (1998).
14 Dhungana, S. *et al*. Purification and characterization of rhodobactin: a mixed ligand siderophore from Rhodococcus rhodochrous strain OFS. *Biometals.* **20,** 853–867 (2007).
15 Finnin, MS. *et al*. Structures of a histone deacetylase homologue bound to the TSA and SAHA inhibitors. *Nature* **401,** 188–193 (1999).
16 Ratledge, C. Iron, mycobacteria and tuberculosis. *Tuberculosis* **84,** 110–130 (2004).
17 Corbin, J. L. & Bulen, W. A. The isolation and identification of 2,3-dihydroxybenzoic acid and 2-N,6-N-di-92,3-dihydroxybenzoyl)-L-lysine formed by iron-deficient Azotobacter vinelandii. *Biochemistry* **8,** 77–762 (1969).